PREDICTION AND ENHANCEMENT OF VOLTAGE STABILITY OF POWER SYSTEMS

A DISSERTATION

SUBMITTED IN PARTIAL FULFILLMENT OF THE REQUIREMENTS
FOR THE AWARD OF THE DEGREE
OF

MASTER OF TECHNOLOGY
IN
POWER SYSTEMS

Submitted by:

Manish Kumar Meena

2K17/PSY/08

Under the supervision of

Prof. Narendra Kumar

DEPARTMENT OF ELECTRICAL ENGINEERING
DELHI TECHNOLOGICAL UNIVERSITY
(Formerly Delhi College of Engineering)
Bawana Road, Delhi-110042

2019

M. Tech (Power System) MANISH KUMAR MEENA 2019

DEPARTMENT OF ELECTRICAL ENGINEERING
DELHI TECHNOLOGICAL UNIVERSITY
(Formerly Delhi College of Engineering)
Bawana Road, Delhi-110042

CANDIDATE'S DECLARATION

I Manish Kumar Meena Roll No.2K17/PSY/08 student of M.Tech. (Power System Engineering) hereby declare that the Dissertation/project entitled "**Prediction and Enhancement of Voltage Stability of Power Systems**" which is submitted by me to the Department of Electrical Engineering, Delhi Technological University, Delhi in partial fulfillment of the requirement for the award of the degree of Master of Technology is original and not copied from any source without proper citation. This work has not previously formed the basis for the award of any Degree, Diploma Associate ship, Fellowship or other similar title or recognition.

Place: Delhi **Manish Kumar Meena**

Date: **2K17/PSY/08**

DEPARTMENT OF ELECTRICAL ENGINEERING
DELHI TECHNOLOGICAL UNIVERSITY
(Formerly Delhi College of Engineering)
Bawana Road, Delhi-110042

CERTIFICATE

I, Manish Kumar Meena, Roll No. 2K17/PSY/08 student of M. Tech. (Power System), hereby declare that the dissertation/project entitled **"Prediction and Enhancement of Voltage Stability of Power Systems"** under the supervision of Prof. Narendra Kumar of Electrical Engineering Department Delhi Technological University in partial fulfillment of the requirement for the award of the degree of Master of Technology has not been submitted elsewhere for the award of any Degree.

Place: Delhi **(Manish Kumar Meena)**

Date:

(Prof. Narendra Kumar)

Former Head, Department of Electrical Engineering

DEPARTMENT OF ELECTRICAL ENGINEERING

DELHI TECHNOLOGICAL UNIVERSITY
(Formerly Delhi College of Engineering)
Bawana Road, Delhi-110042

ACKNOWLEDGEMENT

First and foremost, my utmost gratitude to Prof. Narendra Kumar, my project supervisor. He has been inspiration to me, without which this work is not possible at all. He motivated me very much and encouraging throughout the period of this work was carried out. His readiness for consultation at all times, his educative comments, his concern and assistance even with practical things have been invaluable.

I am very grateful to Prof. Madhusudan Singh (former Head, Electrical Department), Prof. Uma Nangia (Head, Electrical Department) and our M.Tech. Coordinator Prof. Rachana Garg for providing us constant support an environment to complete my work successfully.

I would like to thank all the faculty members of department of Electrical engineering, DTU, Delhi for their constant encouragement.

ABSTRACT

There are many challenges in power system related to stability in the stressed operating condition. Voltage collapse is a frequent phenomenon in stressed condition which leads to degradation the power system performance. So, there is continuously monitoring required to prevent the voltage collapse and major blackout. For this purpose, power system is to be examined to find the weak buses so that voltage stability can be improved.

For the online testing and detection of voltage instability it is required to identify the maximum load taking capacity of the system. Load dynamics is directly related to voltage stability of the bus therefore it is required to consider different load for voltage stability studies.

Previously voltage stability was observed by the P-V and Q-V curves which is time consuming. There are some indexes also provided by the many researchers like L-index, fast voltage stability index (FVSI), new voltage stability index (NVSI), line stability factor (LQP), line collapse proximity index (LCPI), Lmn index, line voltage stability index (LVSI) etc.

In this work a voltage stability index named as Line Collapse Proximity Index (LCPI) has been considered mainly to evaluate the voltage stability and compare with other indices FVSI, Lmn and LQP. The maximum loadability limit of load buses also find out with help of LCPI index and verified with P-V and Q-V curves. LCPI provides highly accurate results in very short time. So precisely monitoring of power system is possible so that we can take necessary action to avoid the voltage instability.

LCPI is also used to identify the reactive power margin for stability. For the effectiveness of this index it is tested on IEEE-30 bus and IEEE-118 bus test system.

CONTENTS

LIST OF FIGURES

LIST OF TABLES

LIST OF ABBREVIATIONS

1.	MW	:	Mega watt
2.	MVAR	:	Mega Volt Ampere Reactive
3.	ANN	:	Artificial Neural Network
4.	LCPI	:	Line Collapse Proximity Index
5.	LVSI	:	Line Voltage Stability Index
6.	LQP	:	Line Stabilization Ratio
7.	Lmn	:	line Stability Index
8.	FVSI	:	Fast Voltage Stability Index
9.	NVSI	:	New Voltage Stability Index
10.	PSO	:	Particle Swarm Optimization
11.	CPF	:	Continuous Power Flow
12.	P-V	:	Power-Voltage
13.	Q-V	:	Reactive Power-Voltage
14.	ABCD	:	Transmission line parameters
15.	N-R	:	Newton-Raphson

NOMENCLATURE

V_R : Voltage at receiving end bus.

V_S : Voltage at sending end bus.

P_R : Active power at receiving end bus.

P_S : Active power at sending end bus.

Q_R : Reactive power at receiving end bus.

Q_S : Reactive power at sending end bus.

R : Transmission line series resistance.

X : Transmission line series reactance.

Z : Transmission line series impedance.

Y : Transmission line shunt admittance.

I : Transmission line current.

θ : Transmission line impedance angle.

α : Angle of parameter A of transmission line.

β : Angle of parameter B of transmission line.

δ : Angle difference between the sending end and receiving end bus voltages.

λ : Loadability factor.

λ_{max} : Maximum value of λ.

CHAPTER 1
INTRODUCTION

1.1 Background

The existing power systems are working under stressed conditions due to the many factors such as environmental issues, regulation & policies, erection cost, equipment cost etc. so that any slight change in working condition may leads to voltage instability [1-11]. Therefore, voltage stability analysis is required to operate the power system within their limits and ensure the voltage stability.

The following are the constraints to operate the secure power system network:

- Regularly increasing power system network size.
- Environmental & Social issues.
- Working with old mechanism for controlling the voltage and power.
- Day by day increasing load on power system network and load-generation unbalancing.

All the above facts are creating stability issues in power system network. The behavior of heavily loaded power system is different from the lightly loaded power system. In the interconnected power system network, it's stability and operations will be severely affected.

1.2 Voltage Stability Issue

Voltage stability is a major issue for power system where the existence of heavy load, faulty condition or lack of reactive power and it affects the reliable and secure operation of power system. Voltage instability occurs due to the continuous increasing load and lake of power transmission capacity to meet this load demand. Voltage stability [7] is the ability of all the buses to maintain its voltage within the limits before and after the disturbances. The definition given by other authors are written in chapter 2.

There are many incidents of blackouts [13] happened due to the voltage instability, such as French black-out in 1978 and 1987 northern Belgium collapses in 1982, Swedish black-out in 1983 Indian Black-out in July-2012[14]. Many of them blackouts occurred due to the loss of major transmission line, loss of generation, increasing the load level etc.

When load bus connected to unique alternator then there are chance of voltage instability. When unique alternator is associated with infinite bus then there are chance of angle instability. When there are combination of unique alternator, infinite bus and load bus then there are chance of both voltage instability and angle instability but the effects cab be separable [15].

The following aspects are playing major role in voltage stability:

1. Characteristics of load
2. Characteristics of reactive power compensation devices.
3. Transmission network strength and level of power transfer.
4. Voltage control limit and reactive power control limit of alternator.
5. Action of voltage controllers such as transformers, on load tap changers (OLTC).
6. Reliable relay operation.
7. Reliable operation of generators.
8. Load distribution.
9. Load restoration mechanism.
10. Load shedding.

Voltage stability problem is attracting many of researchers and engineers to find the appropriate solution. Many of research papers related to voltage stability have been published in different conferences and journals. Voltage instability is a dynamical problem and having both static and dynamic approach to solved it [16]. To secure operation of power system, it to be scrutinized for different operating situations and possibilities. The maximum loadability criteria of the system is defined using static analysis. The effect of system dynamics on voltage stability is quite slow. The static method is having solution of algebraic equations and it is faster with respect to the dynamical method. The various static approaches [17] are given in the literature to get the solution of voltage instability.

1.3 Outline of the thesis

Chapter 1: Short presentation of the voltage stability issues.

Chapter 2: Literature review, an overview of the events and kinds of the voltage instability with few instances. Voltage instability phenomena are described.

Chapter 3: provides voltage stability assessment load modeling and voltage disturbance countermeasures, overview of voltage stability indices.

Chapter 4: Modeling and formation of Line Collapse Proximity Index (LCPI) to get the more accurate results and define the limits of voltage stability for each bus. Also presenting Particle Swarm Optimization (PSO) technique for reactive power compensation.

Chapter 5: Present the simulation result of LCPI and compare with the indices such as Lmn , LQP, FVSI. The reactive power margin is estimated and providing the reactive power support when the system is going to become unstable. The improvement in the LCPI index is shown according to the reactive power support.

Chapter 6: Conclusion of this work and future scope.

CHAPTER 2

LITERATURE REVIEW

2.1 Introduction

Various voltage stability terms can be discovered in the literature [12]. Definitions take into account time frames, system conditions, big or tiny disturbances, etc. The various methods thus show that during a voltage stability course, a wide spectrum of events may happen. Because numerous individuals have distinct phenomenon experiences in result of that variations between the voltage stability definition occurs. It could also show that the phenomenon itself is not sufficiently familiar to create a general concept at this point.

The power system stability classification is given in Fig.2.1 includes Short- or long-term stability with respect to the rotor angle, frequency and voltage according to the type of disturbance (small or big) [40].

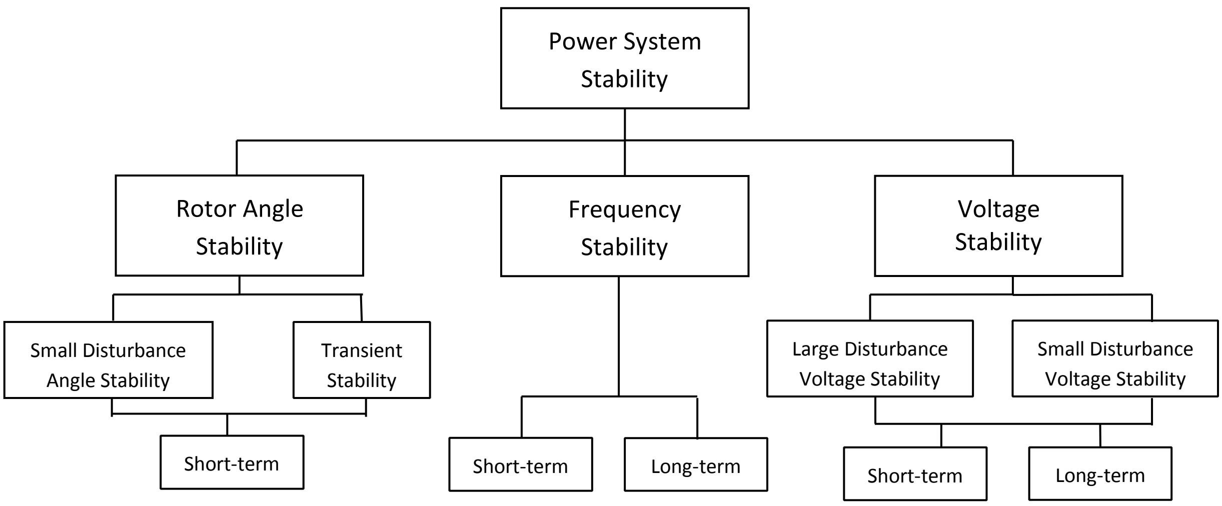

Figure2.1: power system stability classification.

Above classification is necessary to identifies the factors of instability so that we can perform a suitable action to improve the stability. In many cases particularly in extremely loaded system it is difficult to identify the root cause of instability due to the cascade events and several instabilities combined together. Hence for this kind of problem, classification of stability is very useful tool to discriminate the problem and remedy appropriately.

In the following sections we have to discussed about the definition and type of voltage stability.

2.2 CIGRE definitions for voltage stability [40]

CIGRE define the strength of the bus for voltage stability is comparable to other issues related to the dynamic stability.

• A power system for a particular working point is stable with small disturbances if load bus voltage having the same voltage as pre-disturbed value (For assessment, discontinuous designs for tap changers may have to be changed into equal continuous model) The stability of small disturbed voltage leads to associated liberalized dynamic model with eigen values consist negative real part)

• A power system in a given operational stage is referred as voltage stable if voltages close to loads achieve equilibrium state after disturbance. The disturbed state lies in the region where the stable post-disturbed balance exists.

• Whenever voltage at load bus after the disturbances goes below the desired limits Voltage instability occurs. The partial or complete blackout may be occurs due to the voltage instability.

• Instability of voltage is the outcomes of gradual reduction (or boost) of voltage and the lack of reactive power support. However, destabilizing limit checks or other control measures (e.g., load shading), can provide global stability.

2.3 IEEE definitions for voltage stability [40] &[43]

• Voltage stability is the tendency of system to keep the voltage within the desired limits with respect to the increasing in load impedance, or load power. Hence both power and voltage are stably controlled.

• Voltage Collapse is the mechanism through which voltage instability in an important area of the system contributes to voltage failure.

• Voltage security is not only the capacity of a system to function stably, it also maintains stability as a result of a fairly reliable contingency or adverse system changes (in terms of stress on system).

• Voltage instability occurs when voltage decreases very fast due to effect of load raises, fault in system or adverse change in system and controllers fails to maintain the voltage within the desired limits. For a stable operating power system voltage instability occurs within the seconds or 10 to 20 minutes. If the deterioration proceeds unabated, there will be angular instability or voltage instability occurs.

2.4 Hill and Hisken definition for voltage stability [41]

They proposed voltage stability definition according to the static and dynamic part. For static part voltage stability is defined as follow:

- The voltage at the bus should be lie within the appropriate range.
- When reactive power is injected at a particular bus then system must be able to increase the voltage at this bus within the acceptable limits.

The definition as per the dynamic concern as follow:

Voltage stability for small disturbance: when a power system is subjected to small disturbance then the voltage at the respective bus must be equivalent to the pre-disturbed value after the small disturbance then system is called small disturbance voltage stable.

Voltage stability for large disturbance: when a power system is subjected to large disturbance then the voltage at the respective bus must be equivalent to the new post disturbed value. But voltage limit should not be violated, then system is called large disturbance voltage stable.

Voltage collapse: when a power system is subjected to the large disturbance then the voltage at the respected bus is violate the acceptable limits then system undergoes voltage collapse.

2.5 Glavitch definitions[42]

This is a strategy that shows various time frames of failure:

- Transient stability or collapse characterizes to short-term voltage stability when vast disturbances and fast reactions occurs in power system. The time interval is one to a few seconds, that is also refer to the action of automatic controllers at generators [42].
- A big disturbance and consecutive load restoration or load shift on the power system characterizes as long-term Voltage stability. The period is 0.5-30 minutes. Glavitch also presents a difference between dynamic and static approach. The assessment is dynamic if differential equations are engaged. "Static does not signify continuous, that is to say, a static analysis can take time function into consideration”.

From above definitions It is clear that Hill's definition appears to be the nearest to mathematics of voltage stability concepts and the IEEE definition linked to real network. The voltage stability mechanism primarily involves three problems: voltage magnitude must be appropriate; the model must be operationally controllable, and system stability maintained with respect to contingency or change in network.

Figure 2.2 Presents elements and regulators of the power system [44], which perform a role in time-frame and voltage stability.

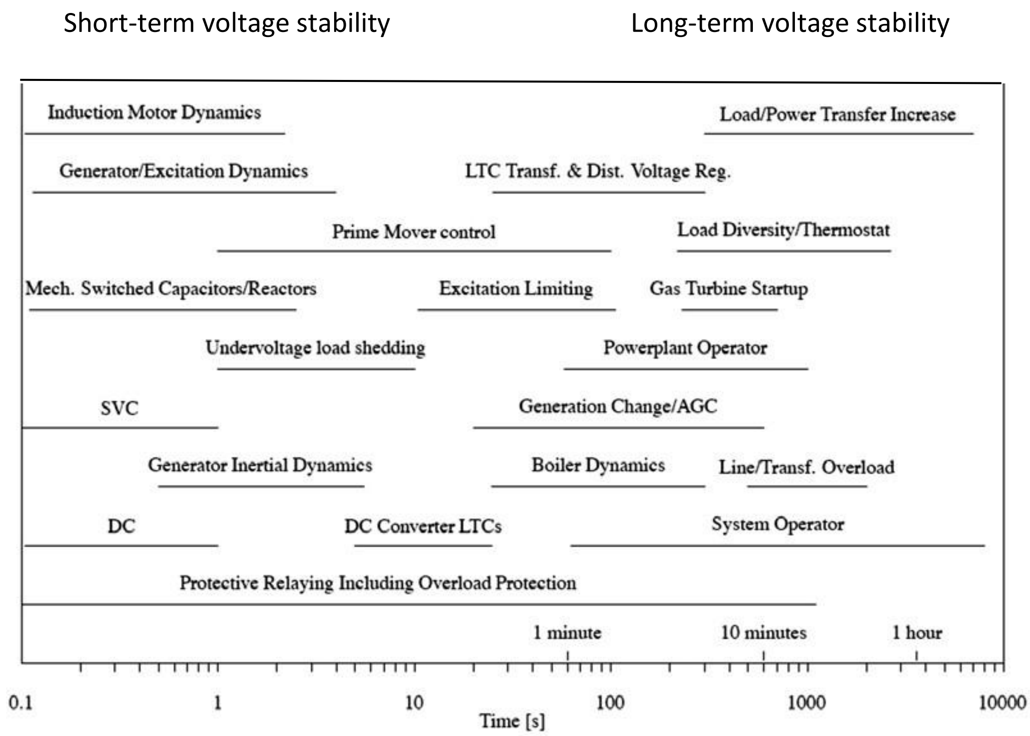

Figure. 2.2 Power system elements and controls time frame.

2.6 Incidence of Voltage instability

The New York voltage collapse in 1970, and the Zealand voltage collapse in Denmark in 1979 are the examples of voltage instability. The New York voltage instability is happened due to the decreasing of the post-contingency voltage by enhanced load on the transmission network and tripping of a 35 MW power generation. At Zealand rapid voltage decrease in that portion was triggered by the tripping of the only plant in the Southern portion of the island generating 270 MW. Within 15 minutes the voltages decreased to 75 percent, which made it difficult to synchronize with the 70 MW gas turbine. Manual load shedding is done to rescue above said voltage collapse [45].

The voltage instability in Belgium also had transmission capability issues on 4 August 1982. The voltage collapse was triggered by a casual trip of some generating stations. As per the economic point of view few generating plant required to serve low load [45] but it led to operate quite near to their boundaries of operation. The nearby region was subjected to lack of reactive power when generating unit tripped and excitation of several generators were limited.

Several blackouts have been happened in many nations in past few years due to the voltage instability issues. Specially, 2003 was a severe year with six significant power outages in the USA, United Kingdom, Italy, Sweden and Denmark [45]. Around 50 million individuals in eight US states and two Canadian territories were impacted by the USA-Canadian blackout of 14 August 2003. The Swedish / Danish power system network was blackout on September 23, 2003 and affected to 2.4 million clients in the same year and a further significant blackout took place five days later on 28 September in continental Europe, which led to failure of entire power system network in Italy.

2.7 Analysis of voltage stability and available methods

The economic constraints, strategies for deregulation and heavy transmission line construction costs are forced to function under strained conditions by current energy structures. Any minor disruption in this country may lead to a crash in voltage [1-11]. For a safe and efficient energy scheme, therefore, voltage stabilization assessment is crucial.

The system voltage stability can be evaluated with dynamic or static methods. The static strategy encodes system snapshots in a distinct time frame, while a dynamic stabi lization assessment needs more time computerization [12]. The scheme is therefore easy to model and analyze.

Different static methods for the analysis of the system voltage stabilization are accessible in literature. The important results of early studies are focused on continuous PV and QV curves [18–22]. The results are important. But these processes need a remedy for the repetitive power flow solution, so it takes time.

Voltage stability indicators based on techniques were created for the fast assessment of voltage stability of power systems. The voltage stability indexes calculate the voltage stability status of the scheme with the graph of the voltage stability index. The previous indicators were focused on the Matrix of Jacobian [23-25] and Proposed Jacobin matrix-based index in [26-28]. However, at the voltage instability stage these indices can't be correctly estimated because of the uncertainty at the critical point.

In order to tackle voltage instability artificial neural network (ANN) indices are suggested [29]. For big network these techniques are very complicated.

The load flow alternative is the basis for establish of L-index in [30]. However, when loads are variable then L-index method is incorrect [31]. The index of line stabilization (Lmn) for the evaluation of the critical situation of line is suggested in [32]. The line stabilization ratio (LQP) index was created in [33] and is used in the control of lines with load flow solution for the voltage stabilization condition. In [34] the proposed fast voltage stabilization index (FVSI) has been used to forecast the critical point of voltage instability and the critical line contingency priority.

The Lmn [32] and FVSI [34] indicators do not take into account actual energy flows for voltage stability forecast, and therefore incorrect outcomes can be achieved in certain working circumstances. The LQP [33] approach uses a simpler transmission line that avoids line resistance so it also gives incorrect assessment when transmission line losses are considered. The [30-34] suggested indicators also over looked the existence of a power line charging capacity while deriving the index equation [8]. It should be pointed out that under ordinary working circumstances line charging capacitance provide quite a great voltage assistance to the system. Ignoring them can result in certain circumstances to a false forecast of the stability of the voltage. Furthermore, the established stability index of the voltage can't be converted into Mega Volt Amp (MVA) load.

To overcome the deficiencies in suggested indices [30-34] a new index Line Collapse Proximity Index (LCPI) is proposed in [35]. The LCPI index considering the line charging reactance and direction of active and reactive power flow, so it gives accurate assessment of voltage stability with respect to the other indices.

Particle Swarm Optimization technique given by James Kennedy and Russell Eberhart in 1997 [36]. PSO technique is used to find optimum bus for reactive power compensation [37-39].

2.8 Power flow analysis:

Power-flow analysis is also referred to load-flow analysis which is frequently used for planning and operation of big complex power systems. The following section will introduce power-flow analysis and its implementation for defining the voltage stability indicators shown in the following chapter.

To determine the power flow, voltage magnitude and corresponding angle at a particular bus of a big power system network the load flow analysis is very useful. Mostly Newton-Raphson Load flow analysis is used for the power flow solution propose.

2.8.1 Type of buses for load flow analysis

The buses in power system network are classified according to their connected elements. The loads are constant and defined by active and reactive power in load flow analysis [46]. The generator voltage is to be considered as constant. The classification of buses are as follow:

- ***Load Buses***: loads are connected on these buses having active power $-P_{Li}$ and reactive power $-Q_{Li}$. The negative sign represents outside flow of power from the bus. These buses are known as P-Q bus. Generators are never connected on these buses. Here we have to find voltage $|V_i|$ and its angle δ_i.
- ***Voltage Controlled Buses***: These buses are having generators governed by prime mover. Generator excitation is responsible for the voltage control at the bus and maintained constant by voltage regulators. The active power also maintains constant by the automatic governors. These buses are known as P-V bus, active power P_{Gi} and voltage $|V_i|$ are specified on these buses. The reactive power Q_{Gi} is generated according to the situation and reactive power limits of generators. We have to find unspecified voltage angle δ_i of the bus voltage by load flow analysis.
- ***Slack or Swing Bus***: This is known as Type-1 usually for the load flow studies. This is also known as reference bus. The voltage angle on this bus is taken 0 degree and other buses voltage angle are comes as per this reference. The voltage magnitude is specified on this bus. For the load flow analysis additional active and reactive power for the line losses are supplied by this bus.

2.8.2 Load flow by Newton-Raphson method

For n number of buses in power system let us assume

n_p = Number of P-Q buses

n_g = Number of P-V buses

$n = n_p + n_g + 1$ = Total number of buses (including one slack bus as bus-1).

ΔP_i = Active power mismatch at i[th] bus

$$\Delta P_i = P_{i,inj} - P_{i,calc} = P_{Gi} - P_{Li} - P_{i,calc} \tag{2.1}$$

ΔQ_i = Reactive power mismatch at i[th] bus

$$\Delta Q_i = Q_{i,inj} - Q_{i,calc} = Q_{Gi} - Q_{Li} - Q_{i,calc} \tag{2.2}$$

Lower subscript G and L are denoting for generator and load of related bus respectively.

The power mismatch should be very small value for convergence of load flow solution.

The Newton-Raphson method [47] is used to solve the non-linear power equations in which jacobian matrix is used for each iteration. The equations are formed as follow:

$$J \begin{bmatrix} \Delta\delta_2 \\ \vdots \\ \Delta\delta_n \\ \dfrac{\Delta|V_2|}{|V_2|} \\ \vdots \\ \dfrac{\Delta|V_{1+n_p}|}{|V_{1+n_p}|} \end{bmatrix} = \begin{bmatrix} \Delta P_2 \\ \vdots \\ \Delta P_n \\ \Delta Q_2 \\ \vdots \\ \Delta Q_{1+n_p} \end{bmatrix} \tag{2.3}$$

The jacobian matrix are divided in parts as:

$$J = \begin{bmatrix} J_{11} & J_{12} \\ J_{21} & J_{22} \end{bmatrix} \tag{2.4}$$

Jacobian matrix dimension is $(n + n_p - 1) \times (n + n_p - 1)$ and dimensions of the submatrices are

J_{11}: $(n - 1) \times (n - 1)$, J_{12}: $(n - 1) \times n_p$, J_{21}: $n_p \times (n - 1)$ and J_{22}: $n_p \times n_p$

here

$$J_{11} = \begin{bmatrix} \frac{\partial P_2}{\partial \delta_2} & \cdots & \frac{\partial P_2}{\partial \delta_n} \\ \vdots & \ddots & \vdots \\ \frac{\partial P_n}{\partial \delta_2} & \cdots & \frac{\partial P_n}{\partial \delta_n} \end{bmatrix} \tag{2.5}$$

$$J_{12} = \begin{bmatrix} |V_2| \frac{\partial P_2}{\partial |V_2|} & \cdots & |V_{1+n_p}| \frac{\partial P_2}{\partial |V_{1+n_p}|} \\ \vdots & \ddots & \vdots \\ |V_2| \frac{\partial P_n}{\partial |V_2|} & \cdots & |V_{1+n_p}| \frac{\partial P_n}{\partial |V_{1+n_p}|} \end{bmatrix} \tag{2.6}$$

$$J_{21} = \begin{bmatrix} \frac{\partial Q_2}{\partial \delta_2} & \cdots & \frac{\partial Q_2}{\partial \delta_n} \\ \vdots & \ddots & \vdots \\ \frac{\partial Q_{1+n_p}}{\partial \delta_2} & \cdots & \frac{\partial Q_{1+n_p}}{\partial \delta_n} \end{bmatrix} \tag{2.7}$$

$$J_{22} = \begin{bmatrix} |V_2| \frac{\partial Q_2}{\partial |V_2|} & \cdots & |V_{1+n_p}| \frac{\partial Q_2}{\partial |V_{1+n_p}|} \\ \vdots & \ddots & \vdots \\ |V_2| \frac{\partial Q_{1+n_p}}{\partial |V_2|} & \cdots & |V_{1+n_p}| \frac{\partial Q_{1+n_p}}{\partial |V_{1+n_p}|} \end{bmatrix} \tag{2.8}$$

2.8.3 Load Flow Algorithm

The following are the step for Newton-Raphson load flow analysis [47]:

Step-1: Assume the initial values of the voltage $|V|^{(0)}$ for all load buses and voltage *angles* $\delta^{(0)}$ for all PQ and PV buses.

Step-2: By using estimated $|V|^{(0)}$ and $\delta^{(0)}$ calculate active power $P_{calc}^{(0)}$ and their mismatch $\Delta P^{(0)}$.

Step-3: By using estimated $|V|^{(0)}$ and $\delta^{(0)}$ calculate reactive power $Q_{calc}^{(0)}$ and their mismatch $\Delta Q^{(0)}$.

Step-3: By using estimated $|V|^{(0)}$ and $\delta^{(0)}$ formulate the Jacobian matrix $J^{(0)}$.

Step-4: Solve (2.3) for $\Delta\delta^{(0)}$ and $\Delta|V|^{(0)}/|V|^{(0)}$.

Step-5: Obtain the updates from

$$\delta^{(1)} = \delta^{(0)} + \Delta\delta^{(0)} \tag{2.9}$$

$$|V|^{(1)} = |V|^{(0)}\left[1 + \frac{\Delta|V|^{(0)}}{|V|^{(0)}}\right] \tag{2.10}$$

Step-6: Observer all the mismatches for small number. If mismatches are come below the small number then end the process. Otherwise come to step-1 again and start the next iteration with the updated values

CHAPTER-3

METHODS OF VOLTAGE STABILITY ANALYSIS

3.1 Introduction

In past study projects, numerous analysis techniques have been suggested to provide a good overview of voltage stability to assess the power system network in working circumstances and to develop suitable monitoring procedures for preventing it from voltage instability. The most suitable and widely use method for finding the maximum loading is P-V and Q-V curve. The P-V and Q-V curve can be drawn by using load flow calculations. The loading margin can be found by using these curves that is the margin between the operating point to the critical point. P-V curve gives the active loading (P) margin and Q-V curve gives the reactive power (Q) margin at the particular operating point [12].

At the critical point or voltage collapse point the convergence problem occurs in the power flow solution. So, to mitigate this load flow convergence problem many of voltage stability indicators are proposed to find the critical line and critical bus in a large power system network. These indices are also based on load flow equations.

3.2 P-V curve

Real Power (P) margin is calculated with the help of P-V curve [49]. P-V curve gives the relation between the active load and voltage at the load bus. The power transfer phenomenon from one bus to another bus can be studied with the help of P-V curve. The power flow solution is required for P-V curve to find the voltage (V) value at respective bus for the different loading condition at a fixed power factor.

$$P = P_o (1 + \lambda) \tag{3.1}$$

P_o is active power at the bus after base case power flow solution, λ is the loading factor by which the active power increment done.

For different active power loading we have to observe voltage value V at the load bus after run the power flow program and draw the characteristic curve between the P and V. The active power margin is the difference of active powers of base case and the active power at the critical point or maximum loading point where the voltage collapse occurs. The typical P-V curve is shown in figure 3.1

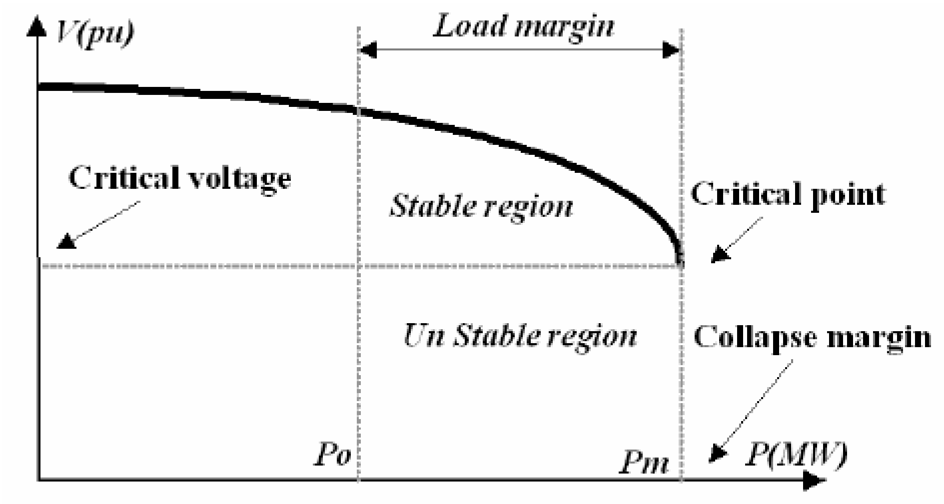

Figure 3.1: Typical P-V curve

3.3 Q-V curve

Q-V curve gives the relation between Reactive power (Q) and voltage (V). Reactive Power (Q) margin is calculated with the help of Q-V curve [48-49]. It can be predicted that voltage stability of a system is maintained or not by using Q-V curve. It shows the injected reactive power (Q) and missing reactive power so that we can take necessary action to prevent the voltage instability. Many of the researchers are used Q-V curve to identify the voltage collapse point and design the system according to that.

The power flow solution is required to find the voltage value at load bus for different reactive power loading with constant active loading.

$$Q = Q_o (1 + \lambda) \qquad (3.2)$$

Q_o is active power at the bus after base case power flow solution, λ is the loading factor by which the reactive power loading increment.

For different reactive power loading we have to observe voltage value V at the load bus after run the power flow program and draw the characteristic curve between the Q and V. The reactive power margin is the difference between voltage axis position and critical point where slope of Q-V curve become zero. The typical P-V curve is shown in figure 3.2

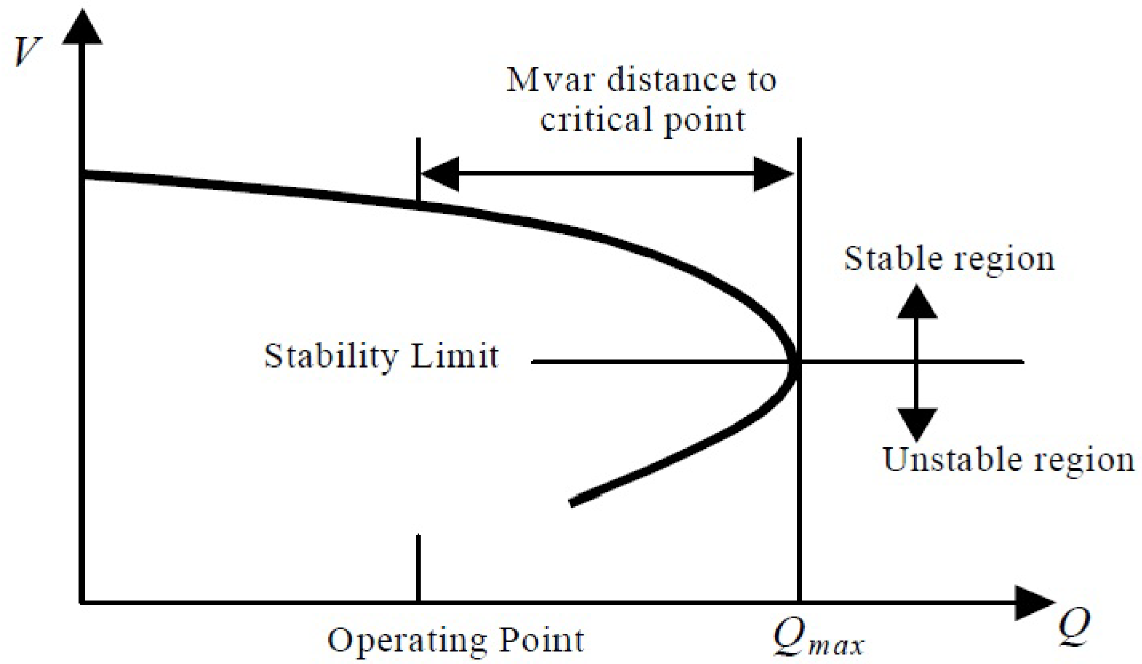

Figure 3.2: Typical Q-V curve

3.4 Disadvantages of P-V and Q-V curve

- The above both methods gives the information for a single bus at a time as per the load variation, so it is difficult to find the critical bus simultaneously. The load flow solution is done for every bus which is time taking for a big power system network.
- The convergence issue occurs in the load flow solution when the load increasing on the load bus and reaches up to the voltage collapse point.
- The cause of voltage instability can't be determined by these curves.

3.5 Minimum singular value of load flow jacobian method

This method is proposed by Thomas and Lof [13] to find the voltage collapse point. It is an index based on determinant of jacobian matrix. When load on load bus increases and voltage reaches to the collapse point at this critical loading power flow has no solution and determinant of jacobian matrix become zero i.e. it becomes singular matrix. The value of jacobian matrix consistently decreasing when loading increases. This method provides an approximate solution for voltage collapse point, the reason for voltage instability, critical line and critical buses can't identify by this method. The behavior of the network is nonlinear from the actual operating condition to the critical operating condition so that this method can't give a linear mechanism to voltage instability point.

3.6 CPF analysis/ continuation power flow method

A predictor corrector system is used in order to locate a remedy [50] is the principle behind the continuity power flow. A tangent predictor is used by a recognized foundation method to predict the next alternative for a specific load increase model.

The corrector step is then provided by a standard power flow with the exact solution.

A new forecast depending on the fresh tangent vector is then expected and a correction step is implemented. This method proceeds until it reaches a critical stage. The location where the vector tangent becomes a null vector is the collapse point.

3.7 Voltage stability indices

The voltage instability condition can be identified by using voltage stability indices. They are taking very less time for calculation and prediction of voltage stability criteria. These indices are based on the power flow solution method and capable to identify the critical bus, critical line, voltage collapse point for voltage instability in a large power system network at a given operating conditions. They are less complex in use and can be used for online or offline studies of power system network.

There are various indices are proposed by the many of researchers to assess the voltage stability. The popular indices are as follow:

3.7.1 Line Stability Index (L_{mn})

In [32], Moghavemmi proposed L_{mn} for a single line based on power flow principle as below figure:

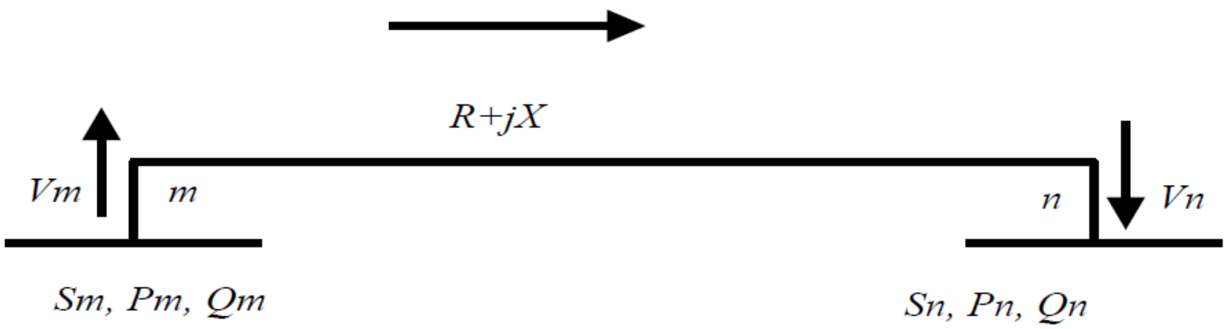

Figure3.3: single line representation of a large power system

Where P_m and P_n are the active power at m and n bus respectively, Q_m and Q_n are the reactive power at m and n bus respectively, S_m and S_n are the complex power at m and n bus respectively and V_m and V_n are the voltage at m and n bus respectively. R is the line resistance and X is the line reactance.

The line stability index (L_{mn}) for the above network is given as-

$$L_{mn} = \left(\frac{4XQ_n}{[V_m Sin(\theta - \delta)]^2} \right) \tag{3.3}$$

For the stability of system the roots of the voltage quadratic equation must be positive or equal to zero. According to this index the line is stable if value of index L_{mn} is lies between 0 to 1. If value of L_{mn} is equal to 1 then it will be a critical for greater than 1 it will be unstable line. If the value of L_{mn} comes leass than 0 then roots are become imaginary it shows that the system is unstable.

3.7.2 L- Index

P. Kessel and H. Glavitsch [30] proposed L- index to assess the voltage stability, which based on single line model and extended for a big network. For a voltage stable system value of L -index is lies between 0 and 1. The L index is derived from the roots of voltage quadratic equation which is obtained from the complex power flow equations. For the system having n number of buses where j numbers non generator bus (PV bus), the generalized L-index is given as below

$$L_j = \left| 1 - \sum_{i=1}^{i=j} F_{ji} \left(\frac{V_i}{V_j} \right) \right| \tag{3.5}$$

Where L_j is the L-index, V_i and V_j are the PV bus and load bus voltages respectively and F_{ji} can be derived from the Y bus matrix of the given power system network.

$$\begin{bmatrix} I_g \\ I_l \end{bmatrix} = \begin{bmatrix} Y_{gg} & Y_{gl} \\ Y_{lg} & Y_{ll} \end{bmatrix} \begin{bmatrix} V_g \\ V_l \end{bmatrix} \tag{3.6}$$

Where subscripts g and l are used to represent the generator bus and load bus respectively for voltage current and related Y bus admittance elements. After rearrangement of above equation, it becomes:

$$\begin{bmatrix} V_l \\ V_g \end{bmatrix} = \begin{bmatrix} Z_{ll} & F_{lg} \\ K_{gl} & Y_{gg} \end{bmatrix} \begin{bmatrix} I_l \\ I_g \end{bmatrix} \tag{3.7}$$

Where $F_{lg} = -[Y_{ll}]^{-1}[Y_{lg}]$

3.7.3 LQP index

LQP index is proposed by A. G. Mohamed [33] to evaluate the voltage stability. This is obtained from the quadratic equation of power, the concept is similar to L_{mn} [32] & FVSI [34] indices. This is derived for single line model with placing the discriminate of power quadratic equation equal to zero or greater zero. This index is also valid for the large power system network as below given generalized form:

$$LQP = 4\left(\frac{X}{V_s^2}\right)\left(\frac{X}{V_s^2} + P_s + Q_r\right) \tag{3.8}$$

Where V_s is the voltage at sending end bus.

X is the line reactance.

P_s is the active power at sending end bus.

Q_r is the reactive power at receiving end bus.

The threshold value of LQP index in ‘1’ for the stability of a power system for each line. Whenever it become greater than 1 then voltage instability occurred in the system and respected lines become unstable.

3.7.4 Fast Voltage Stability Index (FVSI)

This is most popular index to determine the voltage stability and it is proposed by Musirin [34]. It also predicts the line stability and based on power flow concept for the single line model. This index is originated from the roots of voltage quadratic equation. The stability index is given as follow-

$$FVSI_{ij} = \frac{4Z^2{}_{ij}Q_j}{V^2{}_iX_{ij}} \tag{3.4}$$

Where V_i is the sending end bus voltage, Q_j is the reactive power at the receiving end bus, X_{ij} is the line reactance and Z_{ij} is the line impedance.

The critical value of FVSI is 1, if FVSI >1 then line become unstable. For stable condition of line, the value of FVSI must be less than 1. FVSI is also capable to identify the critical line and bus according to the maximum loadability limit on a particular bus.

Modeling of FVSI for two bus power system is as follow:

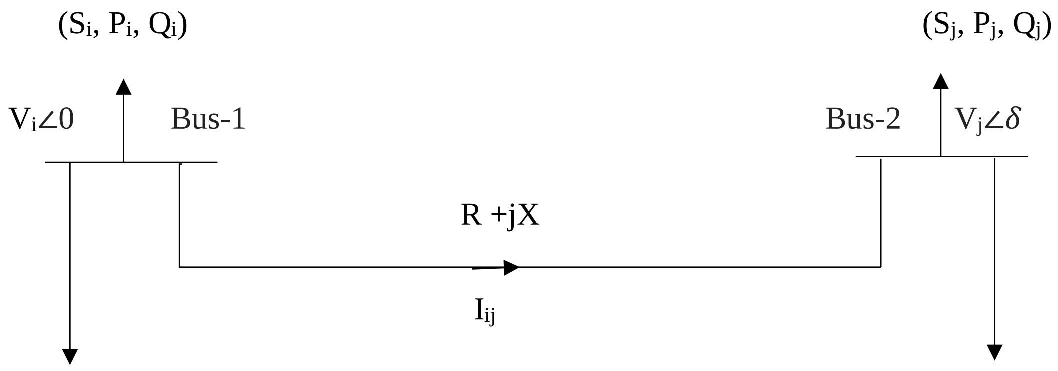

Figure.3.4: Two-bus power system model

In figure 3.4

V_i, V_j = Voltages on sending and receiving end buses respectively.

P_i, Q_j = Active and reactive power on the sending end bus.

P_i, Q_j = Active and reactive power on the receiving end bus.

S_i, S_j = apparent power on the sending and receiving end bus respectively.

δ = angle difference between sending and receiving buses.

I_{ij} = Current flow between the line.

R = resistance of the line.

X = Reactance of the line.

As we know that apparent power

$$S_j^* = (P_j + jQ_j)^* = V_j^* I_j \tag{3.5}$$

$$I_{ij} = (P_j + jQ_j)^* / V_j^* \tag{3.6}$$

$$V_j\angle\delta + (P_j + jQ_j)^* \frac{R+jX}{V_j\angle-\delta} = V_i\angle 0 \tag{3.7}$$

$$V_j^2 + (P_j - jQ_j)(R + jX) = V_i V_j \angle -\delta$$

$$V_j^2 + (P_j R + jP_j X - jQ_j R + Q_j X) = V_i V_j \cos\delta - jV_i V_j \sin\delta$$

Equating real and imaginary parts-

$$V_j^2 + (P_j R + Q_j X) = V_i V_j \cos\delta \tag{3.8}$$

&

$$P_j X - Q_j R = -V_i V_j \sin\delta \tag{3.9}$$

So $$P_j = \frac{Q_j R}{X} - V_i V_j \frac{\sin\delta}{X}$$

From equation (3.8)

$$V_j^2 + R\left(\frac{Q_j R}{X} - V_i V_j \frac{\sin\delta}{X}\right) + Q_j X = V_i V_j \cos\delta$$

$$V_j^2 - V_iV_j\left(\frac{R}{X}Sin\delta + Cos\delta\right) + \left(X + \frac{R^2}{X}\right)Q_j = 0$$

$$V_i = \frac{V_i\left(\frac{R}{X}Sin\delta + Cos\delta\right) \pm \sqrt{\left[\left(V_i\left(\frac{R}{X}Sin\delta + Cos\delta\right)\right)^2 - 4\left(X + \frac{R^2}{X}\right)Q_j\right]}}{2} \tag{3.10}$$

For root must be real & discriminate in above equation

$$\left(V_i\left(\frac{R}{X}Sin\delta + Cos\delta\right)\right)^2 - 4\left(X + \frac{R^2}{X}\right)Q_j \geq 0$$

Since Sinδ is very small so Sinδ = 0 & Cosδ = 1 then

$$V_i^2 - 4\left(X + \frac{R^2}{X}\right)Q_j \geq 0$$

$$\frac{1 - 4\left(X + \frac{R^2}{X}\right)Q_j}{V_i^2} \geq 0$$

$$\frac{4\left(X + \frac{R^2}{X}\right)Q_j}{V_i^2} \leq 1$$

For generalized it, taking ‘j’ as the receiving bus and ‘i’ as the sending bus, we obtained the fast voltage stability index (FVSI) same as equation 3.4.

$$FVSI_{ij} = \frac{4Z^2{}_{ij}Q_j}{V^2{}_iX_{ij}}$$

The following are the conditions of above FVSI index:

- Any line in the system that exhibits FVSI close to 1.00 indicates that the particular line is approaching to its instability point hence may lead to system violation.
- Therefore, FVSI has to be maintained less than unity in order to maintain a stable system.

- When the FVSI of a line approaches unity it means that the line is approaching its stability limits.
- The FVSI of all the lines must be lower than 1 to assure the stability of power system.

3.7.5 New Voltage Stability Index (NVSI)

NVSI index has been explained by author in paper [51], The voltage stability is depended on reactive power available in system. If the indices are calculated from reactive power and active power then it is also depended on the resistance and reactance of the line. But the resistance of the transmission line is very less so a new index named as New voltage Stability Index has been derived with taking the resistance of the transmission line as neglected.

The NVSI is derived from the discriminate and real roots of quadratic equation of voltage at receiving end bus while taking resistance of the transmission line is neglected is comes as:

$$NVSI_{ij} = \frac{2X\sqrt{\left(P_j^2 + Q_j^2\right)}}{2Q_jX - V_i^2} \tag{3.16}$$

To maintain the stability in transmission line the value of NVSI must be less than ‘1’, if value of NVSI index is become ‘1’ or greater than ‘1’then it will be unstable line and there are voltage instability in the power system network.

3.7.6 Line Voltage Stability Index (LVSI)

This index is proposed by [52], This index represents the relation between real power and voltage at the receiving end bus. It is obtained from the discriminate of the voltage quadratic equation for equal to or greater than '0'condition. The LVSI index is given as:

$$LVSI_{ij} = \frac{4RP_j}{[V_i Cos(\theta - \delta)]^2} \quad (3.17)$$

Here θ is the impedance angle of transmission line.

The threshold value of LVSI for the stability of line is also '1'. is LVSI ≥ 1 then line become unstable.

Drawback of LVSI:

- It is seen from the LVSI formula that it depends on the resistance of the line so LVSI index is failed to predict the voltage stability of those line having zero resistance or very less value of resistance.
- The LVSI index is more sensitive to δ so some time it shows instability in healthy line.

3.7.7 Line Collapse Proximity Index (LCPI)

The line charging reactance play the important role in voltage stability but according to the previously explained indices it has neglected, so it is difficult to identify the exact voltage instability or voltage collapse point for a large power system. In view of this an index named Line collapse Proximity Index has been proposed by Rajive Tiwari , K.R. Niazi & Vikas Gupta [35].

$$LCPI_{ij} = \frac{4Acos\alpha(P_j Bcos\beta + Q_j Bsin\beta)}{[V_i Cos\delta]^2} \quad (3.18)$$

For maintain the voltage stability of the power system network LCPI < 1.

This index is explained in detail in chapter-4.

CHAPTER 4

MODELING OF LINE COLLAPSE PROXIMITY INDEX (LCPI)

4.1 Introduction

The Line Collapse Proximity Index (LCPI) approach [35] is a static method to assess the voltage stability. This static approach is taking very less time for computation of whole analysis of a large power system because of no need of repeated power flow solution. The shunt branch reactance and line resistance of transmission line take into consideration for the calculation of ABCD parameter of transmission line. The LCPI is based on ABCD parameter, active power, reactive power, voltage and its angle hence it is clear that LCPI index provides more accurate results for voltage instability with respect to the other indices. The line charging admittance provides support for reactive power and its influence is seen in voltage stability analysis due to neglecting this fact in other indices they provide pessimistic results to assess the voltage stability. The direction of real power flow with respect to the reactive power flow is also take into consideration for evaluation of LCPI so its accuracy is always high in comparison to the other indices.

4.2 Mathematical expression of LCPI

The exact equivalent model of transmission line is derived from the π-model of two port network with help of ABCD parameters. The π-model of two bus system (as figure 3.1) is shown in figure 4.1.

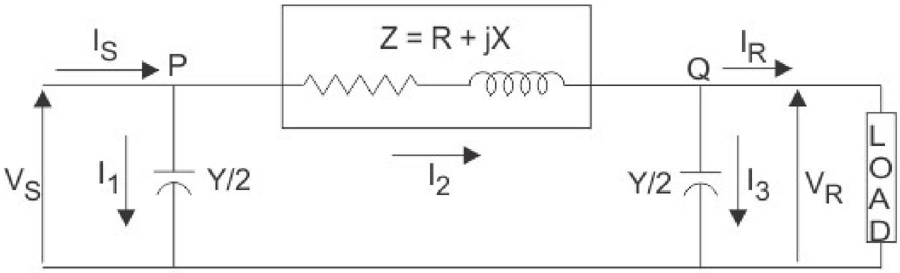

Figure 4.1: π-model of transmission line one-line diagram.

The equation of sending end voltage and current are:

$$V_S = AV_R + BI_R \tag{4.1}$$

$$I_S = CV_R + DI_R \tag{4.2}$$

It can be express in matrix form as:

$$\begin{bmatrix} V_S \\ I_S \end{bmatrix} = \begin{bmatrix} A & B \\ C & D \end{bmatrix} \begin{bmatrix} V_R \\ I_R \end{bmatrix} \tag{4.3}$$

Where A,B,C & D are the transmission line π-model parameters of two port network. These are described as:

$$A = \left(1 + \frac{YZ}{2}\right) \tag{4.4}$$

$$B = Z \tag{4.5}$$

$$C = Y\left(1 + \frac{YZ}{4}\right) \tag{4.6}$$

$$D = A \tag{4.7}$$

The ABCD are the complex variables, Z is the line impedance and Y is the line charging admittance for the relative line of transmission network.

We know the complex power conjugate at the receiving end of transmission line is expressed as:

$$S_R^* = V_R^* I_R = P_R - jQ_R \tag{4.8}$$

Or

$$I_R = \frac{(P_R - jQ_R)}{V_R^*} = \frac{(P_R - jQ_R)}{V_R\angle -\delta_R} \tag{4.9}$$

Now we can write the equation of sending end voltage by using equation (4.1)

$$V_S\angle\delta_s = A\angle\alpha \,.\, V_R\angle\delta_R + \mathrm{B}\angle\beta \,.\, I_R\angle 0 \tag{4.10}$$

Put the values of I_R from equation (4.9) to equation (4.10)

$$V_S\angle\delta_s = A\angle\alpha \,.\, V_R\angle\delta_R + \mathrm{B}\angle\beta \,.\, \frac{(P_R - jQ_R)}{V_R\angle -\delta_R} \tag{4.11}$$

After rearranged the equation (4.11) we get

$$V_S V_R\angle\delta = A\angle\alpha \,.\, V_R^2 + \mathrm{B}\angle\beta \,.\, (P_R - jQ_R) \tag{4.12}$$

Where $\delta = \delta_S - \delta_R$

After separating the real and imaginary part in above equation we get the quadratic equation for voltage

$$V_R^2(Acos\alpha) - V_R(V_S cos\delta) + (P_R Bcos\beta + Q_R Bsin\beta) = 0 \tag{4.13}$$

The roots of above equation are given as

$$V_R = \frac{-V_S cos\delta \pm \sqrt{(V_S cos\delta)^2 - 4Acos\alpha(P_R Bcos\beta + Q_R Bsin\beta)}}{2Acos\alpha} \tag{4.14}$$

The roots of voltage quadratic equation must be real and non-zero to maintain the stability of the system. this requirement is fulfilling when square root part of the above roots are positive i.e.

$$(V_S cos\delta)^2 - 4Acos\alpha(P_R Bcos\beta + Q_R Bsin\beta) > 0 \tag{4.15}$$

To avoid the voltage instability the following condition is obtained from the equation (4.15)

$$\frac{4Acos\alpha(P_R Bcos\beta+Q_R Bsin\beta)}{(V_S cos\delta)^2} < 1 \quad (4.16)$$

Hence, we can define the LCPI as

$$LCPI = \frac{4Acos\alpha(P_R Bcos\beta+Q_R Bsin\beta)}{(V_S cos\delta)^2} \quad (4.17)$$

From the equation 4.17 it is clear that for maintaining the voltage stability of the power system LCPI value of each transmission line must be less than ‘1’.

In the above expression of LCPI Bcosβ and Bsinβ representing the resistive and reactive drop of transmission line respectively due to flow of active and reactive power P_R and Q_R respectively. Transmission line parameter A & B consists the resistive and line charging admittances of system, which are neglected in other indices. LCPI is also consider the magnitude and direction of real and reactive power flow.

When the index LCPI value become nearer to the unity It represents the critical transmission line of the power system. for more than unity value of LCPI voltage instability is arise in the system and the respected transmission line is unstable.

According to the value of LCPI value we can predict the required reactive power compensation to improve the voltage stability of the system. To find the appropriate bus for reactive power compensation here we are using Particle Swarm Optimization (PSO) technique.

4.3 Particle Swarm Optimization (PSO) technique

The Particle Swarm Optimization (PSO) is proposed by Eberhart and Kennedy in 1992 [36]. It is a nonlinear technique based on probability concept, hence it is a stochastic approach. It is inspired by natural process like bird's swarm for searching food in a search space without knowing the exact location of food, behavior of fish schooling etc. here particle is just like a bird for finding the best solution. Every individual particle has a current position and velocity at a particular time in search space and swarm randomly, they can change their position by tuning the velocity. The velocity is depending upon the feedback of neighborhood particle and its past experience. The process for searching the best location is artificially designed for non-linear type optimization problem. For the defined objective function all particles have a fitness value. All the particle has their best value known as personnel best (P-best), they also know the group best performance value known as g-best. The particles adjust their velocity and acceleration according to the p-best and g-best value of individual best and group best respectively. The flow chart of PSO is given in figure 4.2.

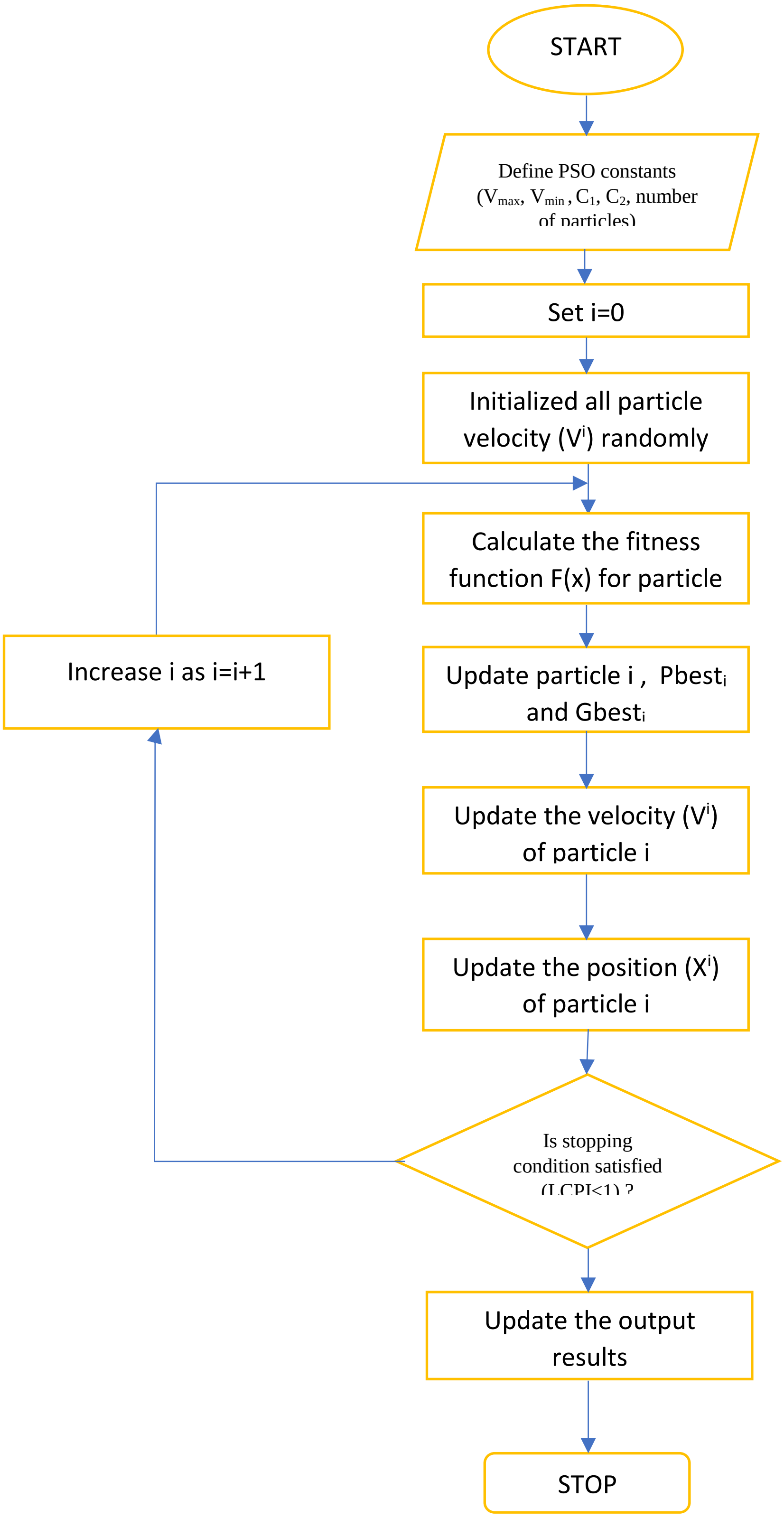

Figure 4.2: Flow Chart of Particle Swarm Optimization technique used for the improvement of voltage stability.

4.3.1 Mathematical formulation of PSO:

Velocity

$$V^{i+1} = V^{i} + C_1 * rand(0,1) * (Pbest_i - X_i) * C_2 * rand(0,1) * (Gbest_i - X_i) \quad (4.18)$$

Position $X^{i+1} = X^{i} + V^{i+1}$ (4.19)

Fitness Function $F = (0.2 - LCPI)^2$ (4.20)

To find proper optimum location and rating of reactive power shunt compensation device [37], we are using PSO technique here as per the following steps:

Step-1: Check weather voltage instability in the system is occurred or not if occurred than only go for step-2 otherwise stop the program.

Step-2: Select the range of shunt compensation ± 600 MVAR as a search space for particles of PSO.

Step-3: Define the length as the number of load buses in the system.

Step-4: Defining the parameters of PSO as

Particles = 50

C_1 = 2.05

C_2 = 2.05

V_{min} = =-0.01* length of search space.

V_{max} = -V_{min}

Step-4: For every particle generate the population and run load flow program.

Step-5: After avoiding the generator buses for reactive power compensation check the fitness function value.

Step-6: Select Pbest and Gbest.

Step-7: According to the above results improve the velocity and position of particles to optimized the fitness function.

Step-8: Select no of iteration (here 50 iteration is selected) and update Pbest and Gbest regularly to optimize the fitness function.

Step-9: Select the optimum buses for reactive power compensation with optimum MVAR rating as per the result of PSO [39].

Step-9: After placing the reactive power compensation observe the improvement in voltage stability.

In the next section we have seen that the PSO is a useful technique to improve voltage stability according to the LCPI index and also compare with other indices.

CHAPTER 5

SIMULATION RESULTS AND DISCUSSION

The voltage stability indices LCPI[35], FVSI[34], Lmn[32] and LQP[33] have been calculated on Matlab7.0 environment for different operating conditions of IEEE-30 bus system and IEEE-118 bus system and compared each other. The loading factor (λ) is used for incrementing the load in multiple of the base case loading. All above said indices have the critical value '1', when the value of any index is approach to unity it shows that the respective line is becoming critical and there are voltage instability in the system.

For the simulation on MATLAB10^{-12} tolerance is taken for convergence of power flow solution and absolute bus power mismatch. The simulation is done for various loading conditions like base case loading, heavy MVA loading, heavy active loading, heavy reactive loading (for complete network and on single bus also). For both systems IEEE-30 bus and IEEE-118 bus we have find the critical lines under the said loading conditions. As per the LCPI Index raking of critical lines is done under various operating conditions and line outage contingency cases and compare with other three indices. Maximum loadability limit is verified from the P-V and Q-V curves.

For IEEE-30 bus system we have predicted the required reactive power for shunt compensation to improve the voltage stability of power system whenever any line goes under unstable state. The optimum bus for shut compensation is determined by the particle swarm optimization (PSO) technique. The improved results after the shunt compensation has been discussed in the following sections.

The flow chart for calculation of LCPI value and LCPI value with shunt compensation are shown in figure 5.1 and figure 5.2 respectively.

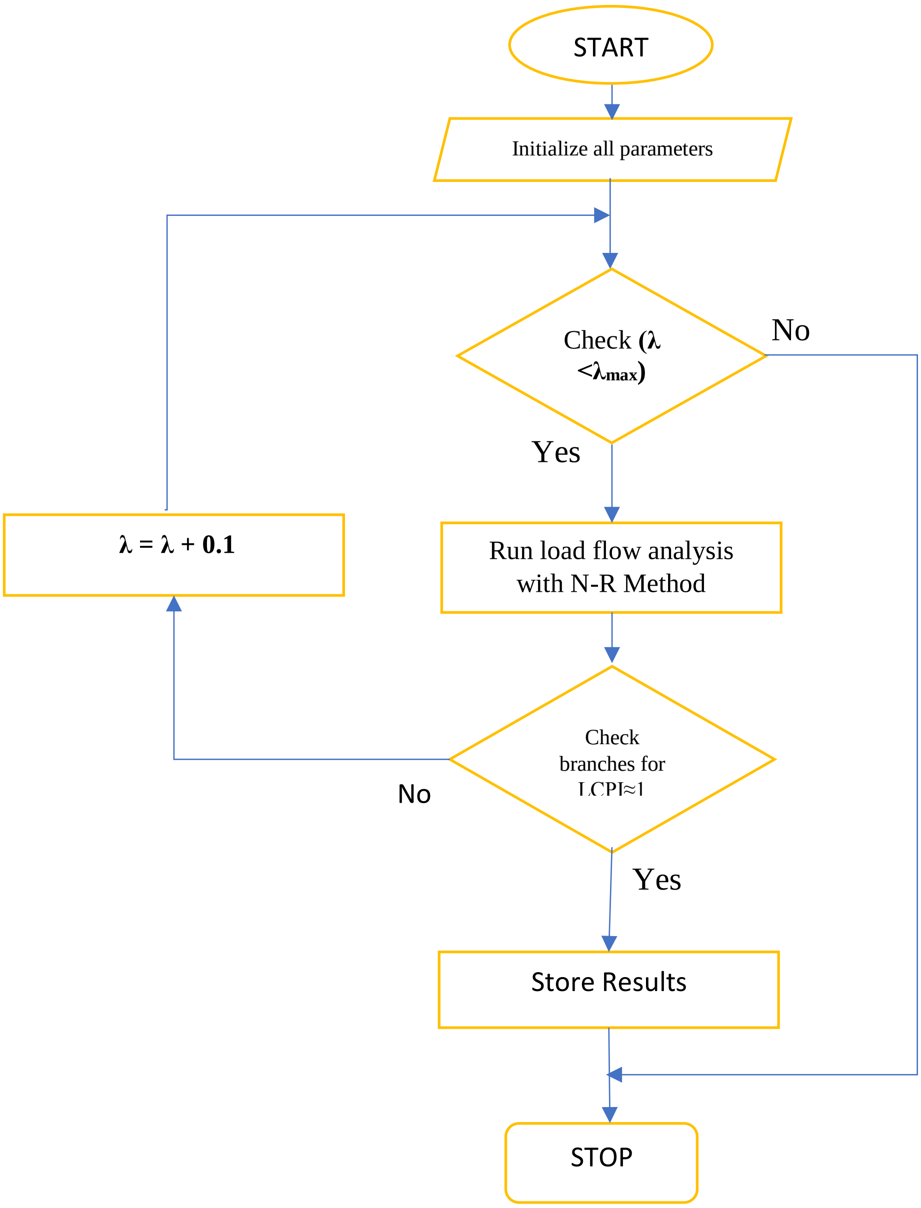

Figure 5.1: Flow Chart of LCPI index calculation.

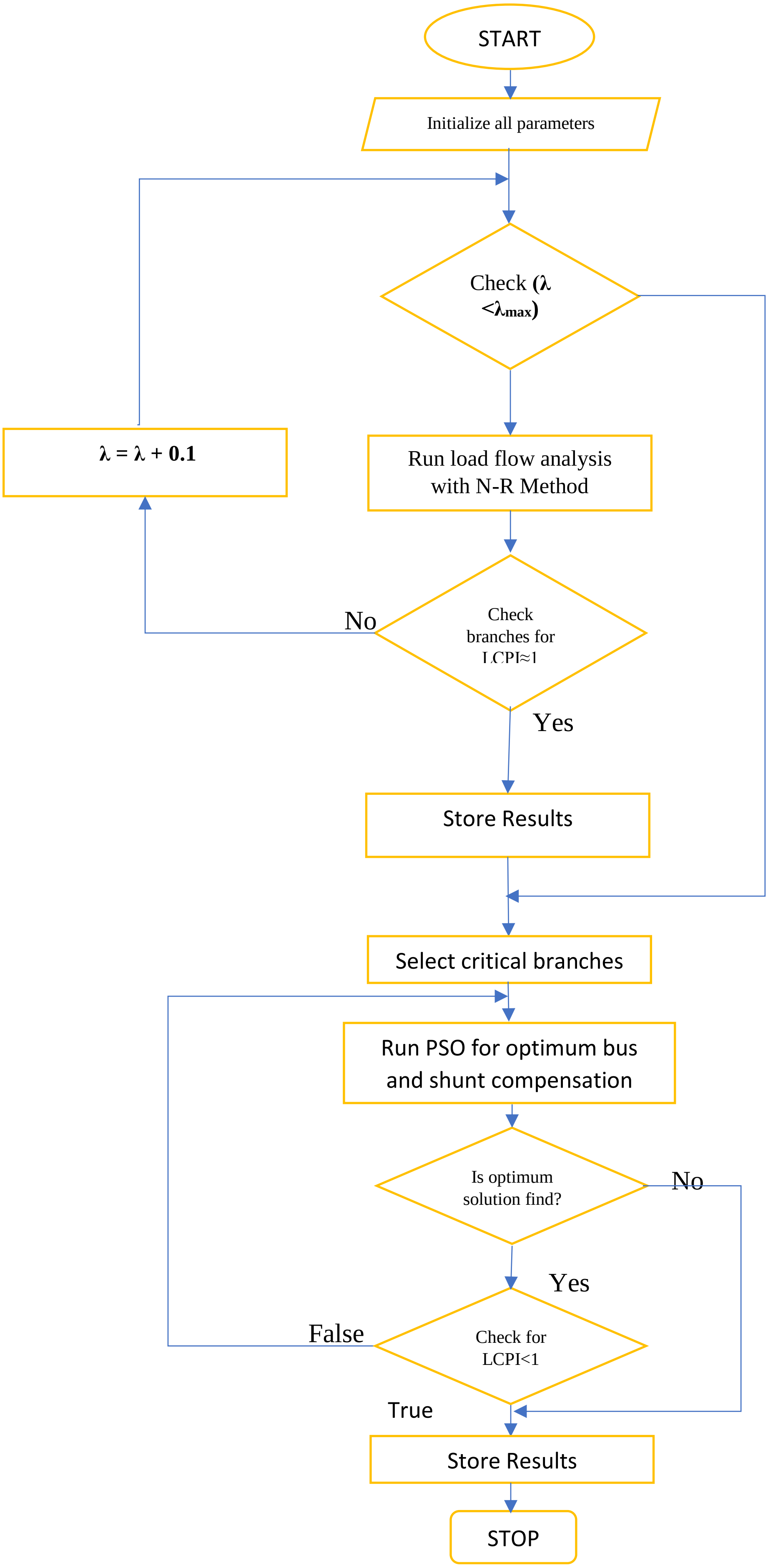

Figure 5.2: Flow Chart of Particle Swarm Optimization technique used for Shunt compensation and LCPI calculation.

The voltage stability analysis for all cases on IEEE-30 and IEEE-118 bus system are as follow:

5.1 IEEE-30 Bus System

The IEEE-30 bus system [52] have 6 numbers generator bus, 24 numbers load buses. The base MVA is 100 MVA. The voltage indices have been calculated on IEEE-30 bus for different operating conditions discussed in following sections.

5.1.1 IEEE-30 bus base case loading

The calculated value of all indices for the base case loading (**λ=1p.u.**) has been shown in Table 5.1. The branch number is representing the serial number of lines which are connected between from bus & to bus. All column of table are sorted according to the LCPI index value in descending order.

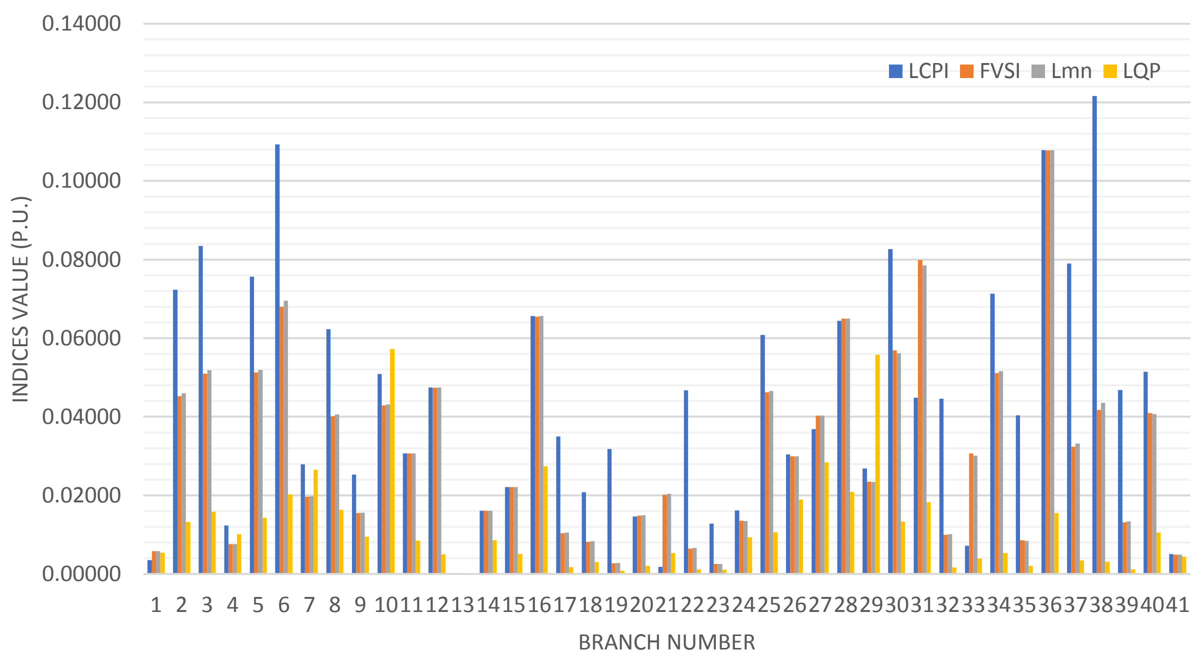

Figure5.3: Indices graph for IEEE-30 bus base case loading.

Table 5.1: IEEE 30 Bus base case loading λ=1p.u.						
Branch Number	**From Bus**	**To Bus**	**LCPI**	**FVSI**	**Lmn**	**LQP**
38	27	30	0.12164	0.04172	0.04356	0.00308
6	2	6	0.10930	0.06801	0.06957	0.02023
36	28	27	0.10782	0.10775	0.10782	0.01553
3	2	4	0.08350	0.05095	0.05186	0.01582
30	15	23	0.08264	0.05690	0.05620	0.01329
37	27	29	0.07898	0.03237	0.03317	0.00346
5	2	5	0.07565	0.05125	0.05194	0.01430
2	1	3	0.07232	0.04529	0.04596	0.01321
34	25	26	0.07135	0.05109	0.05162	0.00535
16	12	13	0.06565	0.06546	0.06565	0.02742
28	10	22	0.06438	0.06496	0.06498	0.02085
8	5	7	0.06231	0.04013	0.04060	0.01633
25	10	20	0.06082	0.04620	0.04655	0.01064
40	8	28	0.05143	0.04092	0.04072	0.01056
10	6	8	0.05085	0.04293	0.04310	0.05723
12	6	10	0.04742	0.04741	0.04742	0.00498
39	29	30	0.04677	0.01317	0.01340	0.00114
22	15	18	0.04673	0.00648	0.00662	0.00119
31	22	24	0.04487	0.07989	0.07850	0.01827
32	23	24	0.04457	0.00993	0.01011	0.00162
35	25	27	0.04038	0.00856	0.00843	0.00205
27	10	21	0.03683	0.04025	0.04032	0.02842
17	12	14	0.03501	0.01038	0.01051	0.00175
19	12	16	0.03177	0.00275	0.00280	0.00084
11	6	9	0.03065	0.03065	0.03065	0.00846
26	10	17	0.03040	0.02995	0.02995	0.01891
7	4	6	0.02788	0.01968	0.01976	0.02652
29	21	22	0.02683	0.02346	0.02343	0.05574
9	6	7	0.02531	0.01551	0.01559	0.00949
15	4	12	0.02210	0.02210	0.02210	0.00507
18	12	15	0.02079	0.00819	0.00831	0.00301
24	19	20	0.01614	0.01353	0.01351	0.00930
14	9	10	0.01605	0.01605	0.01605	0.00859
20	14	15	0.01460	0.01489	0.01490	0.00210
23	18	19	0.01284	0.00257	0.00259	0.00109
4	3	4	0.01231	0.00756	0.00758	0.01015
33	24	25	0.00722	0.03068	0.03012	0.00392
41	6	28	0.00510	0.00494	0.00494	0.00438
1	1	2	0.00350	0.00577	0.00580	0.00537
21	16	17	0.00183	0.02014	0.02037	0.00533
13	9	11	0.00000	0.00000	0.00000	0.00017

Table 5.1 and figure5.3 shows that all indices value are very less with respect to the critical limit ‘1’. Hence simulation for voltage stability analysis for IEEE-30 bus system is working good as the stability of base case loading is proven. The FVSI, Lmn and LQP indices are giving lower value with respect to the LCPI index, but for some branches like as 11,12,14,15,16 LCPI, FVSI and Lmn have same value It is happened due to the direction of active and reactive power flow. The LCPI index considering shunt reactance of each line (based on ABCD parameter) and direction of active and reactive power flow, when the direction of both active and reactive power flow in the same direction then resistive and reactive drops are added together and index value become high. When the shunt admittances and resistance of any branch is zero then the resistive drop in the line due to the active power flow is zero so LCPI index values are equal to the other indices as seen in table 5.1 for branches 11,12,14,15 &16.

5.1.2 IEEE-30 bus heavy MVA loading

The MVA loading means loading on both active power (P) and reactive power(Q) at a bus increase simultaneously with multiple of loadability factor(λ) as follow

$$P = \lambda P_0$$

$$Q = \lambda Q_0$$

Where P_0 and Q_0 are the base case active and reactive power loading respectively

The heavy MVA loading on all load bus with loadability λ = 3.1 p.u. is implemented and results are given in table 5.2 and figure 5.4. It is seen than branch number 23 become unstable according to the LCPI, FVSI and Lmn index but it is still stable as per LQP index. Branch number 28 become critical according to the LCPI and Lmn index, but according to the FVSI it is marginable stable. As the introduction of shunt admittance into the LCPI is providing accurate result for the voltage stability analysis.

Table 5.2: IEEE 30 Bus base test system with heavy MVA loading without shunt compensation λ = 3.1 p.u.

Branch Number	From Bus	To Bus	LCPI	FVSI	Lmn	LQP	Remarks
23	18	19	1.28674	1.23414	1.28674	0.28062	
28	10	22	0.96142	0.87740	0.96142	0.22052	
37	27	29	0.66822	0.61177	0.66822	0.25828	
11	6	9	0.54177	0.23663	0.30235	0.08730	
15	4	12	0.49892	0.26821	0.31712	0.07411	
2	1	3	0.48425	0.46392	0.48425	0.24603	
17	12	14	0.42794	0.51824	0.54140	0.26173	Line no. 23 is become unstable and line number 28 is critical
3	2	4	0.39752	0.25889	0.28567	0.08519	
33	24	25	0.37987	0.12598	0.14832	0.14848	
14	9	10	0.37141	0.37024	0.37141	0.29337	
12	6	10	0.34991	0.01640	0.02229	0.15345	
1	1	2	0.31627	0.42692	0.45149	0.28032	
5	2	5	0.31439	0.15752	0.17361	0.10628	
41	6	28	0.27543	0.27696	0.27727	0.20256	
18	12	15	0.26027	0.11456	0.12473	0.14545	
40	8	28	0.25817	0.25591	0.25817	0.26718	
16	12	13	0.23391	0.19133	0.19610	0.02050	
20	14	15	0.23270	0.16650	0.17265	0.14118	
35	25	27	0.21846	0.12716	0.13394	0.13158	
26	10	17	0.19585	0.28350	0.29657	0.33694	
21	16	17	0.16498	0.04847	0.05172	0.15396	
22	15	18	0.15767	0.06581	0.06924	0.14635	
19	12	16	0.15239	0.16045	0.15978	0.12126	
24	19	20	0.15239	0.14653	0.14698	0.13186	
4	3	4	0.15212	0.04714	0.04495	0.16815	
30	15	23	0.11956	0.05011	0.05221	0.10819	
7	4	6	0.11431	0.10320	0.10380	0.09924	
36	28	27	0.10939	0.40983	0.50987	0.52713	
29	21	22	0.10390	0.11750	0.11829	0.42653	
10	6	8	0.09274	0.02431	0.02595	0.16223	
25	10	20	0.08529	0.00771	0.00811	0.15993	
32	23	24	0.06560	0.03982	0.03933	0.17979	
38	27	30	0.06244	0.06684	0.06670	0.12920	
27	10	21	0.06000	0.14683	0.15338	0.17439	
6	2	6	0.04842	0.02927	0.03064	0.18847	
31	22	24	0.04450	0.01663	0.01688	0.15346	
34	25	26	0.03199	0.14763	0.16321	0.20326	
9	6	7	0.02866	0.09687	0.09136	0.14609	
39	29	30	0.02015	0.07298	0.07501	0.17419	
13	9	11	0.00015	0.06195	0.06407	0.19520	
8	5	7	0.00000	0.00000	0.00000	0.15829	

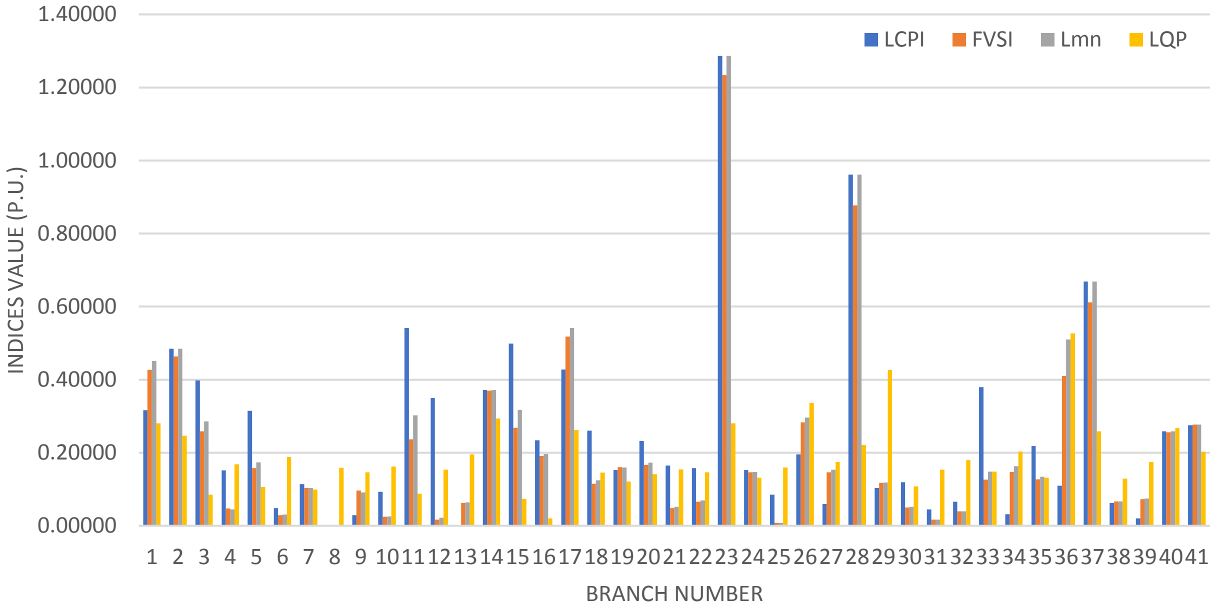

Figure 5.4: IEEE-30 bus heavy MVA loading (λ = 3.1 p.u.) without compensation.

After running the PSO program on the above case of table 5.2 we find the optimum bus location and required MVA capacity for shunt compensation at these locations, the results are shown in table 5.3 and figure5.5.

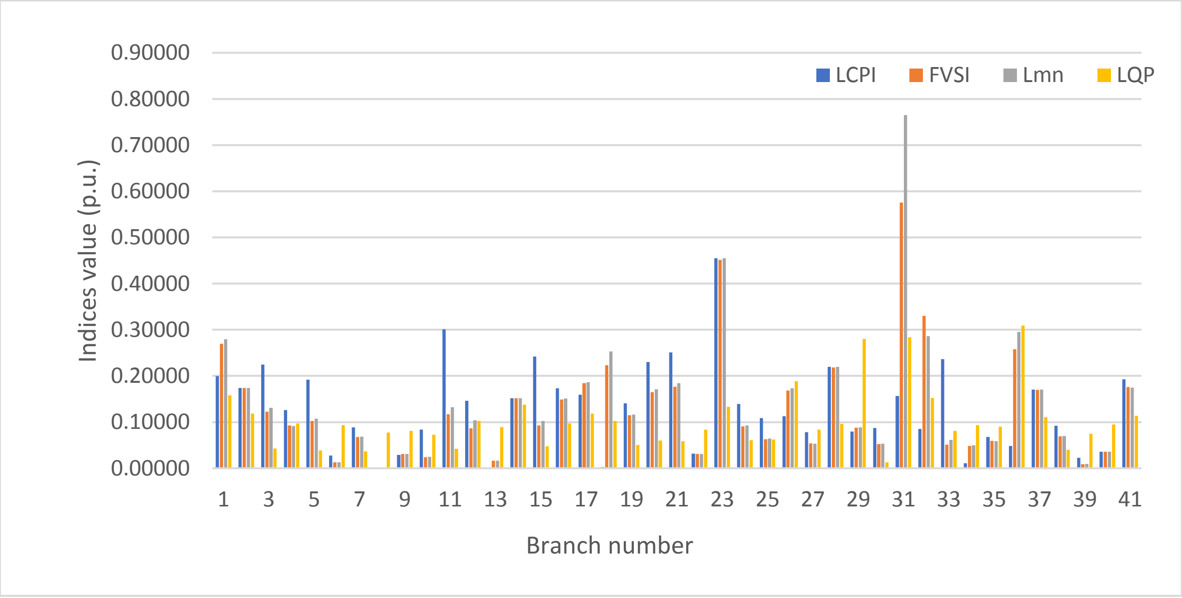

Figure 5.5: IEEE-30 bus heavy MVA loading (λ = 3.1 p.u.) with shunt compensation.

Table 5.3: IEEE 30 Bus base test system with heavy MVA loading and shunt compensation λ = 3.1 p.u.

Branch Number	From Bus	To Bus	LCPI	FVSI	Lmn	LQP	Shunt compensation		Remarks
							Optimum bus location	MVAR capacity (p.u)	
23	18	19	0.45506	0.45171	0.45506	0.13324			
28	10	22	0.21965	0.21865	0.21965	0.09654	10	-0.5352	
37	27	29	0.17076	0.16957	0.17076	0.11108	19	-1.1513	
11	6	9	0.30110	0.11698	0.13234	0.04205	29	0.2178	
15	4	12	0.24203	0.09305	0.10215	0.04795			
2	1	3	0.17396	0.17372	0.17396	0.11824			
17	12	14	0.15967	0.18425	0.18648	0.11816			After shunt compensation system stability improved as shown in LCPI value.
3	2	4	0.22463	0.12278	0.13111	0.04248			
33	24	25	0.23612	0.05142	0.06161	0.08115			
14	9	10	0.15203	0.15161	0.15203	0.13778			
12	6	10	0.14628	0.08679	0.10404	0.10278			
1	1	2	0.19965	0.26946	0.27907	0.15789			
5	2	5	0.19208	0.10227	0.10763	0.03890			
41	6	28	0.19260	0.17604	0.17475	0.11367			
18	12	15	0.00226	0.22312	0.25312	0.10216			
40	8	28	0.03583	0.03580	0.03583	0.09466			
16	12	13	0.17350	0.14891	0.15094	0.09688			
20	14	15	0.23046	0.16490	0.17092	0.06004			
35	25	27	0.06789	0.05913	0.05888	0.09017			
26	10	17	0.11259	0.16859	0.17347	0.18852			
21	16	17	0.25089	0.17652	0.18401	0.05901			
22	15	18	0.03182	0.03130	0.03130	0.08348			
19	12	16	0.14033	0.11479	0.11634	0.05066			
24	19	20	0.13928	0.09056	0.09296	0.06081			
4	3	4	0.12627	0.09286	0.09140	0.09675			
30	15	23	0.08721	0.05221	0.05322	0.01324			
7	4	6	0.08866	0.06769	0.06843	0.03654			
36	28	27	0.04819	0.25794	0.29536	0.30929			
29	21	22	0.07984	0.08795	0.08830	0.28019			
10	6	8	0.08347	0.02385	0.02462	0.07291			
25	10	20	0.10849	0.06279	0.06434	0.06253			
32	23	24	0.08503	0.33027	0.28636	0.15269			
38	27	30	0.09193	0.06887	0.06972	0.03966			
27	10	21	0.07851	0.05397	0.05333	0.08369			
6	2	6	0.02717	0.01283	0.01312	0.09310			
31	22	24	0.15625	0.57589	0.76542	0.28359			
34	25	26	0.01059	0.04845	0.04996	0.09332			
9	6	7	0.02865	0.03097	0.03100	0.08107			
39	29	30	0.02245	0.00911	0.00917	0.07499			
13	9	11	0.00076	0.01655	0.01670	0.08948			
8	5	7	0.00000	0.00000	0.00000	0.07715			

It is clear from above results that after adding the required reactive power as per the table5.3 the LCPI index value of branch number 23 and 28 bring down below the critical limit (1 p.u.) and voltage stability of the system has been improved. The reactive power compensation at bus number 10, 19 and 29 are within the available reactive power margin in Q-V characteristic of the same bus as shown in figure 5.6, 5.7 and 5.8 respectively. The overall performance of the system is also improved.

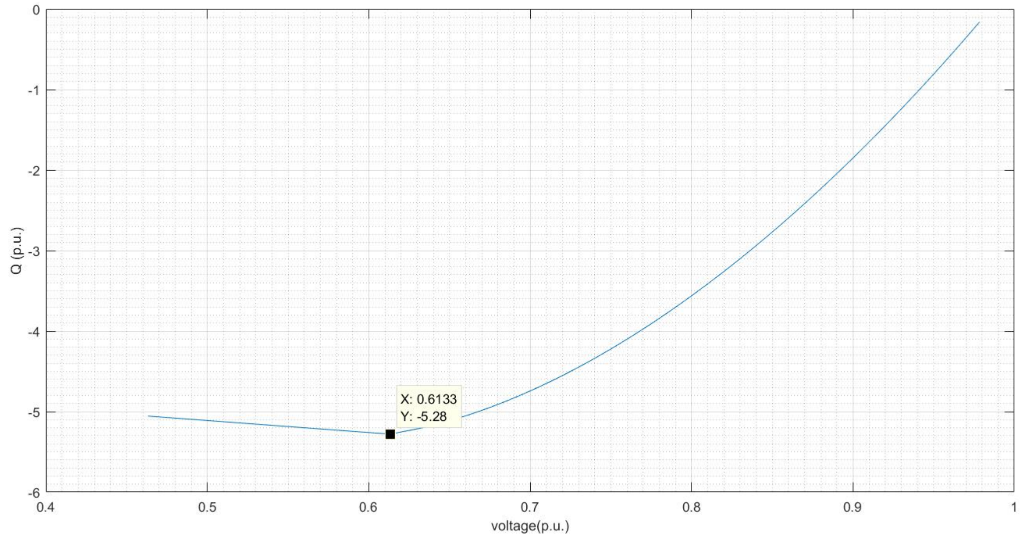

Figure 5.6: IEEE-30 bus system Q-V curve at bus-10.

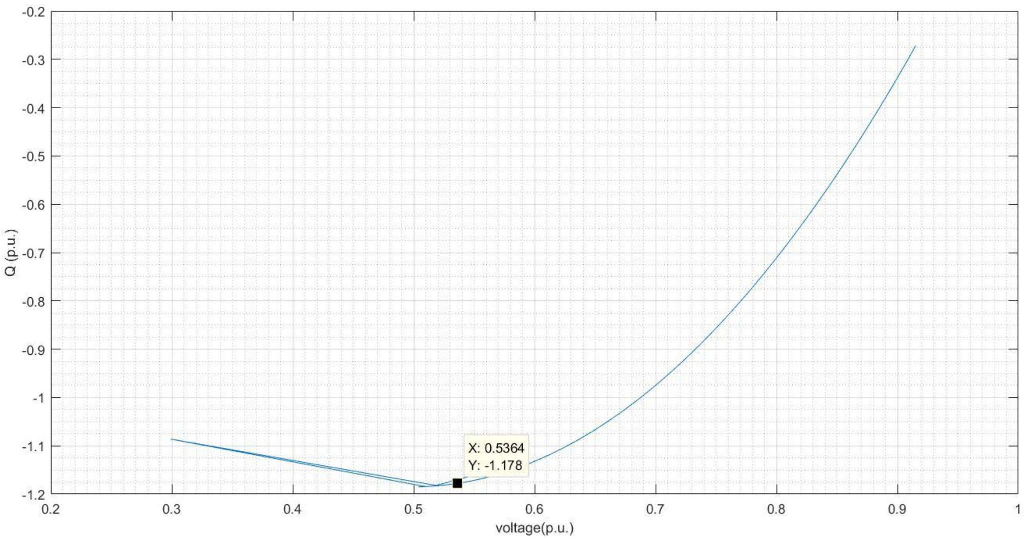

Figure 5.7: IEEE-30 bus system Q-V curve at bus-19.

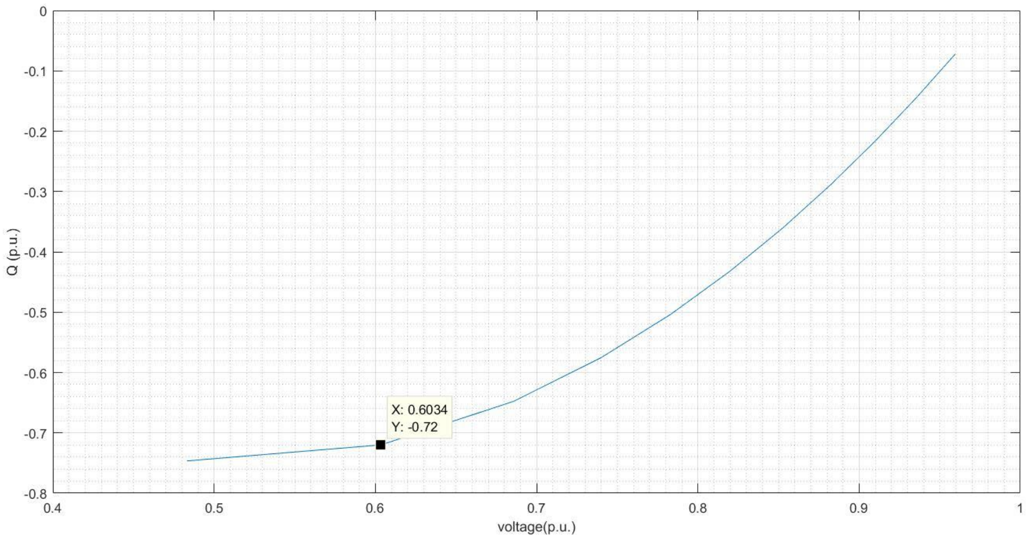

Figure 5.8: IEEE-30 bus system Q-V curve at bus-29.

5.1.3 IEEE-30 bus heavy active loading

The heavy active loading on all load bus with loadability λ = 3.46 p.u. is implemented and results are given in table 5.4 and figure 5.9.

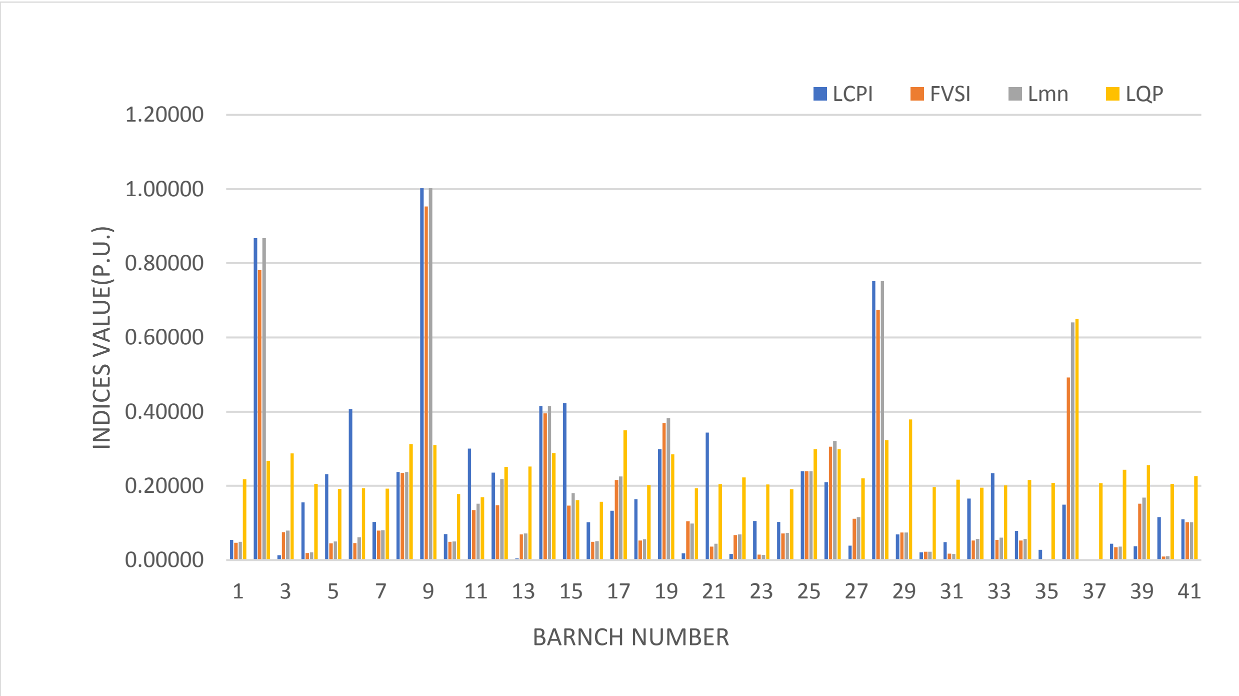

Figure 5.9: IEEE-30 bus heavy Active loading (λ = 3.46 p.u.) without compensation.

Table 5.4: IEEE 30 Bus base test system with heavy active loading without shunt compensation λ = 3.46 p.u.							
Branch Number	**From Bus**	**To Bus**	**LCPI**	**FVSI**	**Lmn**	**LQP**	**Remarks**
9	6	7	1.00274	0.95296	1.00274	0.31029	
2	1	3	0.86733	0.78114	0.86733	0.26750	according to LCPI and Lmn line number 9 become unstable but as per FVSI it is critical.
28	10	22	0.75200	0.67433	0.75200	0.32263	
15	4	12	0.42312	0.14688	0.18035	0.16105	
14	9	10	0.41529	0.39567	0.41529	0.28867	
6	2	6	0.40639	0.04564	0.06158	0.19345	
21	16	17	0.34340	0.03620	0.04428	0.20433	
11	6	9	0.30049	0.13486	0.15212	0.16906	
19	12	16	0.29916	0.36975	0.38276	0.28475	
25	10	20	0.23954	0.23883	0.23954	0.29909	
8	5	7	0.23757	0.23513	0.23757	0.31277	
12	6	10	0.23540	0.14798	0.21831	0.25085	
33	24	25	0.23375	0.05434	0.06042	0.20105	
5	2	5	0.23115	0.04463	0.05010	0.19153	
26	10	17	0.20975	0.30558	0.32091	0.29842	
32	23	24	0.16616	0.05304	0.05658	0.19550	
18	12	15	0.16398	0.05253	0.05583	0.20162	
4	3	4	0.15557	0.01924	0.02078	0.20540	
36	28	27	0.14961	0.49172	0.64067	0.64969	
17	12	14	0.13338	0.21579	0.22522	0.34924	
40	8	28	0.11565	0.00972	0.01031	0.20529	
41	6	28	0.10931	0.10193	0.10161	0.22628	
23	18	19	0.10531	0.01482	0.01403	0.20398	
24	19	20	0.10295	0.07181	0.07298	0.19057	
7	4	6	0.10294	0.07974	0.08071	0.19276	
16	12	13	0.10180	0.04925	0.05074	0.15701	
34	25	26	0.07820	0.05275	0.05677	0.21616	
10	6	8	0.06992	0.04945	0.04998	0.17758	
29	21	22	0.06905	0.07399	0.07417	0.37885	
1	1	2	0.05462	0.04674	0.04941	0.21762	
31	22	24	0.04826	0.01700	0.01675	0.21711	
38	27	30	0.04399	0.03477	0.03643	0.24357	
27	10	21	0.03863	0.11179	0.11598	0.22017	
39	29	30	0.03720	0.15173	0.16874	0.25591	
35	25	27	0.02803	0.00227	0.00230	0.20785	
30	15	23	0.02099	0.02224	0.02223	0.19660	
20	14	15	0.01807	0.10435	0.09854	0.19364	
22	15	18	0.01641	0.06700	0.06878	0.22279	
3	2	4	0.01290	0.07552	0.07963	0.28741	
13	9	11	0.00465	0.06901	0.07146	0.25193	
37	27	29	0.00000	0.00000	0.00000	0.20714	

From the above analysis it is seen that according to LCPI and Lmn branch number 9 become unstable but as per FVSI it is critical.

Now for required reactive power compensation on the above heavy active power loaded system PSO algorithm simulation run and the improved results are as follow:

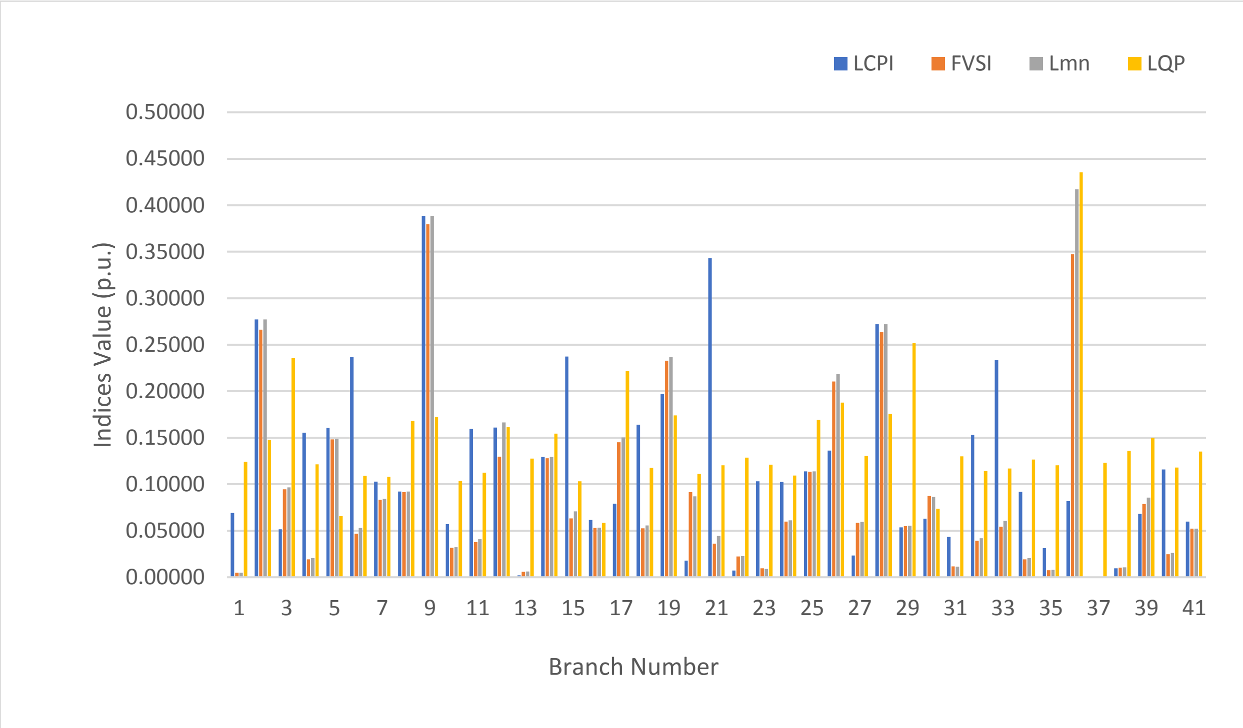

Figure 5.10:IEEE-30 bus heavy Active loading(λ = 3.46 p.u.) with shunt compensation.

Table 5.5: IEEE 30 Bus base test system with heavy active loading and shunt compensation λ = 3.46 p.u.									
Branch Number	**From Bus**	**To Bus**	**LCPI**	**FVSI**	**Lmn**	**LQP**	**Shunt compensation**		Remarks
9	6	7	0.38858	0.37978	0.38858	0.17218	Optimum bus location	MVAR capacity (p.u)	
2	1	3	0.27708	0.26625	0.27708	0.14761	3	-0.5307	
28	10	22	0.27217	0.26371	0.27217	0.17573	7	-1.3038	
15	4	12	0.23734	0.06321	0.07069	0.10321	10	-0.1991	
14	9	10	0.12941	0.12781	0.12941	0.15449			
6	2	6	0.23697	0.04668	0.05297	0.10905			
21	16	17	0.34340	0.03620	0.04428	0.12023			After shunt compensation system stability improved as shown in LCPI value.
11	6	9	0.15943	0.03775	0.04090	0.11239			
19	12	16	0.19710	0.23281	0.23691	0.17403			
25	10	20	0.11391	0.11359	0.11391	0.16927			
8	5	7	0.09204	0.09133	0.09204	0.16812			
12	6	10	0.16100	0.12959	0.16644	0.16132			
33	24	25	0.23375	0.05434	0.06042	0.11696			
5	2	5	0.16076	0.14805	0.14908	0.06579			
26	10	17	0.13626	0.21037	0.21848	0.18790			
32	23	24	0.15289	0.03919	0.04181	0.11417			
18	12	15	0.16388	0.05250	0.05580	0.11753			
4	3	4	0.15557	0.01924	0.02078	0.12131			
36	28	27	0.08197	0.34722	0.41728	0.43554			
17	12	14	0.07922	0.14525	0.15030	0.22177			
40	8	28	0.11585	0.02479	0.02606	0.11811			
41	6	28	0.05971	0.05240	0.05224	0.13508			
23	18	19	0.10323	0.00954	0.00906	0.12101			
24	19	20	0.10257	0.05980	0.06115	0.10925			
7	4	6	0.10287	0.08329	0.08415	0.10802			
16	12	13	0.06144	0.05311	0.05334	0.05848			
34	25	26	0.09165	0.01932	0.02054	0.12654			
10	6	8	0.05711	0.03176	0.03218	0.10345			
29	21	22	0.05377	0.05517	0.05520	0.25200			
1	1	2	0.06897	0.00465	0.00484	0.12415			
31	22	24	0.04338	0.01165	0.01147	0.13016			
38	27	30	0.00969	0.01044	0.01055	0.13580			
27	10	21	0.02328	0.05853	0.05957	0.13022			
39	29	30	0.06813	0.07879	0.08546	0.14982			
35	25	27	0.03111	0.00771	0.00780	0.12054			
30	15	23	0.06279	0.08741	0.08636	0.07356			
20	14	15	0.01797	0.09157	0.08696	0.11120			
22	15	18	0.00709	0.02232	0.02266	0.12853			
3	2	4	0.05166	0.09453	0.09674	0.23588			
13	9	11	0.00204	0.00599	0.00601	0.12770			
37	27	29	0.00000	0.00000	0.00000	0.12305			

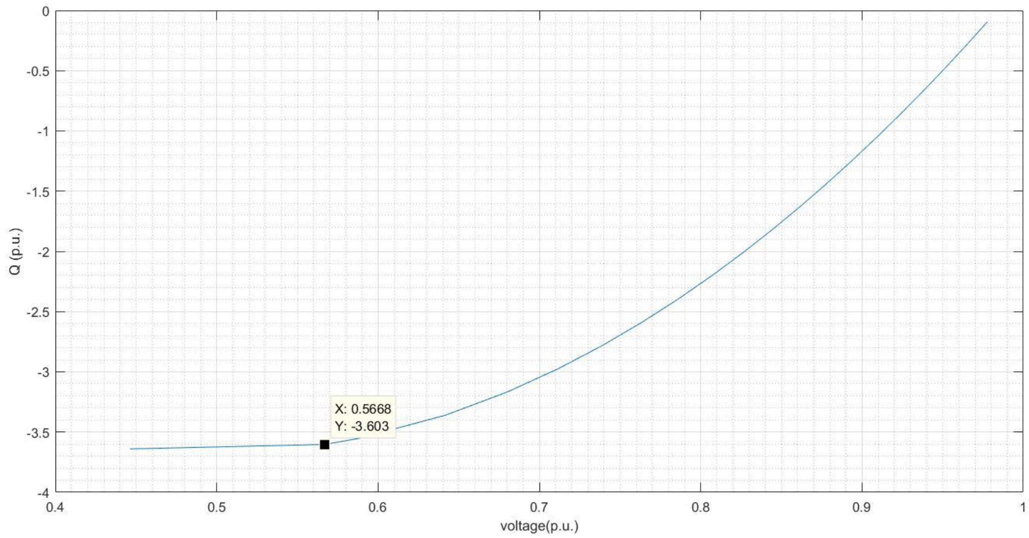

Figure 5.11: IEEE-30 bus Q-V curve at bus-3.

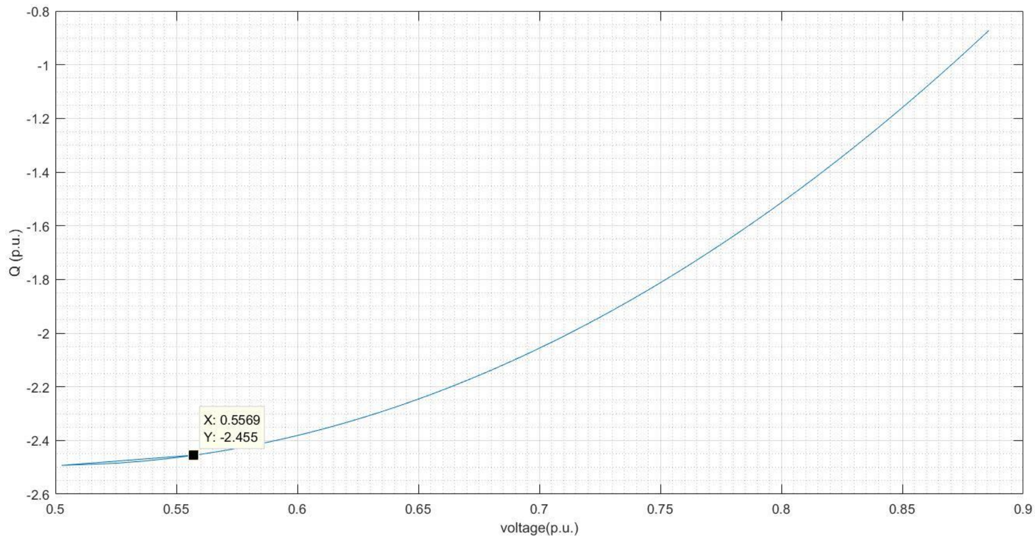

Figure 5.12: IEEE-30 bus Q-V curve at bus-7.

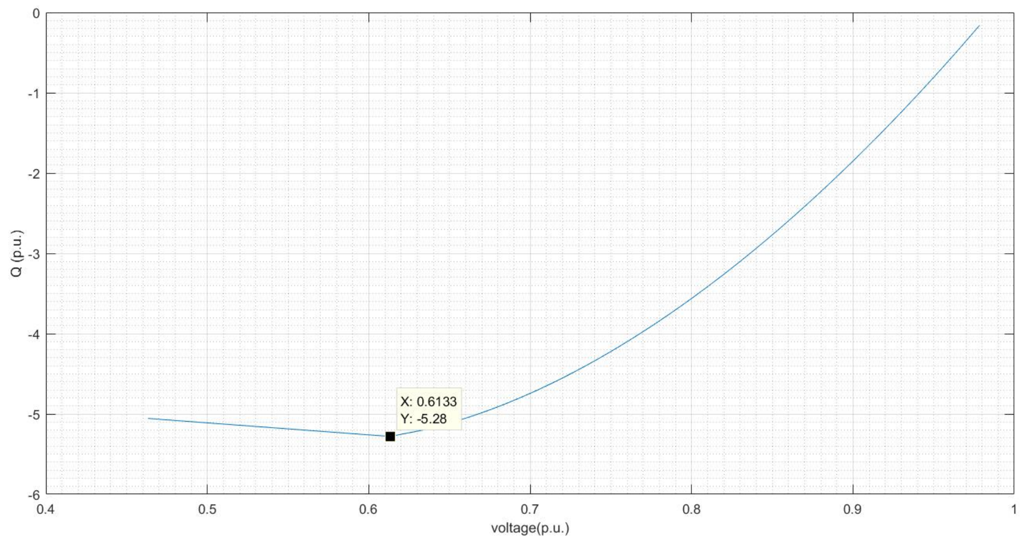

Figure 5.13: IEEE-30 bus Q-V curve at bus-10.

Optimum bus location 3,10 &10 with required reactive power compensation (as per table 5.5) have been found from PSO optimization and improved results are shown in table 5.5 and figure 5.10. the added reactive power are comes within the available margin as shown in Q-V curves figure 5.11, 5.12 & 5.13.

5.1.4 IEEE-30 bus heavy reactive loading

The heavy reactive loading on all load bus with loadability λ = 6.28 p.u. is implemented and results are given in table 5.6 and figure 5.14. The branch number 33 become unstable and LQP index is very inferior to find to critical line.

Table 5.6: IEEE 30 Bus test system with heavy reactive loading without shunt compensation λ = 6.28 p.u.							
Branch Number	**From Bus**	**To Bus**	**LCPI**	**FVSI**	**Lmn**	**LQP**	**Remarks**
33	24	25	1.00288	1.00282	1.00288	0.10490	Line number 33 become unstable
12	6	10	0.57490	0.56824	0.57072	0.16873	
41	6	28	0.52537	0.54305	0.54771	0.08353	
27	10	21	0.49336	0.49173	0.49336	0.17304	
39	29	30	0.48654	0.54260	0.55702	0.10758	
8	5	7	0.48315	0.48231	0.48315	0.03716	
40	8	28	0.44429	0.44297	0.44345	0.13728	
30	15	23	0.42763	0.41792	0.42037	0.11626	
9	6	7	0.39645	0.46706	0.48327	0.13082	
6	2	6	0.38628	0.36766	0.37173	0.10684	
2	1	3	0.38055	0.38872	0.38695	0.37439	
5	2	5	0.32297	0.33256	0.33090	0.10804	
10	6	8	0.30450	0.30426	0.30450	0.06133	
1	1	2	0.29573	0.26521	0.26973	0.01890	
24	19	20	0.27827	0.34365	0.33201	0.03292	
15	4	12	0.23873	0.28197	0.28802	0.17354	
14	9	10	0.22782	0.23961	0.23812	0.04692	
21	16	17	0.20675	0.19504	0.19626	0.02012	
3	2	4	0.20184	0.19709	0.19757	0.21103	
20	14	15	0.19296	0.20550	0.20416	0.03533	
4	3	4	0.19002	0.29603	0.28060	0.06657	
23	18	19	0.18908	0.17021	0.16870	0.03668	
35	25	27	0.17394	0.15561	0.15713	0.02585	
29	21	22	0.15930	0.17687	0.17529	0.09611	
38	27	30	0.14466	0.14464	0.14466	0.06373	
19	12	16	0.13319	0.15585	0.15759	0.35281	
34	25	26	0.12772	0.12772	0.12772	0.02428	
28	10	22	0.11908	0.12093	0.12083	0.05276	
7	4	6	0.11239	0.08394	0.08521	0.01528	
18	12	15	0.10608	0.08612	0.08702	0.00625	
16	12	13	0.08308	0.07841	0.07860	0.08662	
32	23	24	0.08261	0.14115	0.14532	0.01671	
25	10	20	0.07758	0.06078	0.06131	0.00765	
26	10	17	0.06815	0.07329	0.07347	0.03986	
22	15	18	0.05925	0.04876	0.04903	0.01199	
17	12	14	0.03404	0.03290	0.03186	0.00230	
31	22	24	0.01787	0.05077	0.05163	0.01218	
36	28	27	0.00252	0.02814	0.02859	0.02707	
37	27	29	0.00071	0.04879	0.05001	0.01593	
13	9	11	0.00015	0.00585	0.00587	0.00535	
11	6	9	0.00000	0.00000	0.00000	0.00174	

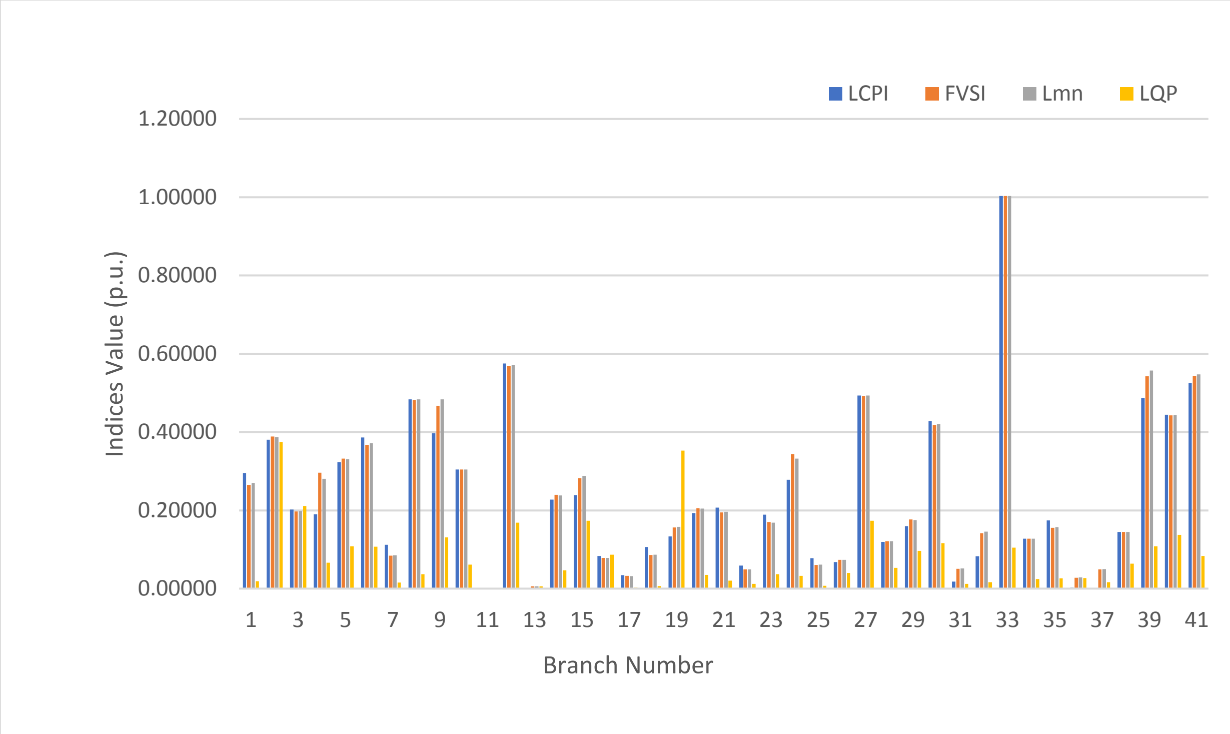

Figure 5.14: IEEE-30 bus heavy Reactive loading (λ = 6.28p.u.) without compensation.

After shunt compensation the results are as follow:

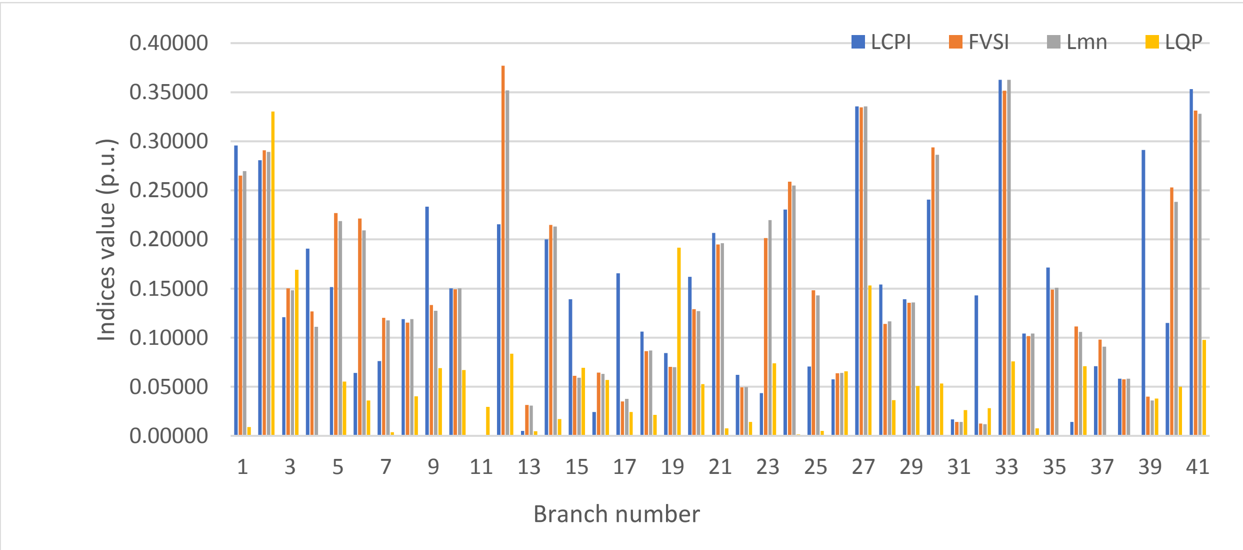

Figure 5.15: IEEE-30 bus heavy Reactive loading (λ=6.28 p.u.) with shunt compensation.

Table 5.7: IEEE 30 Bus test system with heavy reactive loading and shunt compensation λ = 6.28 p.u.

Branch Number	**From Bus**	**To Bus**	**LCPI**	**FVSI**	**Lmn**	**LQP**	**Shunt compensation**		Remarks
							Optimum bus location	MVAR capacity (p.u)	
33	24	25	0.36276	0.35141	0.36276	0.07581			
12	6	10	0.21560	0.37695	0.35176	0.08361	24	-2.3979	
41	6	28	0.35328	0.33125	0.32814	0.09774			
27	10	21	0.33554	0.33451	0.33554	0.15326			
39	29	30	0.29115	0.03992	0.03611	0.03799			Now line number 33 become stable
8	5	7	0.11885	0.11526	0.11885	0.04031			
40	8	28	0.11515	0.25314	0.23831	0.04997			
30	15	23	0.24057	0.29373	0.28644	0.05346			
9	6	7	0.23344	0.13320	0.12744	0.06887			
6	2	6	0.06417	0.22148	0.20931	0.03593			
2	1	3	0.28065	0.29079	0.28922	0.33051			
5	2	5	0.15144	0.22676	0.21860	0.05520			
10	6	8	0.15039	0.14921	0.15039	0.06686			
1	1	2	0.29573	0.26521	0.26973	0.00883			
24	19	20	0.23043	0.25895	0.25509	0.00139			
15	4	12	0.13909	0.06122	0.05909	0.06939			
14	9	10	0.20011	0.21497	0.21331	0.01723			
21	16	17	0.20675	0.19504	0.19626	0.00762			
3	2	4	0.12099	0.15036	0.14823	0.16903			
20	14	15	0.16190	0.12901	0.12703	0.05275			
4	3	4	0.19074	0.12687	0.11095	0.00020			
23	18	19	0.04365	0.20161	0.21970	0.07397			
35	25	27	0.17143	0.14899	0.15077	0.00060			
29	21	22	0.13923	0.13563	0.13588	0.05081			
38	27	30	0.05813	0.05770	0.05813	0.00008			
19	12	16	0.08431	0.07039	0.06992	0.19166			
34	25	26	0.10425	0.10162	0.10425	0.00755			
28	10	22	0.15406	0.11410	0.11660	0.03631			
7	4	6	0.07603	0.12011	0.11752	0.00361			
18	12	15	0.10608	0.08612	0.08702	0.02149			
16	12	13	0.02425	0.06441	0.06323	0.05675			
32	23	24	0.14299	0.01269	0.01180	0.02805			
25	10	20	0.07057	0.14838	0.14292	0.00511			
26	10	17	0.05767	0.06390	0.06410	0.06581			
22	15	18	0.06199	0.04932	0.04964	0.01427			
17	12	14	0.16567	0.03509	0.03774	0.02431			
31	22	24	0.01668	0.01425	0.01404	0.02631			
36	28	27	0.01420	0.11154	0.10578	0.07091			
37	27	29	0.07109	0.09792	0.09078	0.00077			
13	9	11	0.00518	0.03142	0.03088	0.00468			
11	6	9	0.00000	0.00000	0.00000	0.02948			

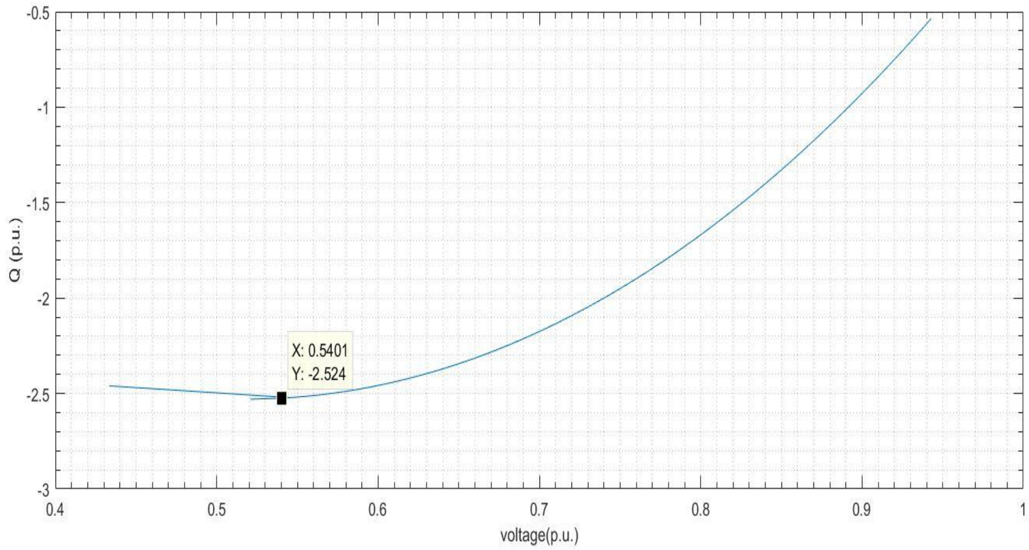

Figure 5.16: IEEE-30 bus Q-V curve at bus-24.

5.1.5 IEEE-30 bus heavy active loading on single bus

In a big power system network loading on all buses can't be increases simultaneously so we have to done analysis for loading on single bus and find the critical line for this increased load on single bus. For the analysis purpose we randomly selected the load buses and increase loadability to get the first critical branch. The analysis results are shown in table5.8

Table 5.8: critical branch of IEEE 30 Bus system with Heavy active loading on single bus

Load Bus	loading (p.u)	Critical Branch	From Bus	To Bus	LCPI	FVSI	Lmn	LQP
8	1.260	36	28	27	0.99562	0.99333	0.99562	0.23023
10	4.900	12	6	10	0.99389	0.76081	0.99389	0.13822
14	1.980	20	14	15	0.99176	0.06402	0.04643	0.02154
15	2.830	30	15	23	0.99362	0.79864	0.74385	0.18942
16	5.510	21	16	17	0.99294	0.45426	0.39497	0.10962
17	3.034	12	6	10	0.99040	0.74128	0.99040	0.14579
18	4.920	30	15	23	0.99403	0.97449	0.96673	0.20463
21	1.581	12	6	10	0.99157	0.79735	0.99157	0.14061
24	2.860	33	24	25	0.99900	0.09455	0.07427	0.09492
29	3.926	39	29	30	0.99225	0.37948	0.31695	0.03266
30	1.002	38	27	30	0.932128	0.040862	0.172722	0.02267

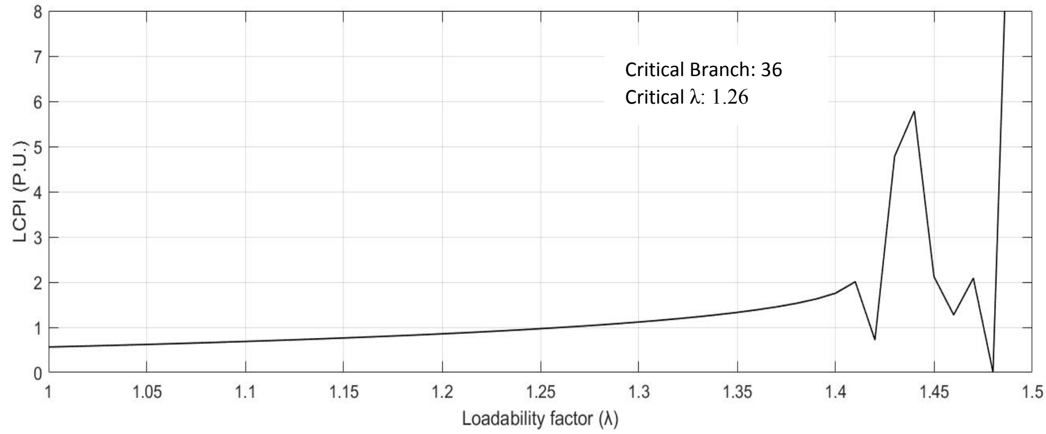

Figure 5.17: IEEE-30 bus heavy active loading (λ) at bus-8 v/s LCPI.

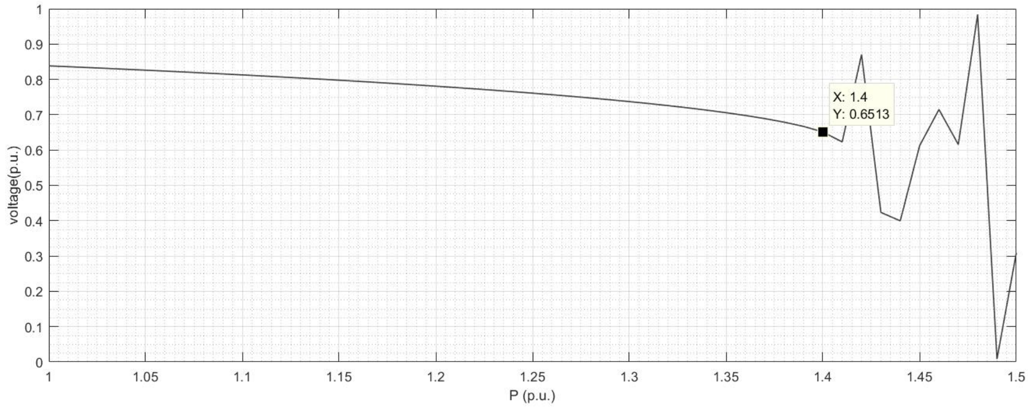

Figure 5.18: IEEE-30 bus system P-V curve at bus-8.

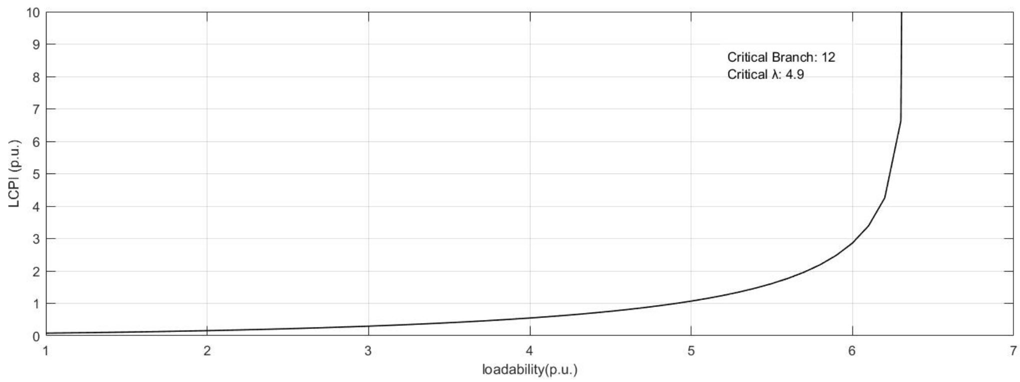

Figure 5.19: IEEE-30 bus heavy active loading (λ) at bus-10 v/s LCPI.

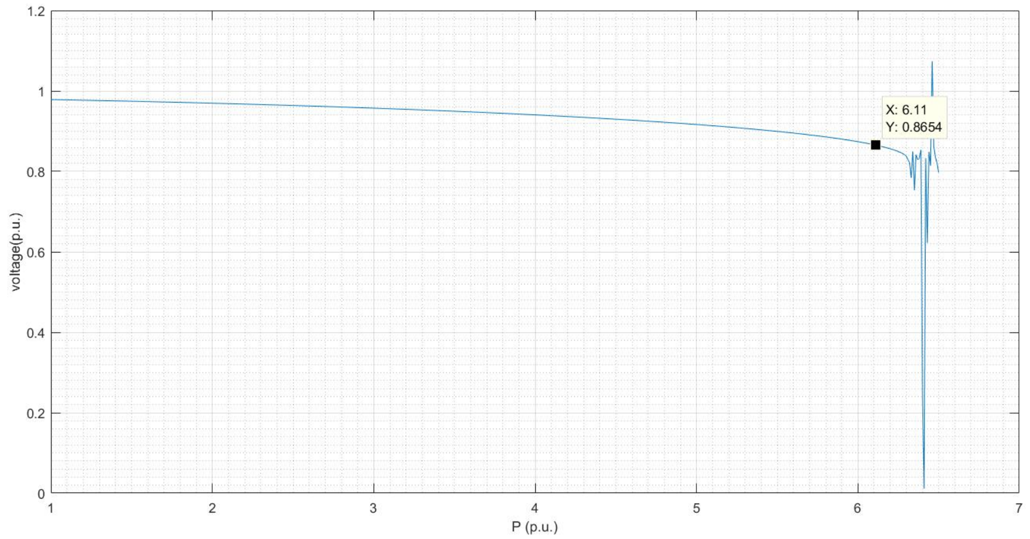

Figure 5.20: IEEE-30 bus system P-V curve at bus-10.

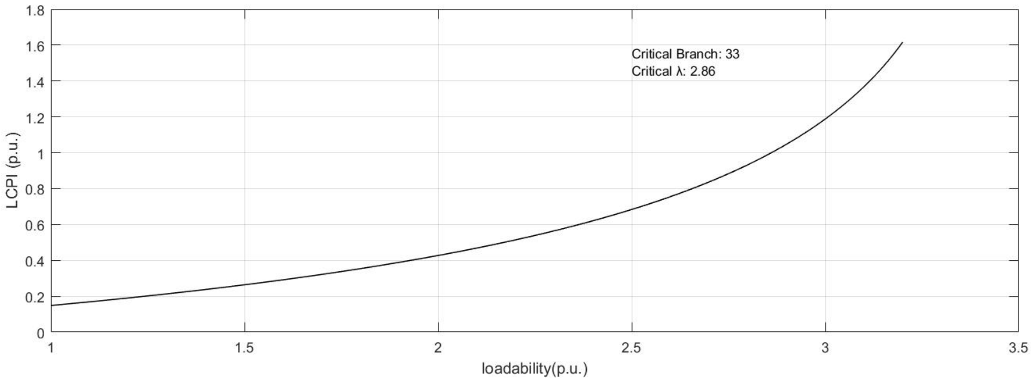

Figure 5.21: IEEE-30 bus heavy active loading (λ) at bus-24 v/s LCPI.

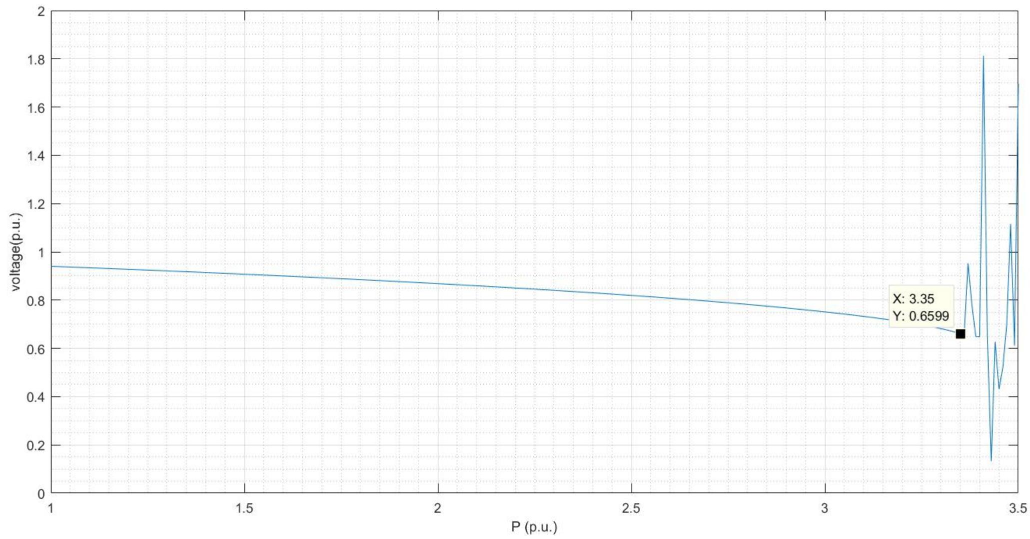

Figure 5.22: IEEE-30 bus system P-V curve at bus-24.

We tested each bus as shown in table5.8 to find the critical branch, when load increases on that bus. The maximum active power loading on the bus is verified by the P-V curve. The behavior of LCPI index with respect to the loading on single bus are shown in above figures 5.17,5.19 & 5.21 for bus number 8,10 & 24 for reference purpose. The P-V curve of these buses are also shown in figure 5.18, 5.20 and 5.22 to verify the maximum allowable loading on these buses.

In table5.8 LCPI value for some critical lines are similar to the FVSI & Lmn, but LQP gives the irrelevant results. From the comparison in table 5.8 it is clear that LCPI gives the accurate result for stability analysis. From this analysis we can predict the maximum loadability limit of each bus in the large power system network and get the detail of most critical line according to the loading on particular bus.

5.1.6 IEEE-30 bus heavy reactive loading on single bus

Similar to the above titled-5.1.5 the analysis for heavy reactive loading on each bus is done and get the critical branch and record the results in table 5.9 (representing some random buses) as follow:

Table 5.9: critical lines of IEEE 30 Bus system with Heavy Reactive loading on single bus

Load Bus	loading (p.u)	**Critical Branch**	**From Bus**	**To Bus**	**LCPI**	**FVSI**	**Lmn**	**LQP**
7	2.822	36	28	27	0.99152	0.99097	0.99152	0.10692
8	1.02	36	28	27	0.99432	0.99386	0.99432	0.10371
10	19	28	10	22	0.97633	1.14409	1.23938	0.26245
14	7.13	20	14	15	0.99573	1.60303	2.15035	0.12318
15	7.25	30	15	23	0.99049	1.14433	1.22891	0.19037
16	8.47	21	16	17	0.99846	1.16679	1.26696	0.16631
17	5.02	28	10	22	0.99541	1.15909	1.25259	0.26858
19	4.42	24	19	20	0.96795	1.08918	1.15251	0.20409
21	8.5	29	21	22	0.99396	1.19211	1.31094	1.98745
24	3.71	33	24	25	0.99442	1.16534	1.26003	0.08963
26	2.315	34	25	26	0.99319	1.27018	0.99502	0.09871
30	4.1	39	29	30	0.99883	1.14242	0.98666	0.04835

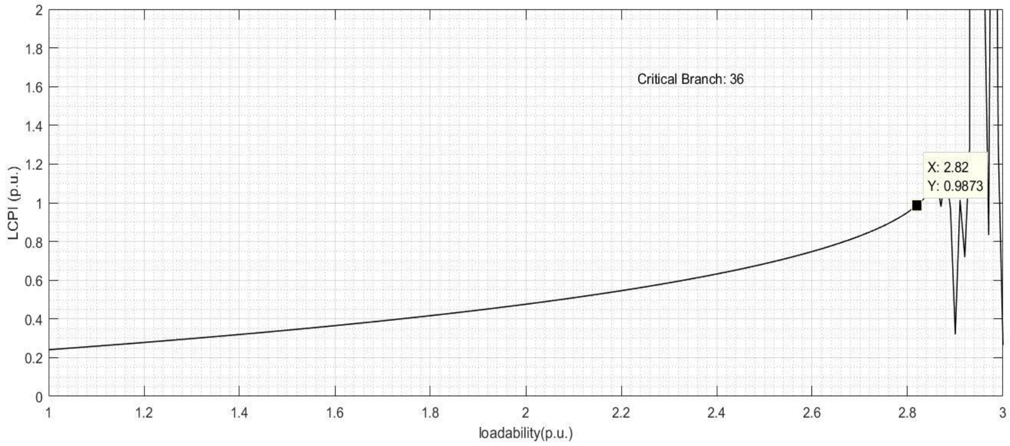

Figure 5.23: IEEE-30 bus heavy reactive loading (λ) at bus-7 v/s LCPI.

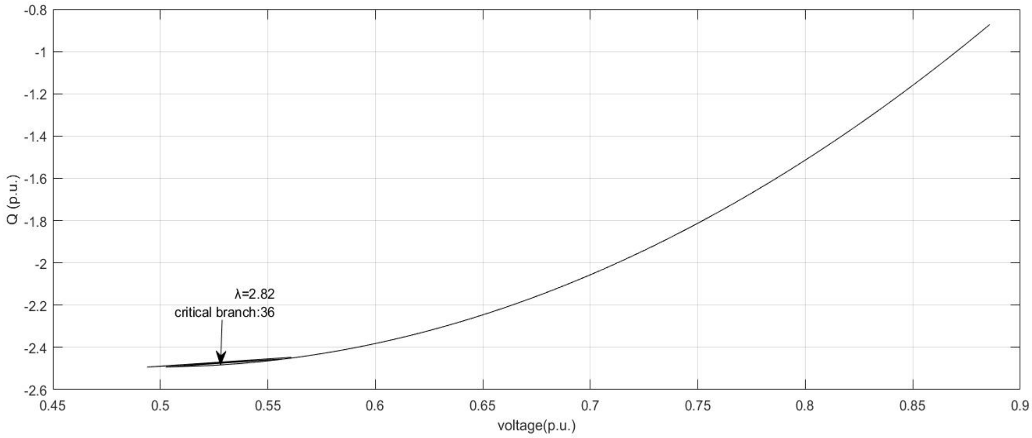

Figure 5.24: IEEE-30 bus heavy reactive loading (λ) at bus-7 Q-V curve.

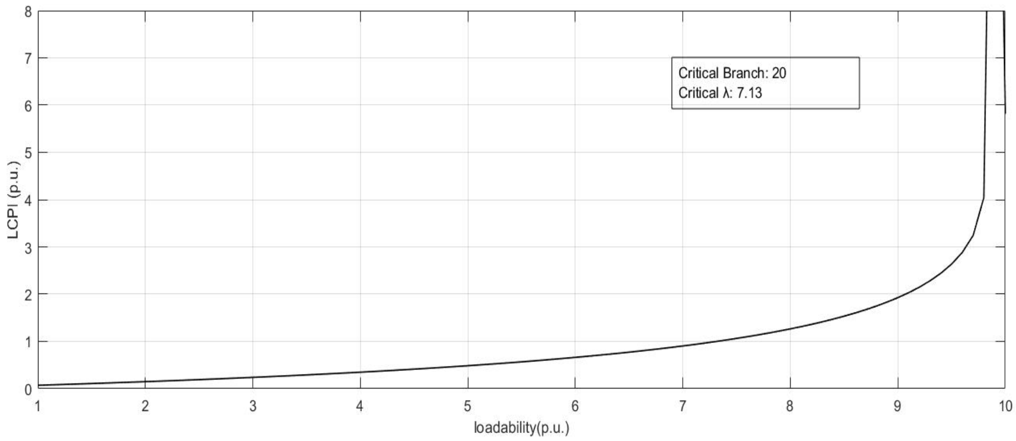

Figure 5.25: IEEE-30 bus heavy reactive loading (λ) at bus-14 v/s LCPI.

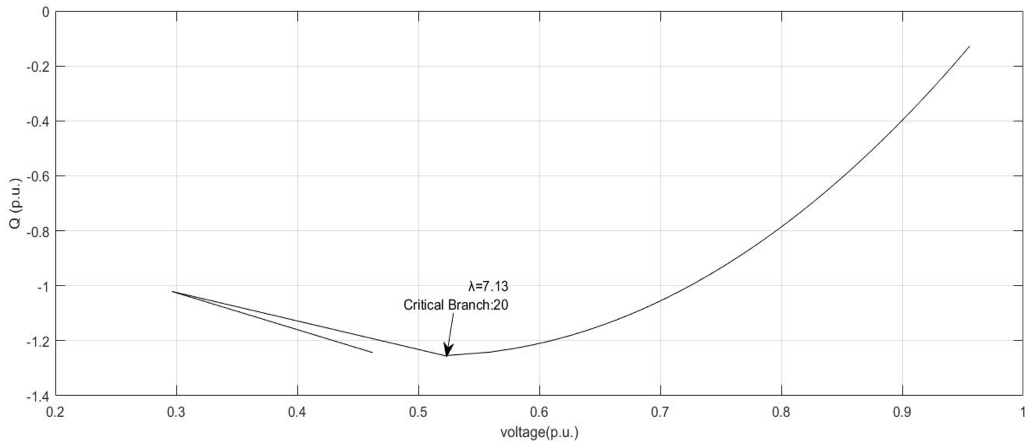

Figure 5.26: IEEE-30 bus heavy reactive loading (λ) at bus-14 Q-V curve.

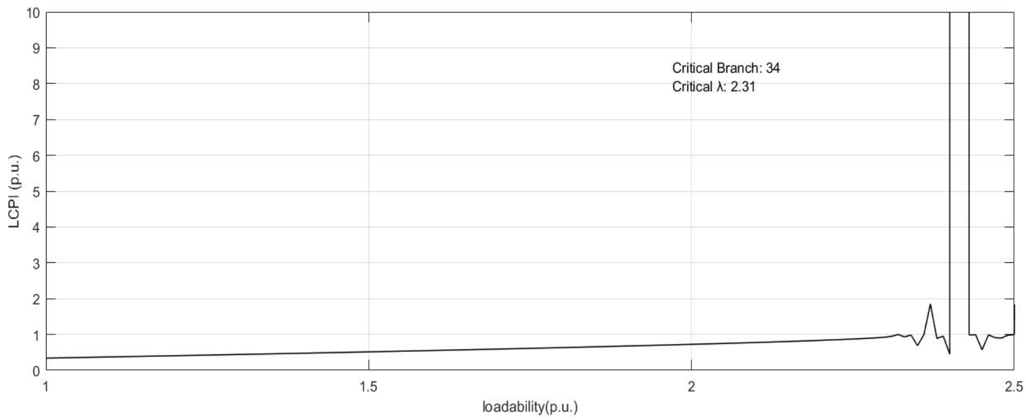

Figure 5.27: IEEE-30 bus heavy reactive loading (λ) at bus-26 v/s LCPI.

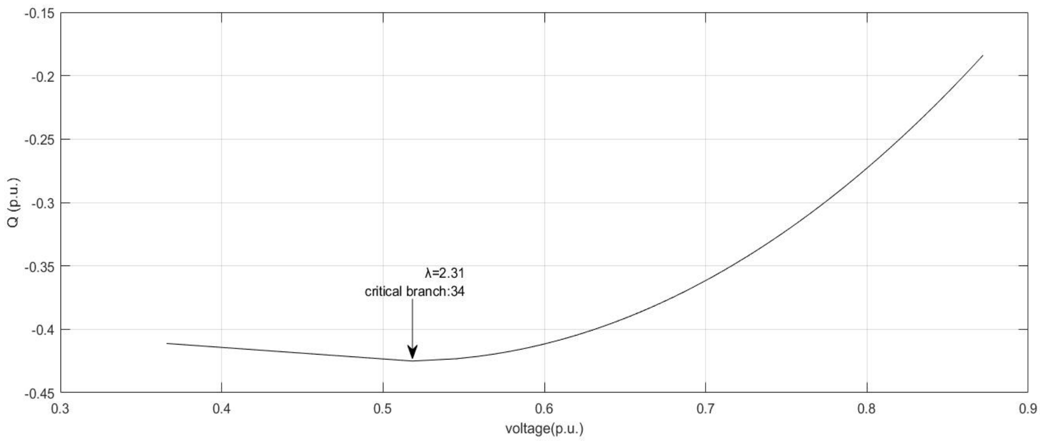

Figure 5.28: IEEE-30 bus heavy reactive loading (λ) at bus-26 Q-V curve.

For explanation purpose bus no.7, 14 and 26 reactive loading v/s LCPI curve and Q-V curve are shown in above figures (figure 5.23 to 5.28).

5.1.7 IEEE-30 bus line contingency analysis

In a large power system network, there are chance of line outage due to any fault, transformer out of service, maintenance of line etc, Line contingency analysis is done to observe the effect of line outage on the voltage stability of entire power system network. Here we done this analysis for pre specified reactive power loading as shown in table5.10 and ranking of critical branches as per LCPI values is done the results are shown in table5.10. In this analysis we observe that the most critical branch is 29 with LCPI index value 0.992195 but according to FVSI and Lmn it is unstable and stable according to LQP index. Branch no.10 is critical according to LCPI but stable according to FVSI, Lmn & LQP. Branch no. 33 is stable according to LCPI, unstable according to FVSI, critical according to Lmn. The LCPI index gives the accurate results consistently and other indices give irregular/incorrect results. The LQP index results are totally different with respect to the other indices.

Table 5.10: critical lines of IEEE 30 Bus system with Pre specified reactive load

Rank	Branch outage	Critical Branch	From Bus	To Bus	LCPI	FVSI	Lmn	LQP	Pre specified Reactive loadability (p.u.)	
									bus no.	**load**
1	29	28	10	22	0.992195	1.097453	1.150828	0.250066		
2	10	40	8	28	0.950838	0.881419	0.85933	0.1393	7	1.41
3	35	33	24	25	0.90455	1.057099	0.946534	0.110934	8	0.51
4	33	34	25	26	0.828693	1.091163	0.919973	0.087371	14	3.57
5	31	34	25	26	0.751158	0.995367	0.856753	0.087526	15	3.63
6	32	34	25	26	0.738938	0.979984	0.846094	0.087512	16	4.24
7	25	34	25	26	0.72532	0.962766	0.83402	0.087131	19	2.21
8	24	34	25	26	0.725161	0.962565	0.833879	0.08721	21	4.25
9	18	34	25	26	0.725008	0.962372	0.833742	0.087514	26	1.16
10	26	34	25	26	0.72485	0.962171	0.833601	0.087533	30	2.05

5.2 IEEE-118 Bus System

The IEEE-118 bus system [53] have 19 numbers generator bus, 91 numbers load buses. The base MVA is 100 MVA. The voltage indices have been calculated on IEEE-118 bus system for different operating conditions and discussed in following sections.

5.2.1 IEEE-118 bus base case loading

The calculated value of all indices for the base case loading **(λ=1p.u.)** has been shown in Table 5.11 and graphical representation is shown in figure 5.29. The branch number is representing the serial number of lines which are connected between from bus & to bus. All column of table is sorted according to the LCPI index value in descending order. After running the simulation on IEEE-118 bus system at base case loading is observed stable according to the all indices (all indices value is less than unity for each branch) value.

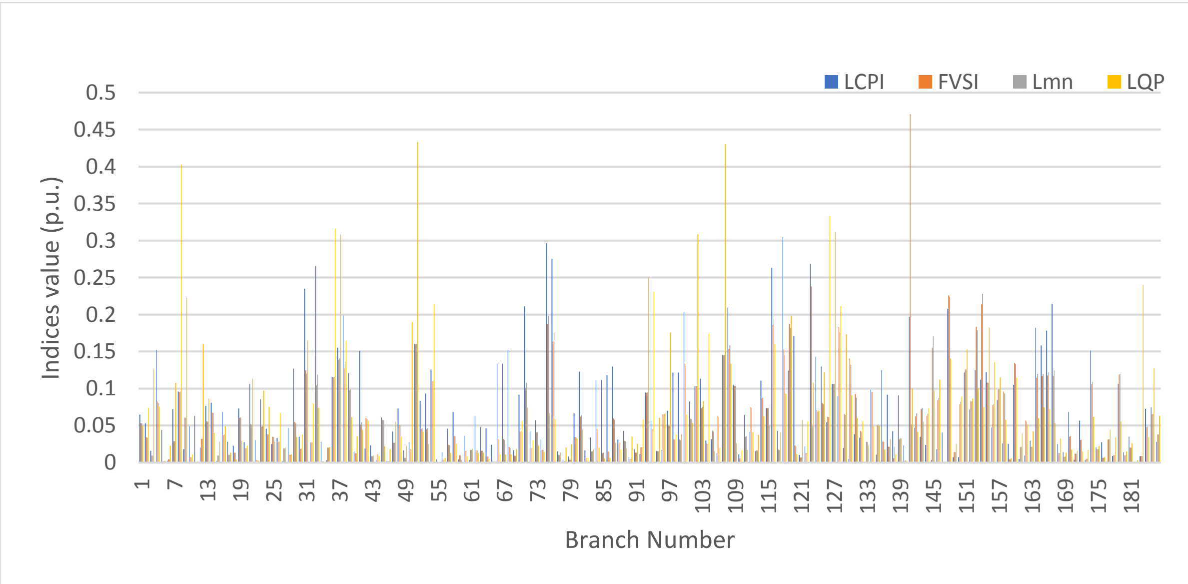

Figure 5.29: IEEE-118 bus base case loading (λ=1) bar chart branch v/s Indices.

Table 5.11: IEEE 118 Bus base case loading λ = 1 p.u.						
Branch Number	**From Bus**	**To Bus**	**LCPI**	**FVSI**	**Lmn**	**LQP**
118	76	77	0.304698	0.153127	0.144968	0.093143
75	49	54	0.296426	0.18694	0.198071	0.066725
76	49	54	0.275223	0.163578	0.175724	0.058709
123	77	80	0.268327	0.238178	0.049293	0.108391
33	25	27	0.265876	0.104346	0.11899	0.073789
116	69	75	0.263323	0.185608	0.19439	0.160111
31	23	25	0.235091	0.124588	0.1205	0.164945
167	100	106	0.214573	0.117277	0.12474	0.05355
71	49	51	0.21119	0.100748	0.107643	0.074485
108	69	70	0.209353	0.153489	0.158744	0.133632
148	80	96	0.207819	0.225705	0.22377	0.140826
100	62	66	0.203234	0.13431	0.130824	0.064768
38	26	30	0.198761	0.127028	0.136147	0.164572
141	89	92	0.196709	0.470735	0.051484	0.099781
164	100	104	0.182198	0.114828	0.119731	0.060114
166	103	105	0.178307	0.117892	0.122059	0.072452
120	75	77	0.171079	0.023222	0.021979	0.011623
51	38	37	0.160644	0.159706	0.160644	0.433043
165	103	104	0.158186	0.116673	0.119438	0.075063
37	8	30	0.155338	0.139017	0.140531	0.308319
68	45	49	0.152504	0.021025	0.019921	0.011335
4	3	5	0.152355	0.082817	0.080583	0.075609
174	103	110	0.151322	0.105999	0.108884	0.061746
41	23	32	0.150826	0.051098	0.054365	0.044426
107	68	69	0.14537	0.144829	0.14537	0.430188
124	77	80	0.143018	0.07083	0.068707	0.070028
66	42	49	0.133605	0.03193	0.030825	0.0107
67	42	49	0.133605	0.03193	0.030825	0.0107
125	79	80	0.12987	0.080304	0.078651	0.121954
87	55	59	0.129856	0.059592	0.057997	0.026837
29	22	23	0.126907	0.054805	0.053307	0.034636
54	30	38	0.125945	0.10978	0.110954	0.214254
136	85	89	0.124916	0.028461	0.02795	0.017841
153	80	99	0.124873	0.183491	0.178931	0.099957
119	69	77	0.124279	0.187211	0.181876	0.198195
81	50	57	0.122836	0.061808	0.063959	0.044314
155	94	100	0.122046	0.108383	0.107725	0.182602
99	49	66	0.121765	0.031362	0.030411	0.038507
98	49	66	0.121765	0.031362	0.030411	0.038507
151	80	97	0.121594	0.125997	0.125723	0.153229
39	17	31	0.12112	0.097767	0.099049	0.06146
86	56	59	0.118158	0.014947	0.014324	0.006287
36	30	17	0.116124	0.115265	0.116124	0.31572
103	66	67	0.113493	0.073652	0.075347	0.082876

154	92	100	0.111981	0.213748	0.228228	0.074891
85	56	59	0.111673	0.012534	0.013248	0.005618
84	54	59	0.111129	0.045892	0.044732	0.01976
114	70	74	0.11057	0.086634	0.087779	0.062923
21	15	17	0.106602	0.052156	0.050908	0.113405
179	32	113	0.106435	0.119162	0.120038	0.0553
127	81	80	0.106349	0.106237	0.106349	0.311714
109	24	70	0.105326	0.103316	0.103905	0.026378
160	100	101	0.105293	0.13455	0.132722	0.114552
102	65	66	0.103401	0.103401	0.103401	0.308498
134	86	87	0.098568	0.095665	0.095549	0.048975
8	8	5	0.096121	0.095384	0.096121	0.402453
93	63	59	0.094643	0.094322	0.094643	0.250544
53	37	40	0.093307	0.045148	0.046377	0.025011
70	49	50	0.091574	0.041814	0.042962	0.056142
137	88	89	0.091571	0.021602	0.021043	0.031811
139	89	90	0.090665	0.031592	0.032716	0.032483
128	77	82	0.08964	0.183335	0.175753	0.211659
23	17	18	0.085616	0.048265	0.049275	0.097194
157	96	97	0.084519	0.09852	0.099242	0.115166
52	37	39	0.083589	0.045325	0.046282	0.041431
101	62	67	0.082551	0.059479	0.058864	0.053575
14	3	12	0.080952	0.067521	0.067127	0.040342
13	2	12	0.076641	0.055785	0.055239	0.08639
185	75	118	0.074859	0.065534	0.065854	0.127541
115	70	75	0.073472	0.073618	0.073639	0.050018
19	14	15	0.073138	0.060609	0.061059	0.029445
48	33	37	0.073051	0.051242	0.050737	0.035019
184	12	117	0.072617	0.048234	0.048885	0.034367
7	8	9	0.072263	0.029114	0.028992	0.107719
152	80	98	0.071902	0.083269	0.082815	0.08643
97	64	65	0.070157	0.050271	0.049938	0.175772
16	11	13	0.068511	0.037319	0.037948	0.048973
170	105	107	0.068272	0.035185	0.035839	0.017409
58	41	42	0.068237	0.035944	0.03542	0.025645
80	56	57	0.066711	0.034758	0.034246	0.032539
1	1	2	0.064777	0.053398	0.053117	0.049584
111	24	72	0.064579	0.034717	0.035303	0.017294
11	5	11	0.063148	0.00062	0.000643	0.001603
62	45	46	0.062891	0.016762	0.016418	0.012848
45	19	34	0.060903	0.057339	0.057324	0.022221
73	52	53	0.057024	0.040731	0.041098	0.022849
172	106	107	0.056545	0.030661	0.031105	0.014981
94	63	64	0.055853	0.045096	0.044903	0.230805
126	68	81	0.054582	0.061767	0.061576	0.333396
2	1	3	0.053429	0.034001	0.033688	0.074009
10	4	11	0.04936	0.007164	0.007391	0.011085
63	46	47	0.047892	0.016143	0.01591	0.013592

156	95	96	0.047525	0.077851	0.079085	0.135888
142	89	92	0.047296	0.062255	0.066735	0.041714
28	21	22	0.046525	0.010726	0.010557	0.011321
64	46	48	0.046227	0.008129	0.007992	0.005006
57	40	42	0.04581	0.023702	0.023472	0.012909
24	18	19	0.045665	0.037931	0.038084	0.075193
5	5	6	0.04413	0.001537	0.001574	0.0023
117	74	75	0.042801	0.017688	0.017479	0.0408
89	59	61	0.042646	0.029621	0.028786	0.019344
138	89	90	0.042504	0.005918	0.02179	0.01103
72	51	52	0.042265	0.019499	0.019733	0.029653
47	35	37	0.04175	0.026985	0.026797	0.055189
112	71	72	0.041323	0.075003	0.073863	0.041197
147	94	95	0.040543	0.000237	0.000243	0.001218
131	83	85	0.038368	0.09268	0.088032	0.059976
60	34	43	0.036462	0.015861	0.016041	0.008753
30	23	24	0.03518	0.01875	0.018914	0.038118
181	27	115	0.035045	0.020366	0.020525	0.026208
143	91	92	0.034741	0.072201	0.07366	0.055338
83	51	58	0.034217	0.015019	0.01517	0.018312
132	84	85	0.033617	0.042785	0.041281	0.056456
26	15	19	0.033463	0.02826	0.028336	0.066964
105	47	69	0.031659	0.043073	0.041745	0.015447
74	53	54	0.031447	0.017491	0.017378	0.014113
88	59	60	0.031086	0.027237	0.026587	0.018368
22	16	17	0.030265	0.003651	0.003608	0.002706
104	65	68	0.030019	0.025482	0.025547	0.174216
163	100	103	0.029447	0.021191	0.021785	0.042527
34	27	28	0.028255	0.001511	0.001533	0.001043
186	76	118	0.028185	0.03808	0.038273	0.063188
17	12	14	0.027974	0.010201	0.010297	0.013494
50	34	37	0.027763	0.018024	0.017938	0.190002
176	110	111	0.027604	0.006381	0.006281	0.007394
20	12	16	0.027594	0.019425	0.019508	0.022802
32	26	25	0.027349	0.027318	0.027349	0.080016
158	98	100	0.026004	0.096138	0.093436	0.057937
159	99	100	0.025491	0.00425	0.004208	0.006253
25	19	20	0.025222	0.034712	0.034556	0.028057
168	104	105	0.025068	0.013079	0.01316	0.032737
65	47	49	0.024299	0.00151	0.001491	0.001826
144	92	93	0.023618	0.063014	0.066214	0.073701
140	90	91	0.023166	0.00277	0.0028	0.002539
43	27	32	0.023138	0.008613	0.008679	0.010038
18	13	15	0.023103	0.013473	0.013559	0.004496
122	78	79	0.022247	0.012835	0.012776	0.055939
175	109	110	0.020684	0.018238	0.01822	0.022333
12	11	12	0.020277	0.032085	0.032277	0.159984
129	82	83	0.019777	0.065807	0.064408	0.173551

42	31	32	0.019163	0.060003	0.058869	0.056478
146	93	94	0.018143	0.084368	0.0875	0.112201
9	9	10	0.018061	0.060831	0.060609	0.222954
91	60	62	0.017982	0.013579	0.01355	0.025637
96	38	65	0.0175	0.065184	0.064702	0.066085
69	48	49	0.01677	0.009399	0.009282	0.018181
82	56	58	0.016413	0.006386	0.006357	0.006537
49	34	36	0.01638	0.006505	0.006538	0.022598
3	4	5	0.01608	0.009623	0.009592	0.12614
113	71	73	0.015681	0.016251	0.016256	0.037532
95	64	61	0.015437	0.015436	0.015437	0.060376
77	54	55	0.015333	0.010513	0.01054	0.013368
40	29	31	0.01522	0.012573	0.012557	0.035574
169	105	106	0.014363	0.007974	0.008	0.01327
180	32	114	0.014001	0.009987	0.010008	0.015123
56	40	41	0.013997	0.003751	0.00377	0.006606
106	49	69	0.012614	0.062642	0.061351	0.019683
92	61	62	0.011582	0.020843	0.020942	0.058044
110	70	71	0.011185	0.005727	0.005712	0.0168
135	85	88	0.010994	0.05066	0.04944	0.050145
121	77	78	0.010214	0.007109	0.007121	0.057521
162	101	102	0.009709	0.056537	0.055396	0.051122
178	17	113	0.009273	0.010539	0.010533	0.034101
183	68	116	0.008812	0.008874	0.008874	0.24018
79	55	56	0.008349	0.003992	0.003984	0.024448
90	60	61	0.007524	0.004629	0.004602	0.034995
150	94	96	0.0074	0.078895	0.082088	0.088936
149	82	96	0.007396	0.014413	0.014266	0.025703
130	83	84	0.004969	0.140845	0.132468	0.090874
161	92	102	0.004555	0.021106	0.021399	0.039347
78	54	56	0.004327	0.002184	0.002186	0.020412
59	43	44	0.004302	0.010075	0.010014	0.00337
55	39	40	0.004108	0.000159	0.000159	0.000437
171	105	108	0.003671	0.012032	0.012085	0.016028
44	15	33	0.003561	0.01106	0.011147	0.009066
145	92	94	0.003559	0.155226	0.170683	0.097211
61	44	45	0.003522	0.017314	0.017145	0.018609
35	28	29	0.00299	0.020329	0.020515	0.021221
173	108	109	0.002821	0.005312	0.005319	0.017343
6	6	7	0.002786	0.004484	0.0045	0.022752
15	7	12	0.002204	0.009342	0.009376	0.028363
27	20	21	0.002045	0.019111	0.018923	0.020918
46	35	36	0.001982	0.001899	0.001899	0.01802
133	85	86	0.00121	0.027907	0.028306	0.022991
177	110	112	0.001093	0.031231	0.031738	0.044729
182	114	115	0.000358	0.000408	0.000408	0.003093

From the above simulation results in table5.11 and figure 5.29 it is seen that all indices value are below '1'. Similar to the IEEE-30 bus base case loading results Values of LCPI, FVSI and Lmn indices are almost equal for some branches such as 8,46,51,55,93,102,107,127,182,183 etc (also highlighted in table 5.11). The LQP index also shows base case stability but results are not similar to the other indices.

5.2.2 IEEE-118 bus heavy MVA loading

The simulation is done for heavy MVA loading with taking loadability λ = 1.492 p.u. for complete 118 bus system and results are shown in table5.12. The bar chart of most critical branches is also shown in figure 5.30.

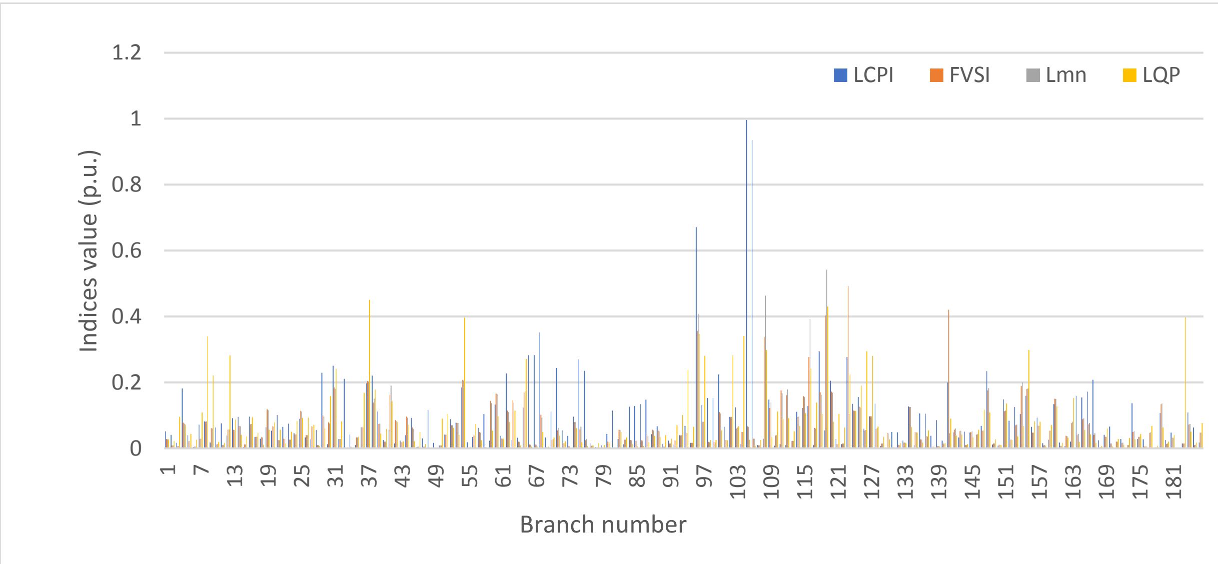

Figure 5.30: IEEE-118 bus heavy MVA loading (λ=1.492) bar chart branch v/s Indices.

Table 5.12: IEEE 118 Bus base test system with heavy MVA loading λ = 1.492 p.u.						
Branch Number	From Bus	To Bus	LCPI	FVSI	Lmn	LQP
105	47	69	0.995838101	0.0671459	0.0655066	0.02586649
106	49	69	0.934822644	0.0294987	0.0293656	0.00774125
96	38	65	0.671044814	0.3560946	0.4083035	0.34624084
68	45	49	0.351790268	0.1015592	0.0931377	0.04993262
118	76	77	0.294331869	0.1698487	0.1620315	0.1044048
66	42	49	0.282822902	0.0115043	0.0109996	0.00545833
67	42	49	0.282822902	0.0115043	0.0109996	0.00545833
123	77	80	0.276842614	0.4921254	0.1040001	0.22439288
75	49	54	0.270197087	0.0576492	0.0660922	0.01893805
31	23	25	0.250769774	0.1848536	0.1804693	0.24133094
71	49	51	0.244030583	0.0546071	0.0618005	0.03889338
76	49	54	0.23515653	0.024589	0.0285817	0.00707807
148	80	96	0.233954509	0.1757954	0.1824076	0.10836865
29	22	23	0.229151364	0.1004014	0.0964905	0.06101914
62	45	46	0.226879795	0.1150512	0.1101352	0.07988026
100	62	66	0.224080464	0.1095431	0.1054709	0.05411609
38	26	30	0.220805102	0.1389215	0.1509644	0.17887963
33	25	27	0.210417361	0.0016346	0.0019839	0.00301659
167	100	106	0.207371638	0.0405284	0.0455713	0.01689235
120	75	77	0.204670058	0.1718095	0.1694571	0.08059348
141	89	92	0.199702528	0.4203358	0.0458301	0.09033626
37	8	30	0.197178943	0.2037121	0.2031242	0.45095662
54	30	38	0.184221626	0.2077792	0.2062872	0.39620347
4	3	5	0.181895679	0.077911	0.075119	0.07187999
166	103	105	0.171566924	0.0724844	0.0768944	0.04311756
155	94	100	0.159404546	0.1794183	0.181291	0.29801008
164	100	104	0.159254563	0.0399589	0.0433848	0.01930733
125	79	80	0.155727124	0.1264345	0.1248094	0.19020803
165	103	104	0.154501401	0.0882335	0.0916913	0.05543368
98	49	66	0.152846289	0.0191647	0.0184748	0.02496231
99	49	66	0.152846289	0.0191647	0.0184748	0.02496231
151	80	97	0.149015914	0.1126438	0.1150581	0.13575233
109	24	70	0.147751352	0.1227215	0.1388314	0.03399548
87	55	59	0.14750057	0.0385421	0.0371368	0.01876456
174	103	110	0.137074679	0.0495318	0.0524258	0.0273232
124	77	80	0.135326968	0.1144491	0.1133614	0.11389635
128	77	82	0.135095434	0.058372	0.0610021	0.06575813
160	100	101	0.134090455	0.1505314	0.1493386	0.127074
86	56	59	0.13400811	0.0245251	0.0230692	0.00734222
60	34	43	0.133251074	0.1662561	0.1637011	0.0970747
97	64	65	0.130760578	0.0810847	0.080579	0.28029538
116	69	75	0.128607132	0.276914	0.3925213	0.24174567
85	56	59	0.12781602	0.0223369	0.0231737	0.00694242

134	86	87	0.127457338	0.125028	0.1249054	0.06413062
84	54	59	0.126425229	0.0251309	0.0242543	0.01229615
153	80	99	0.125433603	0.0697222	0.0720996	0.03639124
103	66	67	0.124393725	0.0603403	0.0627264	0.06660831
65	47	49	0.123711081	0.1694466	0.173581	0.27096837
115	70	75	0.122688769	0.15836	0.1556625	0.10721795
48	33	37	0.116794671	0.0022571	0.0021537	0.0003683
81	50	57	0.114179054	0.0010962	0.0011714	0.00106191
39	17	31	0.111855473	0.0736105	0.0751988	0.04473458
114	70	74	0.111027035	0.0956265	0.0964418	0.06835971
70	49	50	0.1103165	0.0255472	0.0268028	0.03286917
184	12	117	0.108441018	0.071965	0.0734653	0.05044713
179	32	113	0.107312374	0.1343581	0.1363527	0.06343045
136	85	89	0.105778251	0.0268551	0.0263522	0.01803825
137	88	89	0.105256926	0.0365368	0.0356074	0.05414493
58	41	42	0.1036133	0.0037133	0.0035539	0.00070307
154	92	100	0.103575304	0.1897586	0.2001909	0.06772842
21	15	17	0.101048591	0.0250892	0.0242805	0.05607346
127	81	80	0.096767292	0.096718	0.0967673	0.28113096
74	53	54	0.096633525	0.0801619	0.0795636	0.06151514
16	11	13	0.096595598	0.0727064	0.0736428	0.0940436
14	3	12	0.095607686	0.067578	0.0667371	0.04128412
102	65	66	0.095117074	0.0947492	0.0951171	0.28146173
157	96	97	0.093586016	0.0692377	0.0684928	0.08061802
45	19	34	0.092374029	0.0628691	0.0593164	0.02176304
13	2	12	0.09154639	0.0563079	0.0554005	0.08779816
25	19	20	0.08933629	0.1134342	0.1121531	0.09207334
52	37	39	0.08849178	0.0697177	0.0704259	0.06232631
139	89	90	0.08507196	0.0070341	0.007378	0.00553483
152	80	98	0.083835362	0.0259514	0.0268581	0.02529989
8	8	5	0.082026533	0.0808101	0.0820265	0.33969277
53	37	40	0.078090501	0.0764229	0.0765536	0.04123866
11	5	11	0.075545905	0.0099036	0.0104063	0.01652061
23	17	18	0.075252177	0.0259274	0.0266625	0.05049918
7	8	9	0.072262965	0.029114	0.0289923	0.10888421
94	63	64	0.068369491	0.0470637	0.0467492	0.2378626
147	94	95	0.068016101	0.0538563	0.0542558	0.11713781
89	59	61	0.067371666	0.0537178	0.0515947	0.03447233
170	105	107	0.065962629	0.0146514	0.015082	0.00568467
22	16	17	0.065566626	0.0297087	0.0286194	0.01437678
101	62	67	0.065465525	0.0255258	0.0250863	0.02454827
156	95	96	0.06508512	0.0478415	0.047451	0.08247966
36	30	17	0.064115996	0.0631215	0.064116	0.16769059
19	14	15	0.063823824	0.1180653	0.1152006	0.0566595
185	75	118	0.063547015	0.0100313	0.0103312	0.01724865
10	4	11	0.063025002	0.0120076	0.0125296	0.01928215
57	40	42	0.061923426	0.0500811	0.0478483	0.02397924
126	68	81	0.059206517	0.0548929	0.0550284	0.29420314

41	23	32	0.056119854	0.1622712	0.1905204	0.14261877
28	21	22	0.055089022	0.0095716	0.009325	0.00717631
119	69	77	0.054278851	0.40316	0.5416821	0.43013921
72	51	52	0.054026882	0.0152177	0.0155355	0.02105446
20	12	16	0.053800211	0.0669269	0.0665024	0.07907288
1	1	2	0.051789968	0.028043	0.0277341	0.02753057
144	92	93	0.050343231	0.0094853	0.0098052	0.0128409
131	83	85	0.0492691	0.0031887	0.0031152	0.00020454
142	89	92	0.049088009	0.0563648	0.0602343	0.03899735
132	84	85	0.048467256	0.0104438	0.0102563	0.01568135
145	92	94	0.047770354	0.049857	0.0527998	0.03285312
181	27	115	0.047320468	0.0317983	0.0320617	0.04013811
24	18	19	0.045780069	0.0422774	0.0423542	0.08272239
80	56	57	0.043305627	0.0205394	0.0199505	0.0169734
88	59	60	0.042650976	0.0564368	0.0544456	0.03762749
34	27	28	0.0423012	0.0046093	0.0047073	0.00341944
51	38	37	0.041757442	0.0411968	0.0417574	0.10378484
169	105	106	0.041056875	0.0352733	0.0353786	0.05988292
2	1	3	0.040835753	0.0093188	0.0091815	0.02194598
44	15	33	0.040249211	0.0958016	0.0933908	0.07074586
93	63	59	0.039635877	0.0391404	0.0396359	0.10060142
5	5	6	0.039434541	0.0215214	0.0223101	0.04365127
12	11	12	0.038631862	0.0568804	0.0574116	0.28177092
61	44	45	0.03838625	0.0304034	0.0295333	0.02940767
73	52	53	0.038352698	0.0055403	0.0056418	0.00122641
138	89	90	0.038116662	0.0016658	0.0062127	0.00514773
17	12	14	0.034509148	0.0346183	0.0346204	0.04626748
56	40	41	0.033746051	0.0388671	0.0387691	0.07370577
26	15	19	0.033445217	0.0399452	0.0398171	0.09376912
143	91	92	0.033313791	0.0529153	0.0534684	0.04190506
69	48	49	0.032623609	0.0034303	0.0033722	0.00498369
64	46	48	0.032303337	0.0200041	0.0195445	0.00878449
47	35	37	0.029837514	0.0054146	0.0053538	0.01275227
18	13	15	0.029059533	0.0342651	0.0333461	0.01101855
108	69	70	0.028788608	0.3380812	0.4635077	0.29770231
82	56	58	0.028608011	0.056018	0.0552891	0.04948796
32	26	25	0.028427797	0.0284104	0.0284278	0.08207776
172	106	107	0.028027759	0.0170405	0.0174733	0.01043909
121	77	78	0.028000033	0.0129729	0.0130738	0.10436053
175	109	110	0.027810625	0.0350486	0.0351831	0.04330742
176	110	111	0.027603662	0.0063811	0.0062808	0.00622868
27	20	21	0.026823885	0.0668276	0.0656464	0.07115537
159	99	100	0.026227596	0.053051	0.0538198	0.07135573
63	46	47	0.0256305	0.145906	0.1388418	0.11481002
40	29	31	0.025547546	0.0204899	0.0204394	0.05841918
180	32	114	0.025378436	0.0140967	0.0141801	0.02046224
168	104	105	0.02453085	0.0034951	0.0035338	0.0070815
133	85	86	0.023643279	0.0172325	0.0176203	0.01562394

140	90	91	0.023635074	0.0149881	0.0150568	0.01559323
43	27	32	0.02340191	0.0188878	0.0189335	0.02166381
91	60	62	0.023333373	0.015094	0.0150343	0.02951488
59	43	44	0.023282058	0.1437296	0.1374471	0.0530475
113	71	73	0.02134447	0.0221211	0.0221301	0.05186565
163	100	103	0.020281889	0.0763419	0.0807417	0.15259106
55	39	40	0.018821348	0.001753	0.0017387	0.00455591
9	9	10	0.018060659	0.0608308	0.0606088	0.22178913
186	76	118	0.017533148	0.0481054	0.0474084	0.07710848
161	92	102	0.017383969	0.0079356	0.0080445	0.01638652
3	4	5	0.016348317	0.0071579	0.007126	0.09516938
95	64	61	0.016331446	0.0163095	0.0163314	0.06546309
49	34	36	0.016228178	0.0011824	0.0011916	0.00238243
158	98	100	0.015545302	0.0092683	0.0093962	0.0074415
77	54	55	0.015270932	0.0081346	0.0081649	0.00902308
42	31	32	0.014611373	0.0855012	0.0828321	0.079604
183	68	116	0.014592991	0.0146958	0.0146967	0.39734502
90	60	61	0.013379217	0.0053843	0.0053374	0.03954777
122	78	79	0.013102214	0.0143317	0.0143406	0.06298616
83	51	58	0.012999809	0.0259271	0.0264655	0.03357647
104	65	68	0.012898894	0.0499692	0.0496243	0.34111869
30	23	24	0.012798872	0.0786008	0.0756552	0.15798692
111	24	72	0.012494454	0.1758807	0.1666264	0.0892301
92	61	62	0.011788265	0.024613	0.0247769	0.06958444
149	82	96	0.01145904	0.0142633	0.0142872	0.02735736
112	71	72	0.010042302	0.1612361	0.1787843	0.0916322
107	68	69	0.009905102	0.0092973	0.0099051	0.02573081
35	28	29	0.009609715	0.033108	0.0335228	0.03502522
117	74	75	0.009576504	0.0622394	0.0607427	0.13930401
135	85	88	0.009455529	0.0497709	0.0489123	0.04808704
50	34	37	0.009104591	0.0087535	0.0086784	0.09009545
79	55	56	0.008385997	0.0013285	0.0013239	0.00975833
150	94	96	0.008315527	0.0105881	0.0105782	0.00979771
110	70	71	0.007533469	0.0390916	0.0397562	0.11184946
129	82	83	0.007161249	0.0144416	0.0143915	0.03549918
162	101	102	0.00686788	0.0378299	0.0370994	0.03229801
6	6	7	0.004342109	0.0049496	0.0049733	0.02621043
78	54	56	0.004324452	0.001783	0.0017853	0.01537342
46	35	36	0.004255904	0.0048659	0.0048674	0.04962306
15	7	12	0.003872195	0.0116189	0.0116649	0.03624668
146	93	94	0.002802709	0.0414907	0.0423535	0.05608923
177	110	112	0.002061433	0.0470903	0.0482389	0.06826034
171	105	108	0.001839149	0.0203604	0.0205968	0.02781352
173	108	109	0.001821672	0.0095164	0.0095536	3.16E-02
182	114	115	0.001249541	0.0004099	0.0004101	0.00192193
130	83	84	0.000702332	0.0462798	0.0452731	0.02776521
178	17	113	0.000519391	0.0029775	0.0029739	0.00793426

From the above table5.12 and figure5.30 it is clear that LCPI is capable for accurate prediction of voltage instability. The LCPI value for critical branch number 105 is 0.995838 and branch number 106 is 0.934822 which approaches to critical limit '1'(as shown in figure 5.31 and 5.32) but other indices are not approaches nearer to unity for any branch. Hence LCPI is predicting the accurate voltage stability for IEEE-118 bus system also. The LQP index results are very far away from critical limit of stability.

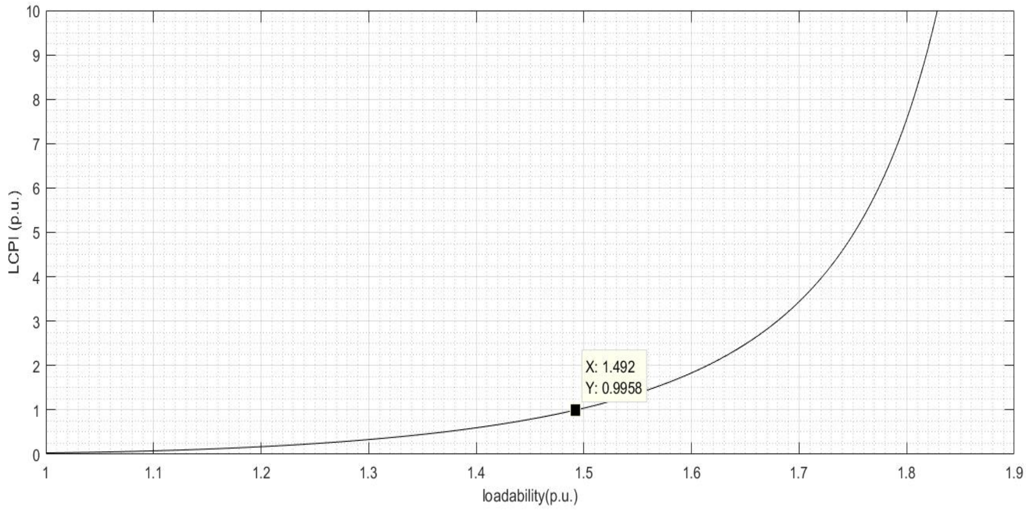

Figure5.31: IEEE-118 bus heavy MVA loading critical line-105 v/s LCPI.

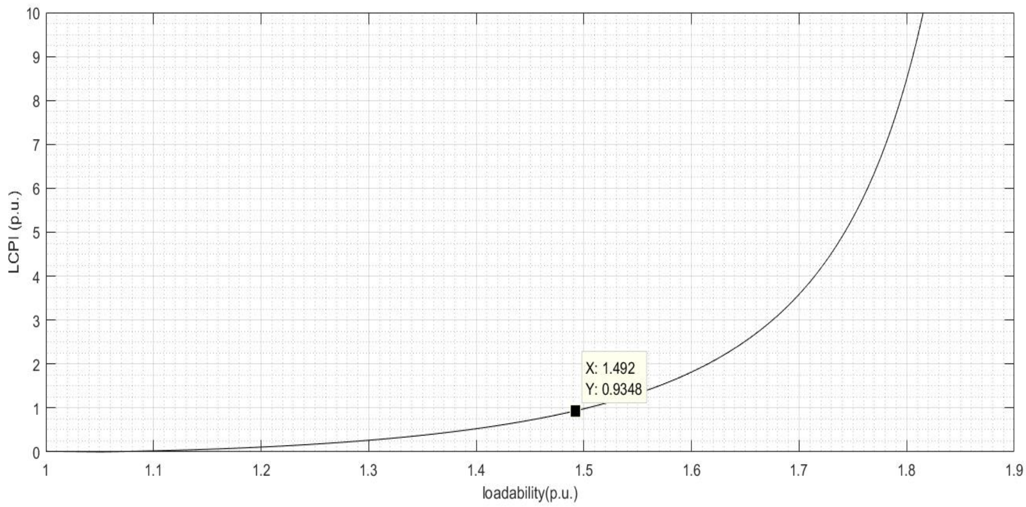

Figure5.32: IEEE-118 bus heavy MVA loading, critical line-106 v/s LCPI.

5.2.3 IEEE-118 bus heavy active loading

The simulation results for heavy active loading with taking loadability factor λ = 1.492 p.u. are shown in table 5.12 and figure5.13.

Table 5.13: IEEE 118 Bus base test system with heavy active loading λ = 1.492 p.u.

Branch Number	From Bus	To Bus	LCPI	FVSI	Lmn	LQP
105	47	69	0.994606509	0.0667817	0.0651423	0.02573829
106	49	69	0.933166275	0.0299472	0.0298055	0.00788586
96	38	65	0.665797887	0.3528329	0.404256	0.34333914
68	45	49	0.295038382	0.0442703	0.040552	0.02331486
118	76	77	0.294263526	0.1699779	0.1621643	0.10448402
66	42	49	0.281888878	0.011346	0.0108474	0.00540992
67	42	49	0.281888878	0.011346	0.0108474	0.00540992
123	77	80	0.276899917	0.4930162	0.1041961	0.22479691
75	49	54	0.270364846	0.0582617	0.0667692	0.01915768
31	23	25	0.244857329	0.1786387	0.1743821	0.23387595
76	49	54	0.235384839	0.0252407	0.0293282	0.00731347
100	62	66	0.224010523	0.1095967	0.1055251	0.05414287
71	49	51	0.222998434	0.0307234	0.0348273	0.02107209
38	26	30	0.220218655	0.1384654	0.1504429	0.17828498
33	25	27	0.210652924	0.0012232	0.0014842	0.00272421
29	22	23	0.1997821	0.0716246	0.0688264	0.04471816
141	89	92	0.19968848	0.4205796	0.0458574	0.09038882
148	80	96	0.197704453	0.1377828	0.1431091	0.08453466
167	100	106	0.196477167	0.0288315	0.0324358	0.01148192
37	8	30	0.196406576	0.2028948	0.2023131	0.44913859
120	75	77	0.195862327	0.162211	0.1599294	0.07648205
54	30	38	0.183777528	0.2072811	0.2057937	0.39542799
4	3	5	0.176485424	0.0726047	0.0700015	0.06729691
62	45	46	0.173323555	0.0598663	0.057247	0.04343042
166	103	105	0.171590971	0.0726198	0.0770324	0.04320035
164	100	104	0.159311111	0.0401147	0.0435502	0.01938858
165	103	104	0.15451242	0.088305	0.0917621	0.05547885
98	49	66	0.152900544	0.019155	0.0184653	0.02495182
99	49	66	0.152900544	0.019155	0.0184653	0.02495182
87	55	59	0.147439586	0.0385914	0.0371852	0.01878742
109	24	70	0.14705165	0.1221539	0.1381473	0.03384803
174	103	110	0.137094898	0.0495975	0.0524935	0.02736065
124	77	80	0.135315832	0.1146051	0.1135244	0.11405028
125	79	80	0.13419952	0.1041186	0.1027404	0.15848814
86	56	59	0.133945018	0.0244072	0.0229595	0.00729679
97	64	65	0.130695746	0.0810443	0.0805385	0.28016173

85	56	59	0.127752481	0.022233	0.0230672	0.0069003
84	54	59	0.126374461	0.0251785	0.0243008	0.01231719
153	80	99	0.125625315	0.0706141	0.0729878	0.03687918
65	47	49	0.123616129	0.1692162	0.173332	0.27061319
155	94	100	0.122461362	0.1394954	0.1407436	0.23596796
151	80	97	0.122287547	0.0846567	0.0865304	0.1015629
116	69	75	0.12153428	0.2839719	0.4025284	0.24786124
103	66	67	0.117646754	0.0532569	0.0553729	0.05857064
115	70	75	0.115707016	0.1508554	0.1483283	0.10204806
81	50	57	0.113996307	0.0012212	0.0013047	0.00097063
39	17	31	0.113063215	0.0747559	0.0763721	0.04548955
160	100	101	0.112566259	0.1280265	0.1270773	0.10779828
114	70	74	0.111032619	0.0957643	0.0965738	0.0684596
134	86	87	0.110005366	0.1072895	0.1071693	0.05572437
179	32	113	0.107284219	0.133982	0.1359461	0.06325932
136	85	89	0.105663475	0.0268559	0.026353	0.01803998
70	49	50	0.104688528	0.0192024	0.0201538	0.02424525
48	33	37	0.103907713	0.0154315	0.0147206	0.00834768
154	92	100	0.103406184	0.1892435	0.1995961	0.06755082
21	15	17	0.102403577	0.0267495	0.0258905	0.05966289
128	77	82	0.097358325	0.0169354	0.0177313	0.01776383
127	81	80	0.096819827	0.096771	0.0968198	0.2812903
60	34	43	0.096751595	0.1287176	0.1268192	0.07473758
137	88	89	0.096085792	0.0273621	0.0266645	0.04118351
58	41	42	0.095413414	0.0118819	0.0113709	0.00634934
102	65	66	0.095103625	0.0947352	0.0951036	0.28141867
45	19	34	0.092217402	0.0626477	0.0591138	0.02167867
14	3	12	0.089564297	0.0611238	0.060351	0.03762037
184	12	117	0.085923253	0.0482339	0.0492701	0.03320048
139	89	90	0.085070453	0.0070281	0.0073717	0.0055273
13	2	12	0.083896204	0.0481263	0.0473383	0.07557719
8	8	5	0.081235781	0.0800328	0.0812358	0.33640633
52	37	39	0.080856667	0.0611561	0.0618072	0.05448478
16	11	13	0.079888555	0.054608	0.0553505	0.07049649
157	96	97	0.079637564	0.0550542	0.0544545	0.06583215
53	37	40	0.079455081	0.0775307	0.0776735	0.04189366
23	17	18	0.076544098	0.027447	0.0282214	0.05360289
152	80	98	0.07399088	0.015948	0.0165058	0.01483328
101	62	67	0.073103467	0.0334578	0.0328866	0.03160281
7	8	9	0.072262965	0.029114	0.0289923	0.10888544
94	63	64	0.068353769	0.047058	0.0467435	0.2378394
11	5	11	0.067736586	0.0183378	0.0192748	0.02902745
89	59	61	0.067336146	0.0536973	0.0515756	0.03445729
25	19	20	0.066468687	0.0900388	0.0890492	0.07270074
170	105	107	0.065989676	0.0148552	0.0152902	0.00578825
19	14	15	0.064836662	0.1190931	0.1162018	0.05719897
36	30	17	0.063773693	0.0627873	0.0637737	0.16686803
74	53	54	0.063266956	0.0456326	0.0452657	0.03635595

57	40	42	0.061751126	0.0496838	0.0474778	0.0237731
41	23	32	0.061720275	0.1557525	0.1827135	0.13731269
1	1	2	0.059286234	0.0362179	0.0358309	0.03501802
126	68	81	0.059203246	0.0549116	0.0550464	0.29430726
185	75	118	0.058620876	0.0048568	0.0050025	0.00743125
10	4	11	0.054315872	0.0214223	0.0223617	0.03295138
22	16	17	0.054229157	0.041134	0.0396205	0.02075455
119	69	77	0.053378154	0.4015856	0.5390606	0.42846788
156	95	96	0.05272733	0.034862	0.0345665	0.06222815
80	56	57	0.049710372	0.0133818	0.0130029	0.01041263
28	21	22	0.049481644	0.0146279	0.014253	0.0121947
142	89	92	0.049079454	0.0563933	0.0602657	0.03901738
147	94	95	0.047623443	0.0319765	0.0322378	0.06997929
72	51	52	0.047178113	0.0081133	0.0082836	0.01051173
2	1	3	0.04664146	0.015655	0.0154285	0.03561146
24	18	19	0.045781923	0.0423897	0.0424643	0.08294578
88	59	60	0.043242083	0.055792	0.0538245	0.03717522
20	12	16	0.041977723	0.0543719	0.054047	0.06389103
51	38	37	0.041912503	0.0413521	0.0419125	0.10426
64	46	48	0.040905239	0.0108497	0.0106035	0.00391667
5	5	6	0.040313719	0.0204875	0.0212363	0.04166152
172	106	107	0.040294973	0.0036513	0.0037419	0.00370305
181	27	115	0.040024185	0.0241814	0.0243857	0.03007922
93	63	59	0.039698561	0.0392028	0.0396986	0.10076526
73	52	53	0.038631769	0.0063884	0.0065032	0.00175283
138	89	90	0.038115525	0.0016677	0.0062196	0.00515261
34	27	28	0.033606693	0.004526	0.0046233	0.0070254
17	12	14	0.033471971	0.0334657	0.0334697	0.04466419
26	15	19	0.033443592	0.0400374	0.0399072	0.09398873
143	91	92	0.033314431	0.0529275	0.053481	0.04191551
132	84	85	0.030279375	0.0107175	0.0105096	0.01246959
47	35	37	0.029454482	0.0050762	0.0050192	0.01208139
12	11	12	0.029375371	0.0467301	0.0471454	0.23285589
169	105	106	0.028955261	0.0224342	0.0225097	0.03741151
32	26	25	0.028417437	0.0283999	0.0284174	0.08204554
108	69	70	0.027982714	0.3369453	0.4616275	0.29670956
176	110	111	0.027603662	0.0063811	0.0062808	0.00622745
144	92	93	0.027215958	0.0347572	0.0359696	0.04212571
44	15	33	0.027169987	0.0816848	0.0796716	0.06004727
61	44	45	0.0268317	0.0411738	0.0400031	0.04173928
56	40	41	0.026239524	0.0306115	0.0305458	0.05765596
159	99	100	0.026188484	0.0527292	0.0534847	0.07093537
158	98	100	0.025994308	0.0022837	0.0023138	0.00046626
63	46	47	0.025513796	0.1459315	0.1388597	0.11482915
168	104	105	0.024533566	0.0035337	0.0035728	0.00717899
175	109	110	0.024354701	0.0311632	0.0312761	0.03877517
69	48	49	0.024102303	0.0129441	0.0127186	0.02404392
140	90	91	0.023634891	0.0149804	0.0150491	0.015583

43	27	32	0.023403279	0.0189966	0.0190415	0.021798
91	60	62	0.022713815	0.0144531	0.0143957	0.02834944
122	78	79	0.021916678	0.0235295	0.0235486	0.10276987
113	71	73	0.021329998	0.0221061	0.0221151	0.05183332
40	29	31	0.021065263	0.0155669	0.0155251	0.0449236
83	51	58	0.020583175	0.0172629	0.0176116	0.02323751
163	100	103	0.020301366	0.0762483	0.0806388	0.15240747
180	32	114	0.018474826	0.0068291	0.0068708	0.00895794
9	9	10	0.018060659	0.0608308	0.0606088	0.2217879
121	77	78	0.017283837	0.0013088	0.0013196	0.00886442
3	4	5	0.017216259	0.0080729	0.0080372	0.10710082
130	83	84	0.016577704	0.0653519	0.0638695	0.04071188
95	64	61	0.016299154	0.0162773	0.0162992	0.06533952
49	34	36	0.016227056	0.0011498	0.0011587	0.00226422
27	20	21	0.015383797	0.0547815	0.053829	0.05872742
77	54	55	0.015271274	0.0081457	0.008176	0.00903672
42	31	32	0.014648028	0.0853477	0.0826897	0.07945656
145	92	94	0.014592631	0.0858727	0.0910775	0.05525045
183	68	116	0.014559626	0.0146622	0.0146631	0.39644852
131	83	85	0.013605593	0.0414977	0.0404871	0.02536107
149	82	96	0.013383544	0.015842	0.0158658	0.03076438
104	65	68	0.012919929	0.049948	0.049603	0.34097207
90	60	61	0.012765376	0.0060135	0.0059611	0.04439824
146	93	94	0.012655135	0.0518394	0.0529298	0.07041914
111	24	72	0.012621388	0.1758201	0.166574	0.08919754
129	82	83	0.012581849	0.0202049	0.0201312	0.05147728
82	56	58	0.011877579	0.0376786	0.0372188	0.03267951
92	61	62	0.011788171	0.0246115	0.0247754	0.06958156
50	34	37	0.010550411	0.0071176	0.0070572	0.07291062
107	68	69	0.010377749	0.0097428	0.0103777	0.02705168
112	71	72	0.009906517	0.1609168	0.1784016	0.09145629
55	39	40	0.009203282	0.008506	0.0084339	0.01134182
79	55	56	0.008386241	0.0013143	0.0013098	0.00967505
133	85	86	0.007684157	0.0344358	0.035233	0.02937589
30	23	24	0.007664682	0.0837426	0.0805998	0.16887968
110	70	71	0.007542943	0.0390634	0.0397267	0.11177148
161	92	102	0.007284195	0.0185411	0.0188004	0.03581524
162	101	102	0.006734495	0.0515708	0.0505687	0.04525724
59	43	44	0.005864654	0.1247988	0.1194142	0.04677933
35	28	29	0.005090047	0.0282358	0.0285844	0.03027015
186	76	118	0.00490767	0.0343857	0.0339061	0.05458826
78	54	56	0.004324649	0.001809	0.0018113	0.01562371
6	6	7	0.003825879	0.005456	0.0054821	0.02870394
15	7	12	0.003349368	0.0109943	0.0110373	0.03440737
46	35	36	0.002434675	0.0029487	0.0029495	0.03082796
173	108	109	0.002376959	0.0101456	0.0101857	0.0336182
18	13	15	0.002104821	0.0628097	0.0610728	0.0220555
177	110	112	0.002061433	0.0470903	0.0482389	0.06826157

117	74	75	0.002019278	0.0540307	0.0527487	0.1206862
178	17	113	0.00184179	0.0043715	0.0043661	0.01252357
150	94	96	0.001059388	0.0004199	0.0004197	0.00138153
171	105	108	0.00100656	0.0236253	0.0239046	0.03197815
135	85	88	0.000952481	0.0410173	0.0403151	0.03930301
182	114	115	0.000730353	0.0001365	0.0001365	0.00311139

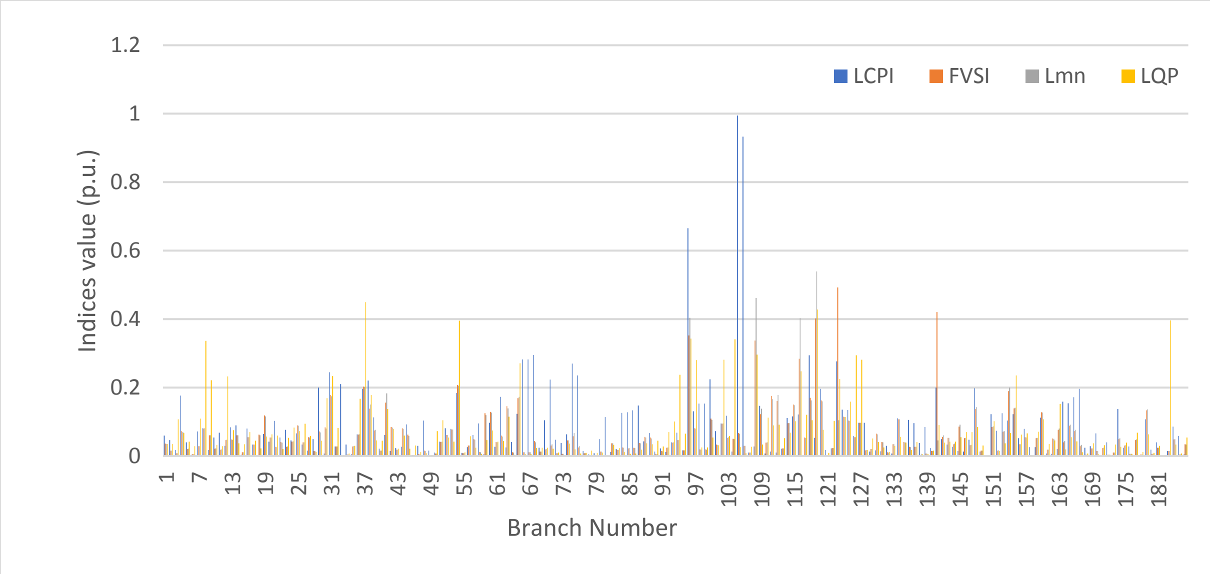

Figure 5.33: IEEE-118 bus heavy active loading (λ=1.492) bar chart branch v/s Indices.

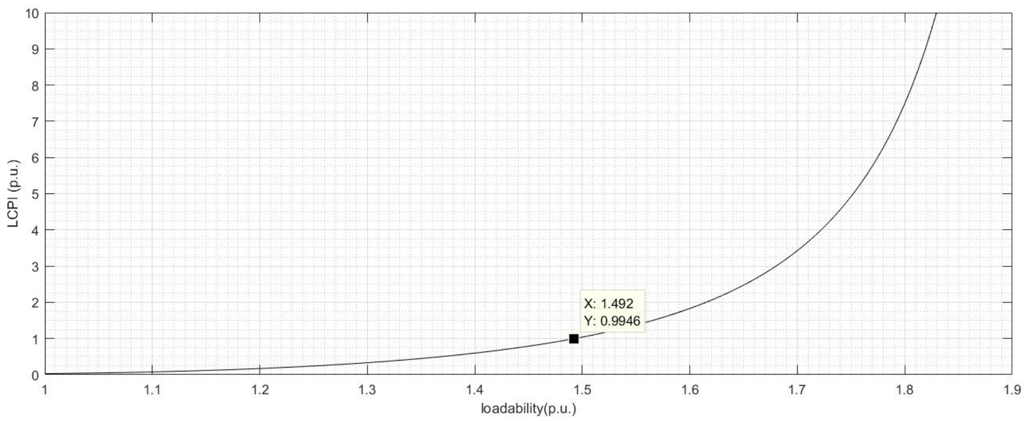

Figure 5.34: IEEE-118 bus heavy active loading, critical line-105 v/s LCPI.

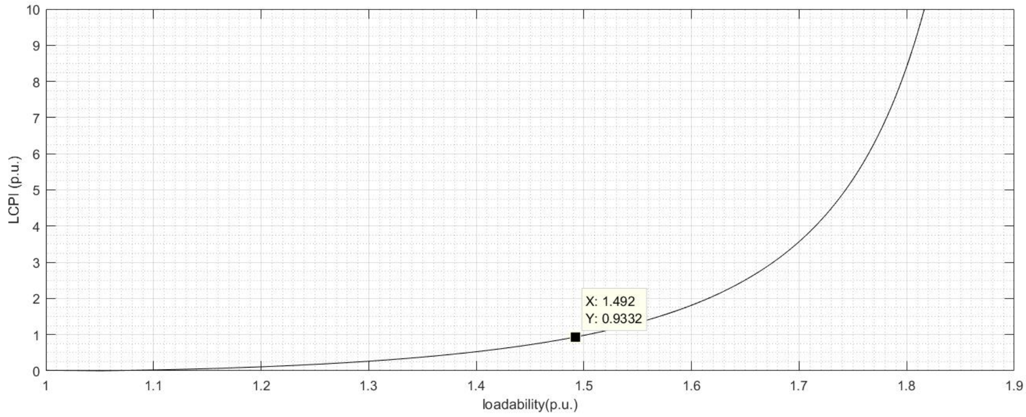

Figure 5.35: IEEE-118 bus heavy active loading, critical line-106 v/s LCPI.

The observations are almost similar to the IEEE-118 bus heavy MVA loading case.

5.2.4 IEEE-118 bus heavy reactive loading

The simulation is done for heavy reactive loading with taking loadability factor **λ** = 6.32 p.u. and results are shown in table 5.14 and figure 5.36.

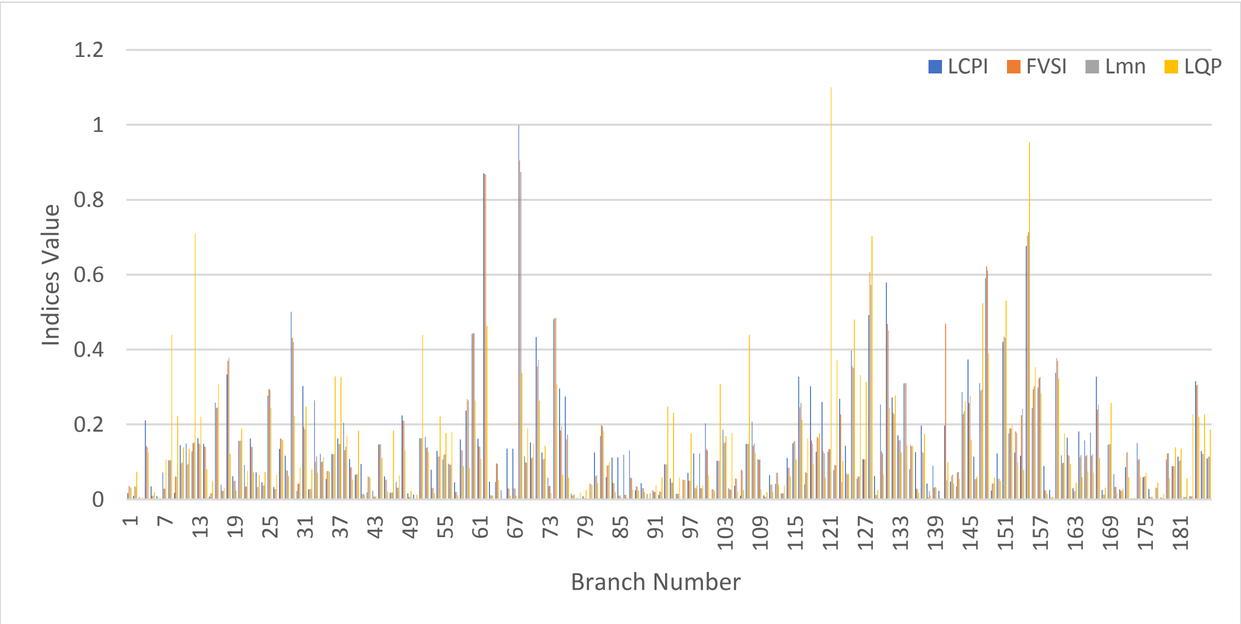

Figure 5.36: IEEE-118 bus heavy reactive loading(λ=6.32) bar chart branch v/s indices.

Table 5.14: IEEE 118 Bus base test system with heavy Reactive loading λ = 6.32 p.u.

Branch Number	From Bus	To Bus	LCPI	FVSI	Lmn	LQP
68	45	49	0.999818	0.904677	0.874336	0.337549
62	45	46	0.870886	0.867869	0.867171	0.46362
155	94	100	0.676554	0.704008	0.713452	0.953022
148	80	96	0.590424	0.621912	0.611317	0.389241
131	83	85	0.579846	0.468598	0.450183	0.244846
29	22	23	0.50051	0.431558	0.421032	0.223322
128	77	82	0.492374	0.607633	0.572996	0.703098
74	53	54	0.481527	0.484096	0.484757	0.307847
60	34	43	0.441646	0.444051	0.443611	0.263536
71	49	51	0.433723	0.354678	0.372551	0.263951
151	80	97	0.42053	0.435061	0.431638	0.530778
125	79	80	0.397471	0.356145	0.350237	0.480843
145	92	94	0.373558	0.257373	0.277498	0.159365
160	100	101	0.337458	0.377386	0.370057	0.322535
18	13	15	0.333915	0.370433	0.377741	0.12218
167	100	106	0.327862	0.239691	0.253667	0.110165
116	69	75	0.327847	0.245448	0.257986	0.211956
184	12	117	0.315794	0.304838	0.306792	0.220847
147	94	95	0.310665	0.289645	0.293089	0.52375
134	86	87	0.309862	0.310434	0.310575	0.143668
31	23	25	0.302658	0.193221	0.186981	0.248095
118	76	77	0.301975	0.157045	0.148943	0.095504
157	96	97	0.298618	0.322597	0.326613	0.282921
75	49	54	0.296097	0.184234	0.195523	0.065754
144	92	93	0.287042	0.227647	0.235738	0.263104
25	19	20	0.277516	0.295223	0.292585	0.243764
76	49	54	0.274576	0.160633	0.172843	0.057644
132	84	85	0.271717	0.231034	0.226838	0.277566
123	77	80	0.268371	0.226861	0.046909	0.103268
33	25	27	0.264169	0.100741	0.115121	0.071221
120	75	77	0.260335	0.128913	0.122736	0.058922
16	11	13	0.258185	0.243881	0.245829	0.307709
130	83	84	0.253517	0.128151	0.121489	0.067
156	95	96	0.244069	0.294576	0.302281	0.353466
59	43	44	0.236732	0.267933	0.264017	0.083281
48	33	37	0.224295	0.210822	0.209605	0.131627
4	3	5	0.211773	0.142368	0.138585	0.125529
108	69	70	0.207363	0.143442	0.149153	0.124845
38	26	30	0.204291	0.131437	0.141073	0.170313
100	62	66	0.203399	0.134	0.130502	0.064615
141	89	92	0.196788	0.469446	0.051339	0.099505
137	88	89	0.196759	0.127017	0.123821	0.175117
103	66	67	0.185847	0.149886	0.153019	0.169371

164	100	104	0.18188	0.113517	0.118448	0.059425
166	103	105	0.178154	0.116596	0.1208	0.071653
152	80	98	0.17616	0.190509	0.189161	0.198627
133	85	86	0.171013	0.157785	0.158946	0.125438
82	56	58	0.170067	0.198504	0.195715	0.18124
52	37	39	0.166699	0.137301	0.139548	0.125935
162	101	102	0.164646	0.118247	0.11598	0.094737
51	38	37	0.163907	0.162903	0.163907	0.439213
13	2	12	0.163651	0.149329	0.148339	0.221085
22	16	17	0.162931	0.140783	0.139437	0.073435
37	8	30	0.162863	0.147145	0.148679	0.32639
61	44	45	0.162185	0.141723	0.140414	0.108402
58	41	42	0.159882	0.131777	0.13014	0.088396
165	103	104	0.158114	0.115981	0.118772	0.074618
20	12	16	0.156026	0.156808	0.156761	0.18892
70	49	50	0.151888	0.110045	0.1126	0.148873
174	103	110	0.151228	0.105497	0.108398	0.061455
115	70	75	0.15014	0.155101	0.154742	0.106143
11	5	11	0.149097	0.092427	0.095443	0.135572
14	3	12	0.14862	0.140279	0.139809	0.080544
107	68	69	0.148243	0.14786	0.148243	0.43932
44	15	33	0.146997	0.147081	0.147127	0.110774
169	105	106	0.145585	0.147457	0.147308	0.257389
10	4	11	0.144787	0.096238	0.098883	0.139035
124	77	80	0.143606	0.068932	0.066805	0.068165
66	42	49	0.135754	0.02985	0.028788	0.010043
67	42	49	0.135754	0.02985	0.028788	0.010043
27	20	21	0.134891	0.162986	0.160823	0.158962
87	55	59	0.130636	0.058226	0.056631	0.026233
54	30	38	0.12934	0.113927	0.115078	0.221474
185	75	118	0.128718	0.12143	0.1219	0.227217
12	11	12	0.128286	0.150263	0.151929	0.709652
121	77	78	0.127562	0.134445	0.133974	1.100036
119	69	77	0.127376	0.166506	0.163472	0.176204
136	85	89	0.126449	0.028709	0.028197	0.017986
153	80	99	0.125625	0.181642	0.177294	0.098947
81	50	57	0.124951	0.062303	0.064534	0.043213
72	51	52	0.124919	0.10683	0.107864	0.142979
150	94	96	0.122918	0.054073	0.056236	0.048068
98	49	66	0.122641	0.030753	0.029811	0.037768
99	49	66	0.122641	0.030753	0.029811	0.037768
34	27	28	0.121921	0.100001	0.101212	0.113643
36	30	17	0.121416	0.12048	0.121416	0.328702
86	56	59	0.118953	0.012261	0.011735	0.005275
161	92	102	0.117177	0.096696	0.097782	0.17645
28	21	22	0.116945	0.078152	0.076858	0.063129
154	92	100	0.116467	0.225531	0.242242	0.078977
69	48	49	0.115052	0.098921	0.09817	0.190098

146	93	94	0.114186	0.05329	0.055147	0.060102
181	27	115	0.113987	0.102928	0.103541	0.135232
85	56	59	0.112495	0.010156	0.010721	0.004678
84	54	59	0.111852	0.044471	0.043318	0.019165
114	70	74	0.110415	0.084193	0.085414	0.061135
186	76	118	0.109149	0.114213	0.113926	0.186785
39	17	31	0.108279	0.085276	0.086374	0.053145
109	24	70	0.107504	0.105794	0.106264	0.027032
127	81	80	0.107002	0.106922	0.107002	0.313737
179	32	113	0.106583	0.122553	0.123658	0.05685
55	39	40	0.10628	0.119239	0.120026	0.177205
8	8	5	0.104917	0.104092	0.104917	0.439264
102	65	66	0.103395	0.103394	0.103395	0.308482
56	40	41	0.095393	0.092995	0.093111	0.180098
41	23	32	0.094775	0.013979	0.014958	0.012666
93	63	59	0.093943	0.093613	0.093943	0.248602
21	15	17	0.092004	0.034561	0.03369	0.075374
139	89	90	0.090671	0.031622	0.032746	0.032518
158	98	100	0.089795	0.024546	0.023913	0.014809
180	32	114	0.088647	0.08846	0.088473	0.139334
172	106	107	0.086133	0.124266	0.126858	0.059896
135	85	88	0.081008	0.144602	0.140949	0.144404
53	37	40	0.079016	0.030349	0.031181	0.016462
122	78	79	0.078154	0.092151	0.09152	0.372205
7	8	9	0.072263	0.029114	0.028992	0.107714
23	17	18	0.0721	0.03272	0.033443	0.06521
97	64	65	0.070809	0.050455	0.050116	0.176378
170	105	107	0.068105	0.033397	0.034049	0.016494
40	29	31	0.065257	0.067573	0.067653	0.183688
111	24	72	0.065052	0.039346	0.039915	0.019695
19	14	15	0.0622	0.04967	0.050038	0.023871
129	82	83	0.062012	0.012178	0.011906	0.025341
45	19	34	0.060937	0.052892	0.052763	0.020546
83	51	58	0.059924	0.090412	0.091844	0.099527
175	109	110	0.058778	0.060967	0.061046	0.071721
73	52	53	0.058018	0.036059	0.036497	0.016553
94	63	64	0.056045	0.045102	0.044905	0.230774
126	68	81	0.05525	0.061415	0.06125	0.331579
35	28	29	0.054523	0.075624	0.076462	0.073396
63	46	47	0.047748	0.011214	0.011028	0.009646
142	89	92	0.047343	0.062105	0.066569	0.04161
64	46	48	0.046934	0.096476	0.094325	0.050608
47	35	37	0.046356	0.031412	0.031191	0.063505
57	40	42	0.046013	0.020556	0.020325	0.011282
24	18	19	0.04563	0.037016	0.037182	0.073367
89	59	61	0.04301	0.030215	0.029354	0.01975
138	89	90	0.042509	0.005927	0.021823	0.011053
112	71	72	0.041843	0.071771	0.070795	0.039397

117	74	75	0.040088	0.072063	0.070964	0.162754
17	12	14	0.039224	0.022899	0.023095	0.031148
105	47	69	0.03613	0.056517	0.054404	0.02048
143	91	92	0.034735	0.072134	0.07359	0.055283
5	5	6	0.034501	0.009647	0.009891	0.019327
26	15	19	0.033456	0.027783	0.027864	0.065826
104	65	68	0.029654	0.025991	0.026044	0.177714
163	100	103	0.029348	0.022017	0.022644	0.044153
176	110	111	0.027604	0.006381	0.006281	0.007399
32	26	25	0.027476	0.027447	0.027476	0.080403
171	105	108	0.027063	0.023157	0.023207	0.028849
159	99	100	0.025371	0.005269	0.00522	0.007583
168	104	105	0.025052	0.012693	0.012774	0.031755
65	47	49	0.024771	0.000646	0.000639	0.001755
88	59	60	0.024693	0.034648	0.033808	0.023556
91	60	62	0.024672	0.020572	0.020531	0.038357
149	82	96	0.023963	0.0425	0.042127	0.058831
140	90	91	0.023168	0.002812	0.002842	0.002593
30	23	24	0.023165	0.042108	0.042528	0.085314
43	27	32	0.023096	0.007562	0.007624	0.008735
42	31	32	0.018952	0.061662	0.060448	0.058064
9	9	10	0.018061	0.060831	0.060609	0.222959
46	35	36	0.017771	0.018852	0.018862	0.184529
1	1	2	0.016611	0.035409	0.035093	0.031746
49	34	36	0.016384	0.006684	0.006717	0.023243
113	71	73	0.015626	0.016195	0.016199	0.037399
77	54	55	0.015333	0.01053	0.010556	0.013395
95	64	61	0.015072	0.015071	0.015072	0.058928
90	60	61	0.014157	0.002151	0.002139	0.017205
50	34	37	0.012402	0.001121	0.001115	0.012454
92	61	62	0.011588	0.020965	0.021066	0.058375
110	70	71	0.011224	0.006512	0.006497	0.019005
106	49	69	0.009773	0.079212	0.076953	0.025075
2	1	3	0.009528	0.034771	0.034351	0.074303
6	6	7	0.00837	0.001023	0.001027	0.004355
79	55	56	0.008347	0.004209	0.0042	0.025733
183	68	116	0.008311	0.00837	0.00837	0.226627
15	7	12	0.007868	0.016053	0.01612	0.048108
3	4	5	0.006434	0.000566	0.000564	0.006696
182	114	115	0.006137	0.006506	0.006505	0.057244
178	17	113	0.004749	0.004316	0.004315	0.014825
78	54	56	0.004326	0.002008	0.00201	0.018718
173	108	109	0.003214	0.001579	0.001581	0.004197
80	56	57	0.002619	0.042751	0.04195	0.038499
96	38	65	0.001249	0.052397	0.052039	0.052687
177	110	112	0.001093	0.031231	0.031738	0.044724
101	62	67	0.000401	0.026747	0.026426	0.023105

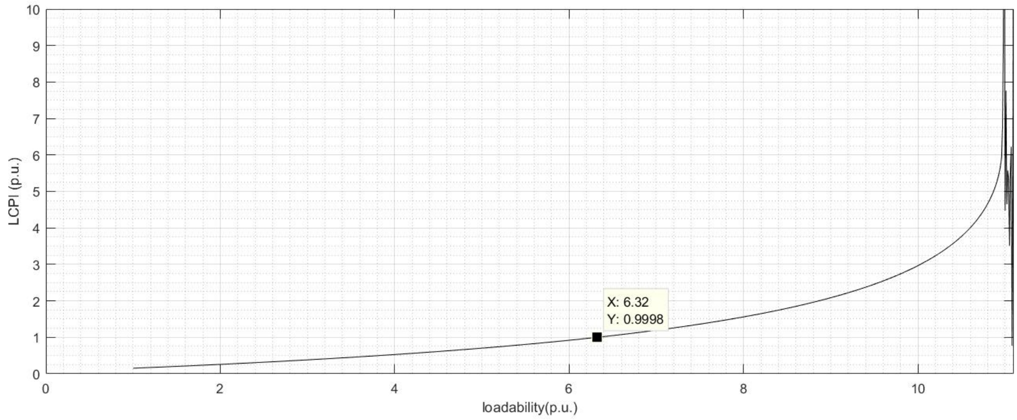

Figure 5.37: IEEE-118 bus heavy reactive loading, Critical branch-68 v/s LCPI.

Branch number 65 (45-49), become critical according to LCPI, FVSI and Lmn. but LQP shows it stable. According to the LQP index here branch number 121(77-78) become unstable and branch number 155(94-100) become critical. Hence from the comparable analysis it is clear that LCPI index predict accurate result, FVSI and Lmn also predicted marginable acceptable results but LQP results are not acceptable in any case.

5.2.5 IEEE-118 bus heavy active loading on single bus

The simulation on IEEE-118 bus system is done for heavy active loading on single bus as mentioned in second column of table 5.15. The most critical branch for each single bus is observed from the observed results which are mentioned in table5.15. the loadability verses LCPI index graph for some buses (2, 13, 52 ,115) also shown in figures 5.38, 5.40,5.42 and 5.44 and P-V curve also shown in figure 5.39, 5.41, 5.43 and 5.45 for verifying maximum active power loadability limit of the same buses.

Table 5.15: critical lines of IEEE 118 Bus system with Heavy active loading on single bus								
Load Bus	**loading (p.u)**	**Critical Branch**	**From Bus**	**To Bus**	**LCPI**	**FVSI**	**Lmn**	**LQP**
1	1.15	96	38	65	0.990294	0.527564	0.642106	0.766271
2	2.8	13	2	12	0.994973	0.463077	0.424224	0.647475
3	1.45	4	3	5	0.995207	0.443054	0.437669	0.449951
7	3.26	96	38	65	0.997191	0.531051	0.647145	0.502275
13	1.1	18	13	15	0.977996	0.413369	0.378856	0.122003
14	3.2	19	14	15	0.980915	0.334596	0.308286	0.128461
16	1.6	22	16	17	0.946439	0.404955	0.387082	0.179866
20	1.8	29	22	23	0.910569	0.591579	0.566844	0.28078
21	1.7	29	22	23	0.932551	0.584819	0.561667	0.278676
28	3.5	96	38	65	0.99494	0.527749	0.644085	0.50093
33	1.48	48	33	37	0.987319	0.477796	0.440577	0.248962
41	1.39	66	42	49	0.993065	0.237734	0.253537	0.075217
52	1.88	73	52	53	0.977532	0.629374	0.593023	0.196498
75	1.5	120	75	77	0.999571	0.329569	0.305493	0.134681
83	2.9	131	83	85	0.925197	0.603603	0.559755	0.292365
93	5.2	146	93	94	0.938093	0.423307	0.387457	0.37976
101	2.2	162	101	102	0.992803	0.523013	0.509041	0.310258
110	1.3	174	103	110	0.97136	1.118438	2.499626	0.659422
112	1.7	174	103	110	0.945601	1.103253	2.43689	0.650478
114	7.8	96	38	65	0.967186	0.512997	0.623356	0.488171
115	2.9	96	38	65	0.978202	0.51854	0.631369	0.493129
118	1.9	118	76	77	0.968008	0.164664	0.156713	0.100104

For load bus 110 and 112 LCPI predicted 174(103-110) as critical branche but FVSI and Lmn shows that this branch crosses the voltage stability limit and become unstable. It is happened due to the consideration of shunt branch admittance for LCPI calculation which is not considered in FVSI and Lmn index, hence there are still stability margin available to reach the instability stage.

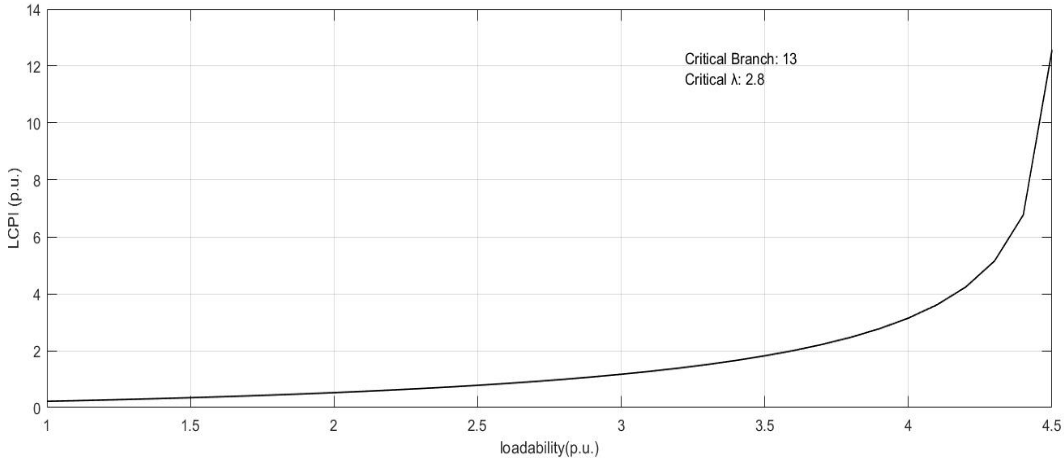

Figure 5.38: IEEE-118 bus heavy active loading (c) at bus-2 v/s LCPI.

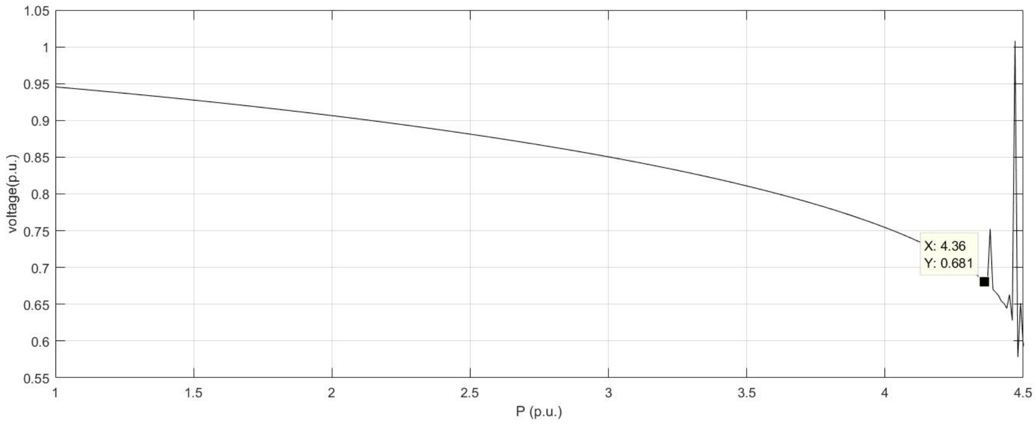

Figure 5.39: IEEE-118 bus system P-V curve at bus-2.

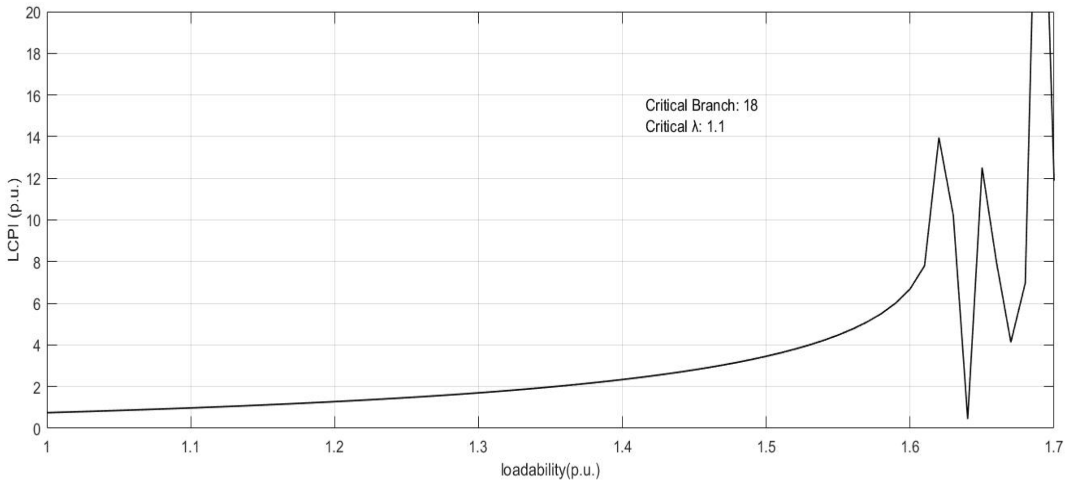

Figure 5.40: IEEE-118 bus heavy active loading (λ) at bus-13 v/s LCPI.

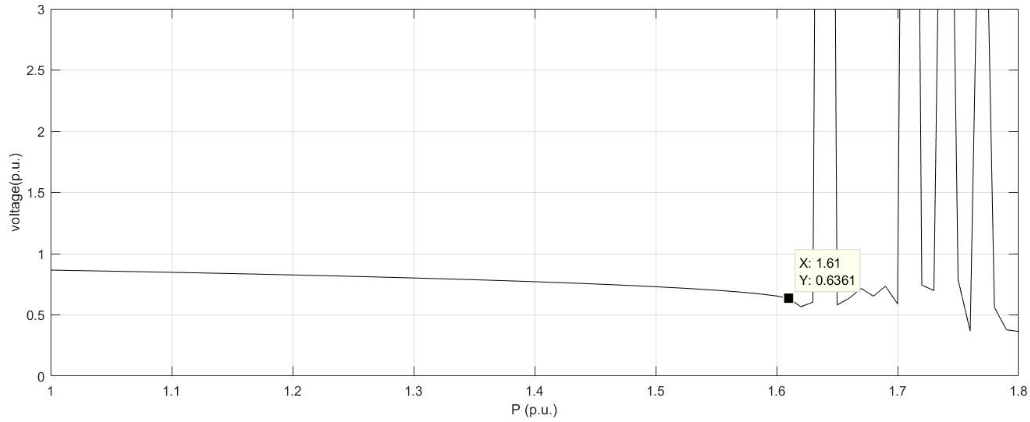

Figure 5.41: IEEE-118 bus system P-V curve at bus-13.

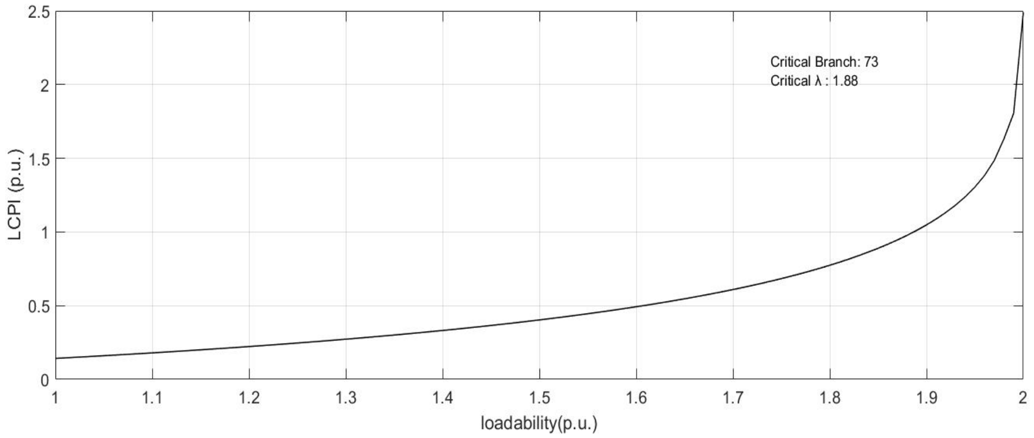

Figure 5.42: IEEE-118 bus heavy active loading (λ) at bus-52 v/s LCPI.

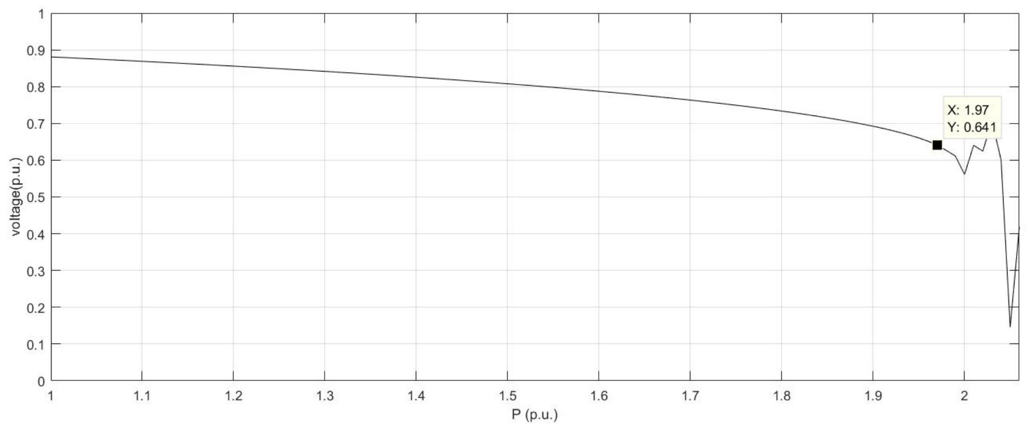

Figure 5.43: IEEE-118 bus system P-V curve at bus-52.

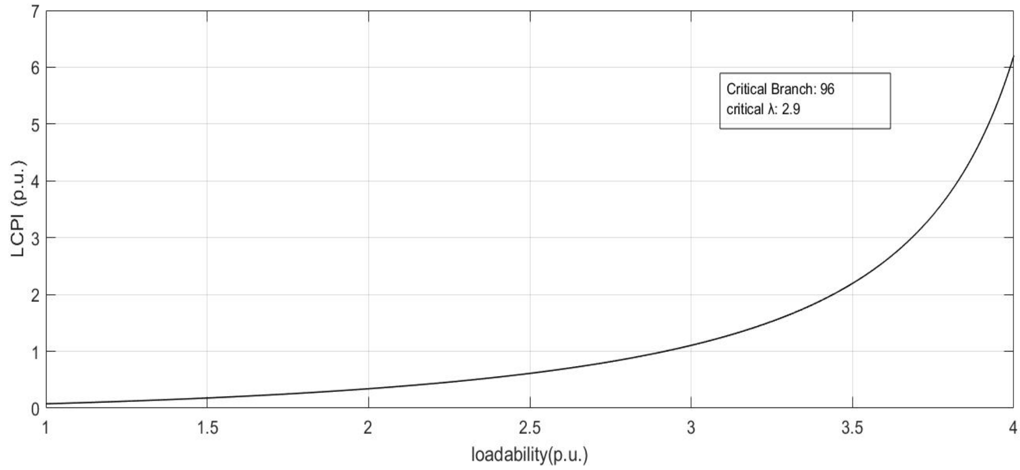

Figure 5.44: IEEE-118 bus heavy active loading (λ) at bus-115 v/s LCPI.

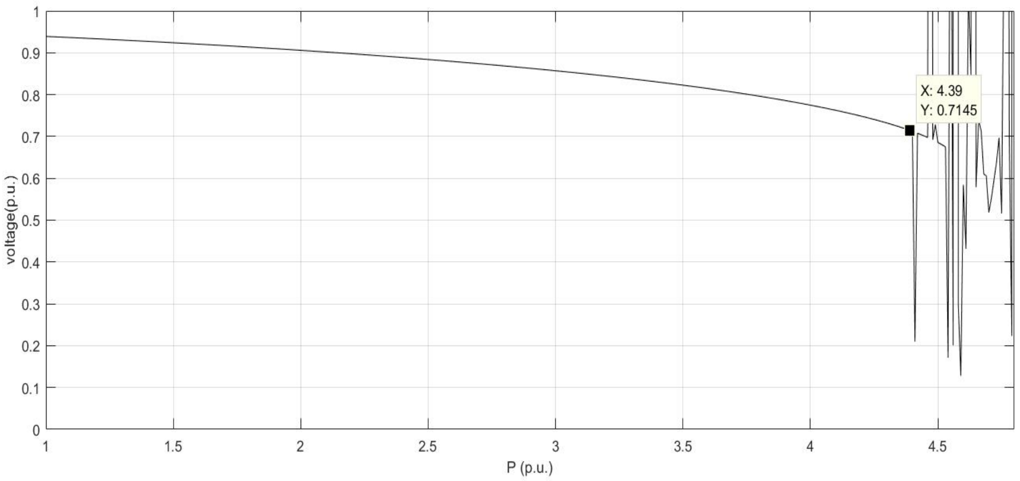

Figure 5.45: IEEE-118 bus system P-V curve at bus-115.

5.2.5 IEEE-118 bus heavy reactive loading on single bus

The simulation of IEEE-118 bus for heavy reactive loading is shown in table 5.16.

Table 5.16: critical lines of IEEE 118 Bus system with Heavy Reactive loading on single bus

Load Bus	loading (p.u)	Critical Branch	From Bus	To Bus	LCPI	FVSI	Lmn	LQP
2	4.5	13	2	12	0.9687	1.004462	1.020597	1.110612
3	5.7	4	3	5	0.987888	0.92853	0.9097	0.615104
13	1.7	4	3	5	0.987888	0.92853	0.9097	0.615104
16	3	22	16	17	0.963958	0.973162	0.977628	0.373463
20	9.3	29	22	23	0.97881	0.913055	0.893305	0.397964
22	2.9	29	22	23	0.999375	0.936839	0.917436	0.405445
28	5.5	35	28	29	0.987392	1.052959	1.087491	0.655959
33	2.7	48	33	37	0.995348	1.027465	1.042675	0.484254
39	3.9	55	39	40	0.991612	1.069255	1.110031	1.150671
43	2.7	59	43	44	0.926423	0.94547	0.954515	0.215884
48	4.1	69	48	49	0.967064	1.026413	1.054268	1.441745
51	5.1	73	52	53	0.970459	1.041805	1.08028	0.313455
67	8.4	103	66	67	0.996974	1.009774	0.997279	1.14494
75	6.99	120	75	77	0.998227	0.860943	0.823917	0.301195
82	2.48	131	83	85	0.994304	0.904189	0.876374	0.41202
86	2.1	134	86	87	0.993745	1.005307	1.010841	0.367128
93	6.3	146	93	94	0.988516	1.131294	1.222163	0.920597
101	2.14	162	101	102	0.991786	0.962921	0.952604	0.51193
109	12.4	175	109	110	0.992361	1.096859	1.152719	0.909119
115	11.1	181	27	115	0.991475	1.022697	0.994698	1.349758
118	5.93	120	75	77	0.997774	0.813144	0.769457	0.286228

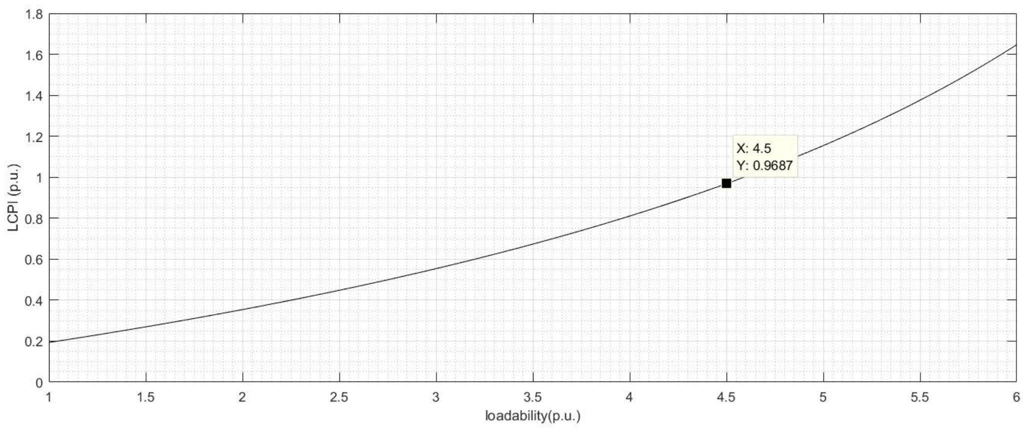

Figure 5.46: IEEE-118 bus heavy reactive loading (λ) at bus-2 v/s LCPI.

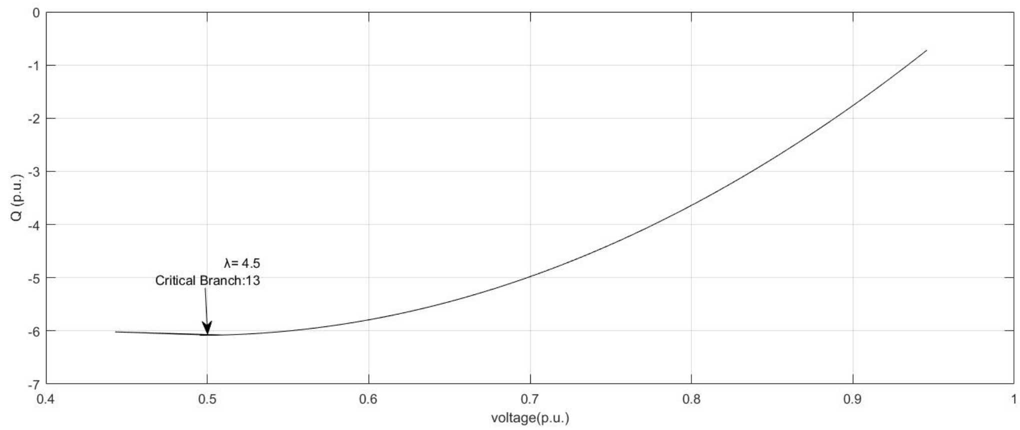

Figure 5.47: IEEE-118 bus system Q-V curve at bus-2.

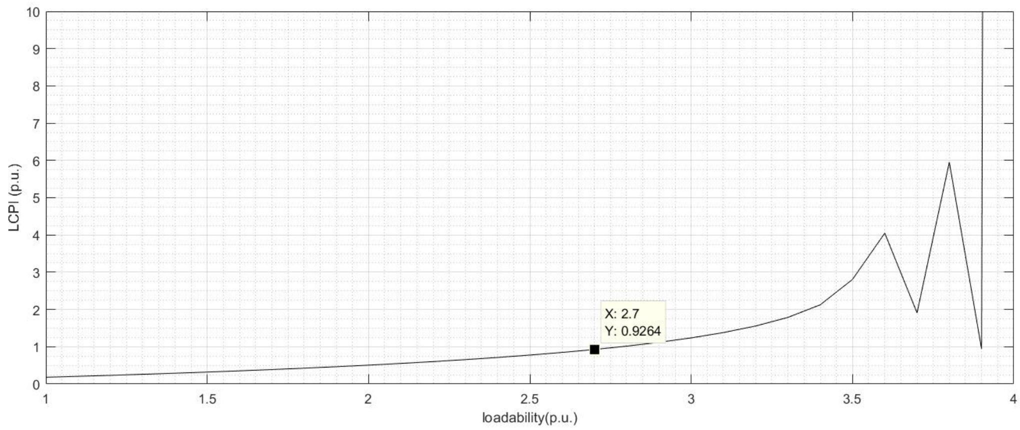

Figure 5.48: IEEE-118 bus heavy reactive loading (λ) at bus-43 v/s LCPI.

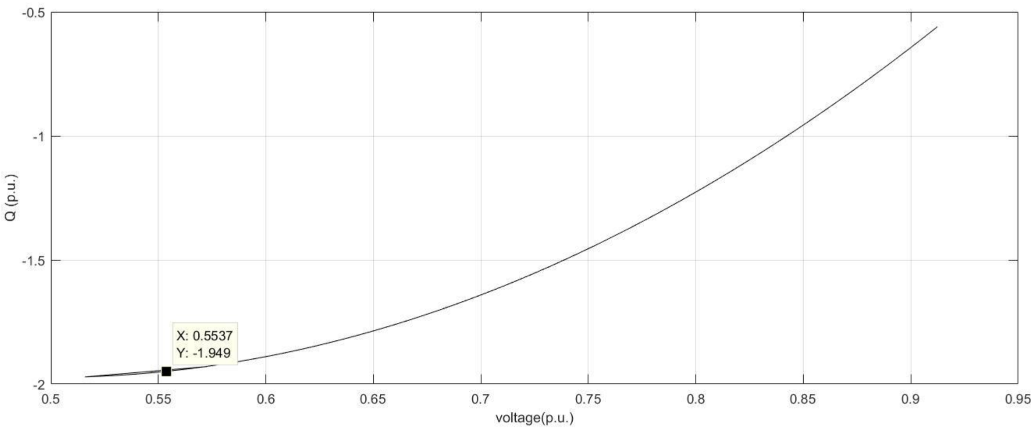

Figure 5.49: IEEE-118 bus system Q-V curve at bus-43.

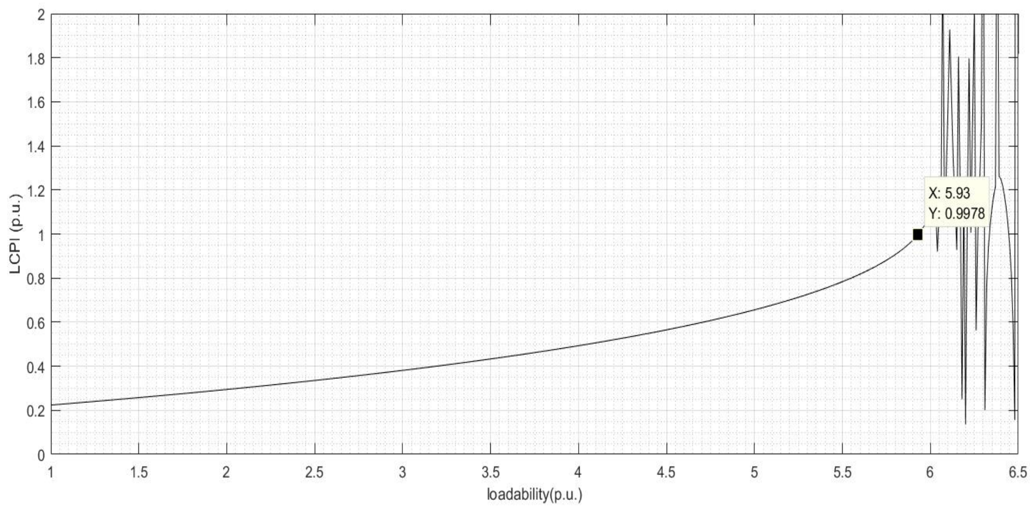

Figure 5.50: IEEE-118 bus heavy reactive loading (λ) at bus-118 v/s LCPI.

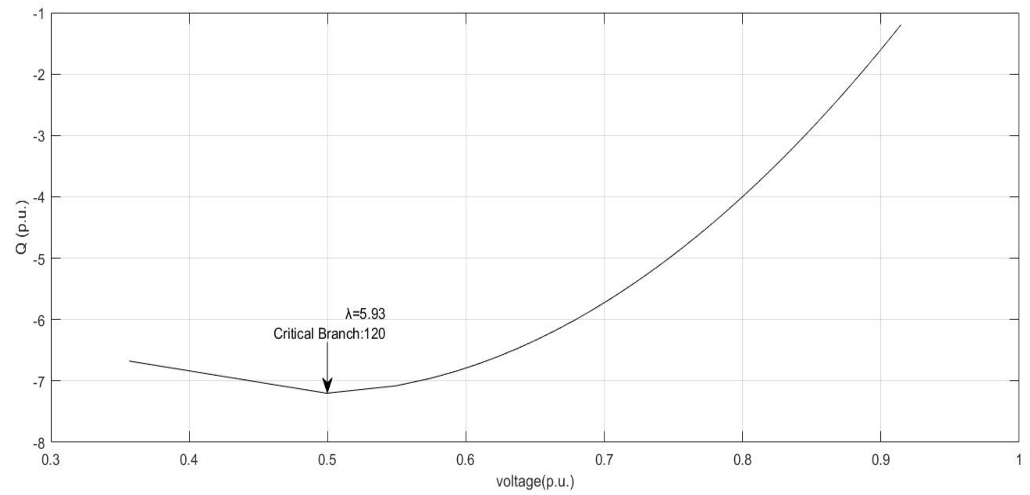

Figure 5.51: IEEE-118 bus system Q-V curve at bus-118.

For bus no. 2, 43 and 118 λ v/s LCPI and Q-V curve are shown in above figures (5.46 to 5.51). It shows the reactive power loading limit for said buses and behavior of LCPI for heavy reactive power loading.

5.2.6 IEEE-118 bus line contingency analysis

In the line contingency analysis, we have to outage every branch one by one and find the respective critical branch for IEEE-118 bus system with pre specified reactive load. The simulation of IEEE-118 bus for line contingency are similar to IEEE-30 bus system and ranking of critical buses are given in table 5.17.

Table 5.17: critical lines of IEEE 118 Bus system with Pre specified reactive load λ=2.9 p.u.

Rank	Branch outage	Critical Branch	From Bus	To Bus	LCPI	FVSI	Lmn	LQP
1	16	18	13	15	0.991667	0.888346	0.857984	0.234491
2	62	68	45	49	0.934569	0.741353	0.695462	0.2844
3	121	125	79	80	0.738288	0.676406	0.661604	0.809885
4	68	62	45	46	0.577556	0.483036	0.466284	0.2858
5	60	68	45	49	0.564915	0.422769	0.401034	0.182453
6	25	29	22	23	0.479717	0.420217	0.411067	0.220239
7	155	148	80	96	0.429418	0.450125	0.445297	0.281532
8	151	148	80	96	0.424505	0.452458	0.446054	0.282994
9	51	68	45	49	0.424473	0.24741	0.231774	0.113027
10	96	68	45	49	0.41822	0.245435	0.230203	0.112515
11	147	148	80	96	0.411952	0.429486	0.425586	0.268592
12	128	148	80	96	0.406338	0.457659	0.446817	0.286256
13	74	71	49	51	0.397984	0.299401	0.318429	0.222705
14	38	31	23	25	0.394679	0.181668	0.175294	0.233984
15	59	68	45	49	0.393438	0.285051	0.273059	0.130943
16	8	22	16	17	0.391806	0.029628	0.027982	0.020338
17	157	148	80	96	0.387508	0.420874	0.413992	0.263192
18	69	68	45	49	0.384065	0.225079	0.211927	0.104426
19	50	68	45	49	0.381334	0.244188	0.23156	0.113078
20	63	68	45	49	0.378871	0.231239	0.218512	0.107348

CHAPTER 6
CONCLUSIONS AND FUTURE SCOPE

6.1 Conclusions

The voltage stability assessments for IEEE-30 bus system and IEEE-118 bus system are done in this work by using LCPI [35], FVSI [34], Lmn [32] and LQP [33] indices. The various cases like MVA loading, active loading, reactive loading on complete power system network and single bus are taken to observe the voltage stability of system and ranking of critical line is done according to the operating conditions. We also observe the voltage stability for line contingencies cases for both IEEE-30 bus and IEEE-118 bus system. The maximum loadability factor (λ) is computed and verified by P-V and Q-V curve on different loading conditions.

It is observed that the LCPI index provides accurate results for voltage stability and also able to point out the exact voltage instability point. The accuracy of LCPI index is high with respect to the other indices because of the following reasons:

- Exact transmission line model (including bus charging data) is used for the calculation of LCPI index.
- The direction of active power flow with respect to the reactive power flow in the line is considered in it.
- The magnitude of both active and reactive power at every bus is considered in it.
- Due to the consideration of ABCD parameters the effect of transformer on voltage stability is inherently included in it.

In the comparative study of LCPI, FVSI, Lmn and LQP indices it is observed that sometimes FVSI and Lmn indices gives the results similar to the LCPI index but LQP index gives entirely different results from the LCPI index except base case loading.

The LCPI index in also capable to identify the required reactive margin for the critical or unstable system to bring back it into the stable region, it is shown in section 5.1.2, 5.1.3 and 5.1.4 for IEEE-30 bus system.

The reactive power compensation with PSO algorithm for IEEE-30 bus system in section 5.1.2, 5.1.3 and 5.1.4 are verified from Q-V curve and it is found that the injected reactive power is comes under the available margin of reactive power.

6.2 Future Scope of Research

- This work is useful for voltage stability analysis for a big power system network even it can be implemented for bigger than IEEE-118 bus.
- In future work it is possible to design the suitable reactive power compensation system to improve the voltage stability of system.
- Load modeling according to the available stability margin is possible.

REFERENCES

[1] NERC. 1996 System Disturbances (2008): Review of selected electric system disturbances in North America; Available: http://www.nerc.com/files/ disturb96.pdf.

[2] DHA L . Voltage stability assessment using equivalent nodal analysis. IEEE Trans Power Syst 2016;31(1):454–63 .

[3] Moger T , Dhadbanjan T . A novel index for identification of weak nodes for reactive compensation to improve voltage stability. IET Gener, Transm Distrib 2015;9(14):1826–34.

[4] Aldeen M , Saha S , Alpcan T , Evans RJ . New online voltage stability margins and risk assessment for multi-bus smart power grids. Int J Control 2015;88(7):1338–52.

[5] Phadke AR , Fozdar M , Niazi KR . A new technique for computation of closest saddle-node bifurcation point of power system using real coded genetic algorithm. Int J Electr Power Energy Syst 2011;33(5):1203–10.

[6] Phadke AR , Fozdar M , Niazi KR , Bansal RC , Mithulananthan N . On-line monitoring of proximity to voltage collapse using a new index based on local signals. Electr Power Compon Syst 2010;38(13):1498–512.

[7] Pourbeik P , Kundur P , Taylor CW . The anatomy of a power grid blackout. IEEE Power Energy Mag 2006;4(5):22–9.

[8] Andersson G , Donalek P , Farmer R , Hatziargyriou N , Kamwa I , Kundur P , et al. Causes of the 2003 major grid blackouts in north america and europe, and recommended means to improve system dynamic performance. IEEE Trans Power Syst 2005;20(4):1922–8.

[9] Singh B , Nehru K . Prevention of voltage instability by using FACTS controllers in power systems: a literature survey. Int J Eng Sci Technol 2010;2(5):980–92.

[10] RSS R , Manohar TG . Literature review on voltage stability phenomenon and importance of FACTS controllers in power system environment. Global J Res Eng Electr Electron Eng 2012;12(3):1–6.

[11] Tiwari R , Niazi KR , Gupta V . Line collapse proximity index for prediction of voltage collapse in power systems. Int J Electr Power Energy Syst 2012;41(1):105–11.

[12] Kundur P . Power system stability and control. New York: McGraw Hill; 1994.

[13] PA Lof, T Smed, G Andersson, DJ Hill. Fast calculation of a voltage stability index IEEE Transactions on Power Systems 7 (1), 54-64

[14] Liu, Shuran & Deng, Hui & Su, Guo. (2013). Analyses and Discussions of the Blackout in Indian Power Grid. 10.3968/j.est.1923847920130601.2627.

[15] C. D. Vournas, P. W. Sauer, and M. A. Pai, \Relationships between voltage and angle Stability of power systems," Electric Power Systems Research, vol. 18, no. 8,
pp. 493-500, November 1996.

[16] B. Gao, G. K. Morison, and P. Kundur, \Voltage stability analysis using Static and dynamic approaches," IEEE Transactions on Power Systems, vol. 8, no. 3, pp. 1159-1171, Aug. 1993.

[17] Luis Aromataris, Patricia Arnera, and Jean Riubrugent, \Improving static techniques for the analysis of voltage stability," Electric Power System Research, vol. 33, no. 4, pp. 901-908, May 2011.

[18] Glavic M , Van Cutsem T . A short survey of methods for voltage instability detection. In: Power and energy society general meeting. IEEE; 2011. p. 2011.

[19] Taylor CW . Power system voltage stability. McGraw-Hill; 1994.

[20] Ajjarapu V , Christy C . The continuation power flow: a tool for steady state voltage stability analysis. IEEE Trans Power Syst 1992;7(1):416–23.

[21] Chowdhury BH , Taylor CW . Voltage stability analysis: VQ power flow simulation versus dynamic simulation. IEEE Trans Power Syst 20 0 0;15(4):1354–9.

[22] Mittelstadt WA , Chowdhury BH , Taylor CW . Voltage stability analysis: VQ power flow simulation versus dynamic simulation [discussion and closure]. IEEE Trans Power Syst 2001;16(4):931–2.

[23] Araposthatis A , Sastry S , Varaiya P . Analysis of power-flow equation. Int J Electr Power Energy Syst 1981;3(3):115–26.

[24] Lof PA , Smed T , Andersson G , Hill DJ . Fast calculation of a voltage stability index. IEEE Trans Power Syst 1992;7(1):54–64.

[25] Gao B , Morison GK , Kundur P . Voltage stability evaluation using modal analysis. IEEE Trans Power Syst 1992;7(4):1529–42.

[26] Kwatny HG , Pasrija AK , Bahar LY . Static bifurcations in electric power networks: loss of steady-state stability and voltage collapse. IEEE Trans Circuits Syst 1986;33(10):981–91.

[27] Ajjarapu V , Lee B . Bifurcation theory and its application to nonlinear dynamical phenomena in an electrical power system. IEEE Trans Power Syst 1992;7(1):424–31.

[28] Canizares CA . On bifurcations, voltage collapse and load modeling. IEEE Trans Power Syst 1995;10(1):512–22.

[29] Devaraj D , Roselyn JP . On-line voltage stability assessment using radial basis function network model with reduced input features. Int J Electr Power Energy Syst 2011;33(9):1550–5.

[30] Kessel P , Glavitsch H . Estimating the voltage stability of a power system. IEEE Trans Power Delivery 1986;1(3):346–54.

[31] Overbye TJ . Effects of load modelling on analysis of power system voltage stability. Int J Electr Power Energy Syst 1994;16(5):329–38.

[32] Moghavvemi M , Omar FM . Technique for contingency monitoring and voltage collapse prediction. In: IEE proceedings-generation, transmission & distribution; 1998. p. 634–40.

[33] Mohamed A , Jasmon GB . A new clustering technique for power system voltage stability analysis. Electr Mach Power Syst 1995;23(4):389–403.

[34] Musirin I , TKA R . On-line voltage stability based contingency ranking using fast voltage stability index (*FVSI*). Transm Distrib Conf Exhibit 2002 . Asia Pacific

[35] RajiveTiwari, K.R.Niazi, VikasGupta. Line collapse proximity index for prediction of voltage collapse in power systems International Journal of Electrical Power & Energy Systems Volume 41, Issue 1, October 2012, Pages 105-111.

[36] James Kennedy and Russell Eberhart, Particle Swarm Optimization (PSO). 0-7803-2768-3/95/$4.00 0 1995 IEEE, 1942-1948.

[37] I. J. Hasan, C. K. Gan, M. Shamshiri, M. R. Ab. Ghani and I. bin Bugis. 2014. Optimal Capacitor Allocation in Distribution System Using Particle Swarm Optimization. Appl. Mech. Mater. 699: 770- 775.

[38] S.Sakthivel and Dr.D.Mary, Particle Swarm Optimization Algorithm for Voltage Stability Enhancement by Optimal Reactive Power Reserve Management with Multiple TCSCs. International Journal of Computer Applications (0975 – 8887) Volume 11– No.3, December 2010 19.

[39] M. Ettappan and 2 Dr. M. Rajaram A Particle Swarm Optimization Algorithm for Reactive Power Compensation, International Journal of Electrical Engineering. ISSN 0974-2158 Volume 5, Number 6 (2012), pp. 669-678

[40] Kundur, P., et al., *Definition and classification of power system stability IEEE/CIGRE joint task force on stability terms and definitions.* Power Systems, IEEE Transactions on, 2004. 19(3): p. 1387-1401.

[41] D. J. Hill, I. A. Hiskens, “Load recovery in voltage stability analysis and control”, Bulk Power System Phenomena III, Voltage Stability, Security and Control, pp. 579-595,ECC, Davos, Aug. 1994.

[42] H. Glavitsch, “Voltage stability and collapse - A review of basic phenomena and methods of assessment”, Bulk Power System Phenomena III, Voltage Stability, Security and Control, pp. 9-14, ECC, Davos, Aug. 1994.

[43] IEEE Committee Report, Voltage Stability of Power Systems: Concepts, Analytical Tools, and Industry Experience, IEEE/PES 90TH0358-2-PWR, 1990.

[44] C.L. Wadhwa, Electrical Power Systems, New Age International, 2005 ISBN-9788122417227.

[45] IEEE Committee Report, Voltage Stability of Power Systems: Concepts, Analytical Tools, and Industry Experience, IEEE/PES 90TH0358-2-PWR, 1990.

[46] V. Ajjarapu and C. Christy, "The continuation power flow: a tool for steady state voltage stability analysis," *[Proceedings] Conference Papers 1991 Power Industry Computer Application Conference*, Baltimore, MD, USA, 1991, pp. 304-311

[47] F. Milano, "Continuous Newton's Method for Power Flow Analysis," in *IEEE Transactions on Power Systems*, vol. 24, no. 1, pp. 50-57, Feb. 2009. doi: 10.1109/TPWRS.2008.2004820.

[48] T. J. Overbye, I. Dobson and C. L. DeMarco, "Q-V curve interpretations of energy measures for voltage security," in *IEEE Transactions on Power Systems*, vol. 9, no. 1, pp. 331-340, Feb. 1994. doi: 10.1109/59.317593.

[49] S. Lian, S. Minami, S. Morii and S. Kawamoto, "Analysis method of voltage stability for bulk power system by P-V and Q-V curves considering dynamic load," *2009 IEEE/PES Power Systems Conference and Exposition*, Seattle, WA, 2009, pp. 1-6. doi: 10.1109/PSCE.2009.4840156

[50] G. C. Ejebe, G. D. Irisarri, S. Mokhtari, O. Obadina, P. Ristanovic and J. Tong, "Methods for contingency screening and ranking for voltage stability analysis of power systems," *Proceedings of Power Industry Computer Applications Conference*, Salt Lake City, UT, USA, 1995, pp. 249-255.

[51] R. Kanimozhi and K. Selvi, “A Novel Line Stability Index for Voltage Stability Analysis and Contingency Ranking in Power System Using Fuzzy Based Load Flow,” Journal of Electrical Engineering and Technology, vol. 8, no. 4, pp. 694–703, Jul. 2013.

[52] Nai-shan, H.; Xu, T.; Liao, Q.; Lu, Z. The analysis of abundance index of voltage stability based circuit theory. Guangxi Electr. Power 2006, 2, 12–14.

[53] Power System Test Archive-UWEE, University of Washington. <http://www.ee.washington.edu/research/pstca>.

Appendix-A

Data for IEEE-30 bus test system

The IEEE 30-bus test system is shown in Figure A.1 The system data is taken from [53] and buses are renumbered. The base MVA is 100. The relevant data are provided in following tables

TableA.1: Generator data nomenclature

Column number	Name	Description
1.	Bus	Bus Number
2.	Pg	Real power output (MW)
3.	Qg	Reactive power output (MVAr)
4.	Qmax	Maximum reactive power output (MVAr)
5.	Qmin	Minimum reactive power output (MVAr)
6.	Vg	Voltage magnitude setpoint (p.u.)
7.	Base MVA	MVA base of this machine
8.	Status	Status=1 machine in service Status=0 machine out of service
9.	Pmax	Maximum real power output (MW)
10.	Pmin	Minimum real power output (MW)

TableA.2 Bus data nomenclature

Column number	Name	Description
1.	Bus	Bus number
2.	Type	1: PQ bus 2: PV bus 3: Reference bus 4: Isolate bus
3.	Pd	real power demand (MW)
4.	Qd	reactive power demand (MVAr)
5.	Gs	shunt conductance (MW demanded at V = 1.0 p.u.)
6.	Bs	shunt susceptance (MVAr injected at V = 1.0 p.u.)
7.	Vm	voltage magnitude (p.u.)
8.	Va	voltage angle (degrees)
9.	Base kV	base voltage (kV)
10.	Vmax	maximum voltage magnitude (p.u.)
11.	Vmin	minimum voltage magnitude (p.u.)

TableA.3: Branch data nomenclature

Column number	Name	Description
1.	Branch Number	Branch/Line Number
2.	From bus	from bus number
3.	To bus	to bus number
4.	R	resistance (p.u.)
5.	X	reactance (p.u.)
6.	B	total line charging susceptance (p.u.)
7.	rateA	MVA rating A (long term rating), set to 0 for unlimited
8.	rateB	MVA rating B (short term rating), set to 0 for unlimited
9.	rateC	MVA rating C (emergency rating), set to 0 for unlimited
10.	ratio	transformer off nominal turns ratio (= 0 for lines)
11.	angle	transformer phase shift angle (degrees), positive => delay
12.	Status	initial branch status, 1 - in service, 0 - out of service
13.	ang min	minimum angle difference, angle (Vf) - angle(Vt) (degrees)
14.	ang max	maximum angle difference, angle (Vf) – angle (Vt) (degrees)

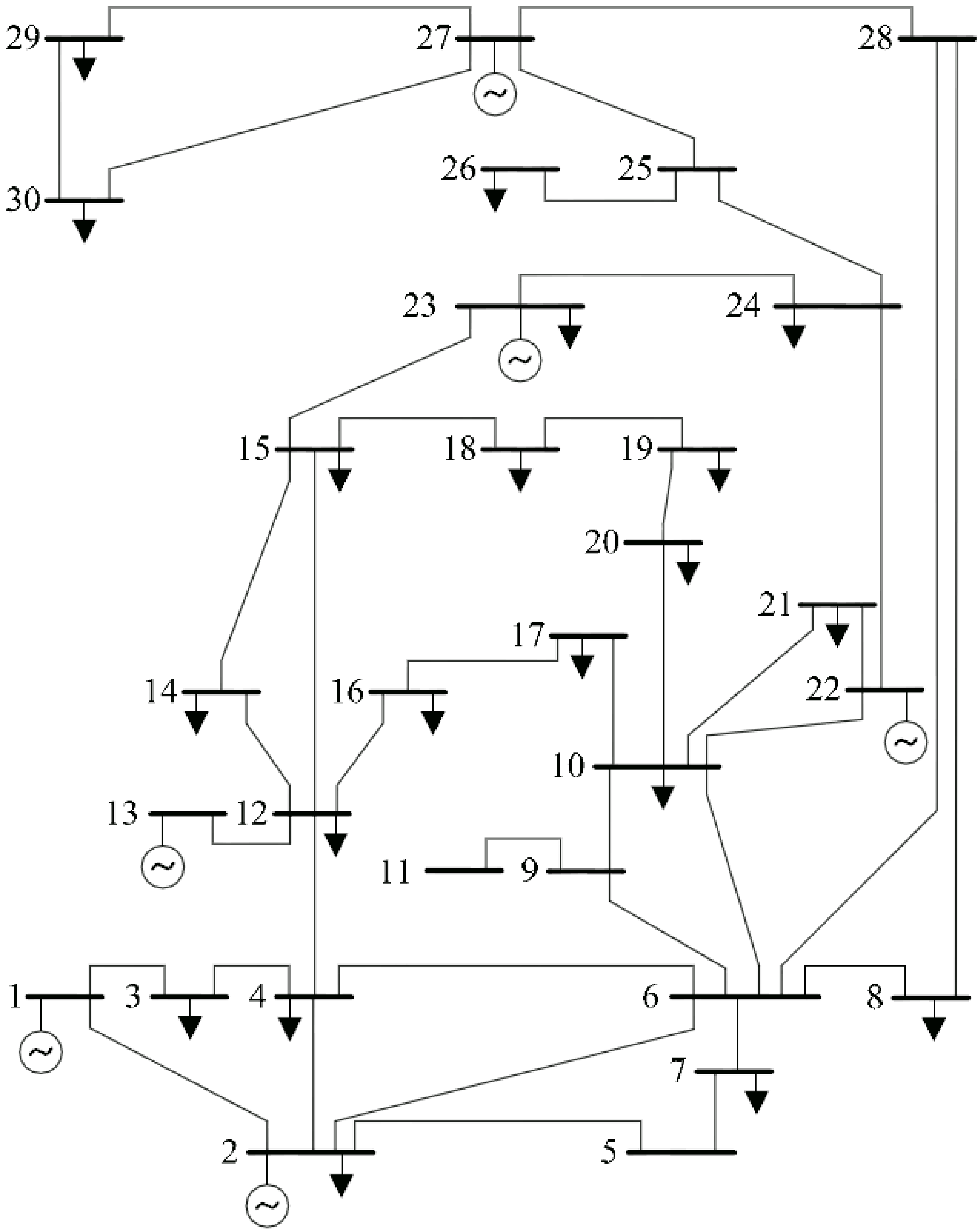

FigureA.1: One-line diagram of IEEE-30 bus test system

Table A.4: Generator bus data

Bus	Pg	Qg	Qmax	Qmin	Vg	Base MVA	Status	Pmax	Pmin
1	23.54	0	150	-20	1	100	1	80	0
2	60.97	0	60	-20	1	100	1	80	0
3	0	0	0	0	1	100	0	0	0
4	0	0	0	0	1	100	0	0	0
5	0	0	0	0	1	100	0	0	0
6	0	0	0	0	1	100	0	0	0
7	0	0	0	0	1	100	0	0	0
8	0	0	0	0	1	100	0	0	0
9	0	0	0	0	1	100	0	0	0
10	0	0	0	0	1	100	0	0	0
11	0	0	0	0	1	100	0	0	0
12	0	0	0	0	1	100	0	0	0
13	37	0	44.7	-15	1	100	1	40	0
14	0	0	0	0	1	100	0	0	0
15	0	0	0	0	1	100	0	0	0
16	0	0	0	0	1	100	0	0	0
17	0	0	0	0	1	100	0	0	0
18	0	0	0	0	1	100	0	0	0
19	0	0	0	0	1	100	0	0	0
20	0	0	0	0	1	100	0	0	0
21	0	0	0	0	1	100	0	0	0
22	21.59	0	62.5	-15	1	100	1	50	0
23	19.2	0	40	-10	1	100	1	30	0
24	0	0	0	0	1	100	0	0	0
25	0	0	0	0	1	100	0	0	0
26	0	0	0	0	1	100	0	0	0
27	26.91	0	48.7	-15	1	100	1	55	0
28	0	0	0	0	1	100	0	80	0
29	0	0	0	0	1	100	0	0	0
30	0	0	0	0	1	100	0	0	0

Table A.5: load bus data

Bus	Type	Pd	Qd	Gs	Bs	Vm	Va	Base KV	Vmax	Vmin
1	3	0	0	0	0	1	0	135	1.05	0.95
2	2	21.7	12.7	0	0	1	0	135	1.1	0.95
3	1	2.4	1.2	0	0	1	0	135	1.05	0.95
4	1	7.6	1.6	0	0	1	0	135	1.05	0.95
5	1	0	0	0	0.19	1	0	135	1.05	0.95
6	1	0	0	0	0	1	0	135	1.05	0.95
7	1	22.8	10.9	0	0	1	0	135	1.05	0.95
8	1	30	30	0	0	1	0	135	1.05	0.95
9	1	0	0	0	0	1	0	135	1.05	0.95
10	1	5.8	97.6	0	0	1	0	135	1.05	0.95
11	1	0	0	0	0	1	0	135	1.05	0.95
12	1	11.2	7.5	0	0	1	0	135	1.05	0.95
13	2	0	0	0	0	1	0	135	1.1	0.95
14	1	6.2	1.6	0	0	1	0	135	1.05	0.95
15	1	8.2	2.5	0	0	1	0	135	1.05	0.95
16	1	3.5	1.8	0	0	1	0	135	1.05	0.95
17	1	9	5.8	0	0	1	0	135	1.05	0.95
18	1	3.2	0.9	0	0	1	0	135	1.05	0.95
19	1	9.5	3.4	0	0	1	0	135	1.05	0.95
20	1	2.2	0.7	0	0	1	0	135	1.05	0.95
21	1	17.5	11.2	0	0	1	0	135	1.05	0.95
22	2	0	0	0	0	1	0	135	1.1	0.95
23	2	3.2	1.6	0	0	1	0	135	1.1	0.95
24	1	8.7	6.7	0	0.04	1	0	135	1.05	0.95
25	1	0	0	0	0	1	0	135	1.05	0.95
26	1	3.5	2.3	0	0	1	0	135	1.05	0.95
27	2	0	0	0	0	1	0	135	1.1	0.95
28	1	0	0	0	0	1	0	135	1.05	0.95
29	1	2.4	0.9	0	0	1	0	135	1.05	0.95
30	1	10.6	1.9	0	0	1	0	135	1.05	0.95

Table A.6: Branch data

Branch Number	From Bus	To Bus	R	X	B	rateA	rateB	rateC	ratio	Angle	Status	ang min	ang max
1.	1	2	0.02	0.06	0.03	0	130	130	0	0	1	-360	360
2.	1	3	0.05	0.19	0.02	0	130	130	0	0	1	-360	360
3.	2	4	0.06	0.17	0.02	0	65	65	0	0	1	-360	360
4.	3	4	0.01	0.04	0	0	130	130	0	0	1	-360	360
5.	2	5	0.05	0.2	0.02	0	130	130	0	0	1	-360	360
6.	2	6	0.06	0.18	0.02	0	65	65	0	0	1	-360	360
7.	4	6	0.01	0.04	0	0	90	90	0	0	1	-360	360
8.	5	7	0.05	0.12	0.01	0	70	70	0	0	1	-360	360
9.	6	7	0.03	0.08	0.01	0	130	130	0	0	1	-360	360
10.	6	8	0.01	0.04	0	0	32	32	0	0	1	-360	360
11.	6	9	0	0.21	0	0	65	65	0	0	1	-360	360
12.	6	10	0	0.56	0	0	32	32	0	0	1	-360	360
13.	9	11	0	0.21	0	0	65	65	0	0	1	-360	360
14.	9	10	0	0.11	0	0	65	65	0	0	1	-360	360
15.	4	12	0	0.26	0	0	65	65	0	0	1	-360	360
16.	12	13	0	0.14	0	0	65	65	0	0	1	-360	360
17.	12	14	0.12	0.26	0	0	32	32	0	0	1	-360	360
18.	12	15	0.07	0.13	0	0	32	32	0	0	1	-360	360
19.	12	16	0.09	0.2	0	0	32	32	0	0	1	-360	360
20.	14	15	0.22	0.2	0	0	16	16	0	0	1	-360	360
21.	16	17	0.08	0.19	0	0	16	16	0	0	1	-360	360
22.	15	18	0.11	0.22	0	0	16	16	0	0	1	-360	360
23.	18	19	0.06	0.13	0	0	16	16	0	0	1	-360	360
24.	19	20	0.03	0.07	0	0	32	32	0	0	1	-360	360
25.	10	20	0.09	0.21	0	0	32	32	0	0	1	-360	360
26.	10	17	0.03	0.08	0	0	32	32	0	0	1	-360	360
27.	10	21	0.03	0.07	0	0	32	32	0	0	1	-360	360
28.	10	22	0.07	0.15	0	0	32	32	0	0	1	-360	360
29.	21	22	0.01	0.02	0	0	32	32	0	0	1	-360	360
30.	15	23	0.1	0.2	0	0	16	16	0	0	1	-360	360
31.	22	24	0.12	0.18	0	0	16	16	0	0	1	-360	360
32.	23	24	0.13	0.27	0	0	16	16	0	0	1	-360	360
33.	24	25	0.19	0.33	0	0	16	16	0	0	1	-360	360
34.	25	26	0.25	0.38	0	0	16	16	0	0	1	-360	360
35.	25	27	0.11	0.21	0	0	16	16	0	0	1	-360	360
36.	28	27	0	0.4	0	0	65	65	0	0	1	-360	360
37.	27	29	0.22	0.42	0	0	16	16	0	0	1	-360	360
38.	27	30	0.32	0.6	0	0	16	16	0	0	1	-360	360
39.	29	30	0.24	0.45	0	0	16	16	0	0	1	-360	360
40.	8	28	0.06	0.2	0.02	0	32	32	0	0	1	-360	360
41.	6	28	0.02	0.06	0.01	0	32	32	0	0	1	-360	360

Appendix-B

Data for IEEE-118 bus test system

The IEEE 118-bus test system is shown in Figure B.1 The system data is taken from [53] and buses are renumbered. The base MVA is 100. The relevant data are provided in following tables.

The nomenclature are same as mentioned in appendix-A.

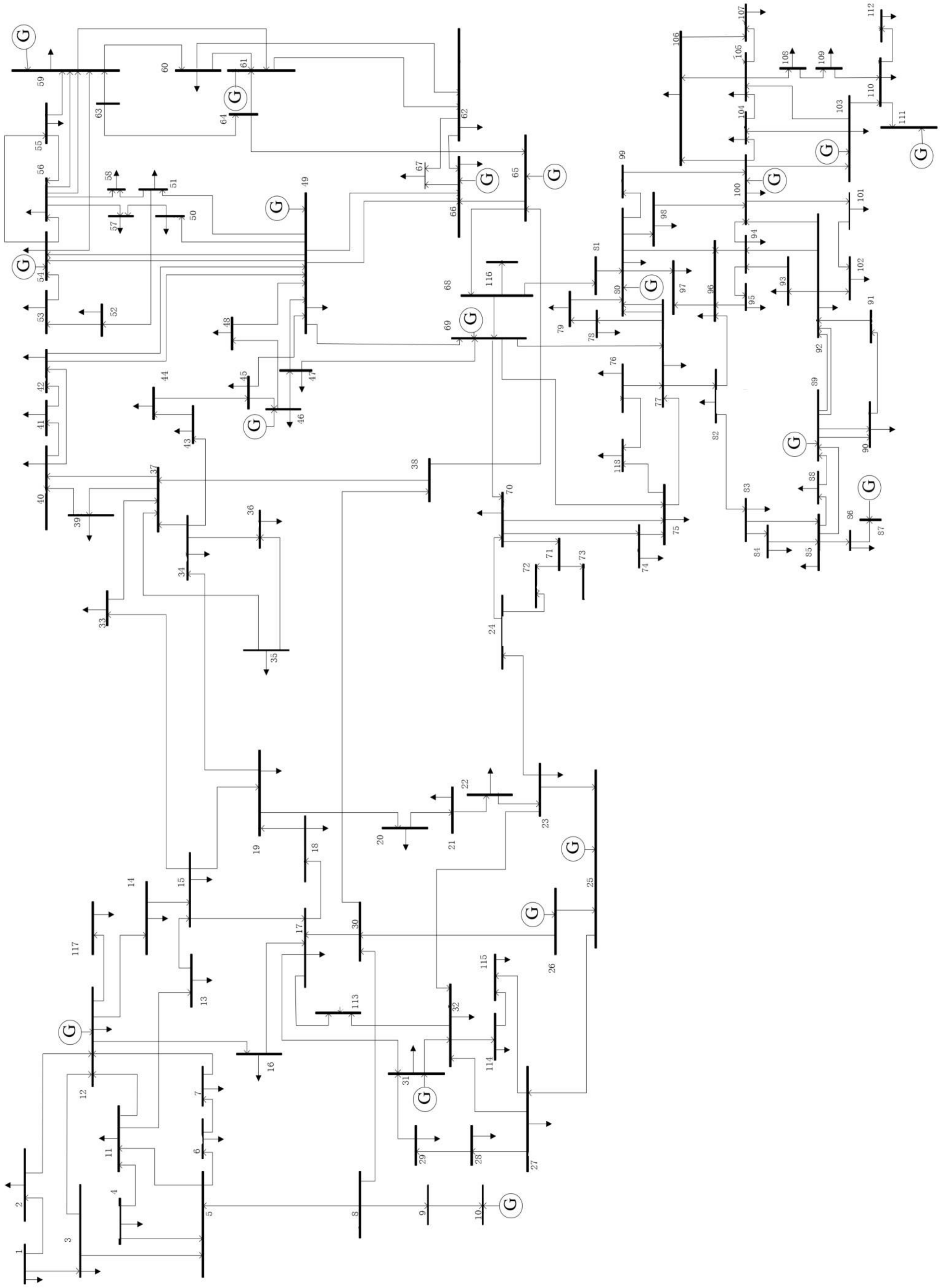

Figure B.1: One-line diagram of IEEE-118 bus test system

Table B.1: Generator bus data

Bus	Pg	Qg	Qmax	Qmin	Vg	Base MVA	Status	Pmax	Pmin
1	0	0	15	-5	0.955	100	1	100	0
2	0	0	0	0	0.955	100	0	100	0
3	0	0	0	0	0.955	100	0	0	0
4	0	0	300	-300	0.998	100	1	100	0
5	0	0	0	0	0.955	100	0	0	0
6	0	0	50	-13	0.99	100	1	100	0
7	0	0	0	0	0.955	100	0	0	0
8	0	0	300	-300	1.015	100	1	100	0
9	0	0	0	0	0.955	100	0	0	0
10	450	0	200	-147	1.05	100	1	550	0
11	0	0	0	0	0.955	100	0	0	0
12	85	0	120	-35	0.99	100	1	185	0
13	0	0	0	0	0.955	100	0	0	0
14	0	0	0	0	0.955	100	0	0	0
15	0	0	30	-10	0.97	100	1	100	0
16	0	0	0	0	0.955	100	0	0	0
17	0	0	0	0	0.955	100	0	0	0
18	0	0	50	-16	0.973	100	1	100	0
19	0	0	24	-8	0.962	100	1	100	0
20	0	0	0	0	0.955	100	0	0	0
21	0	0	0	0	0.955	100	0	0	0
22	0	0	0	0	0.955	100	0	0	0
23	0	0	0	0	0.955	100	0	0	0
24	0	0	300	-300	0.992	100	1	100	0
25	220	0	140	-47	1.05	100	1	320	0
26	314	0	1000	-1000	1.015	100	1	414	0
27	0	0	300	-300	0.968	100	1	100	0
28	0	0	0	0	0.955	100	0	0	0
29	0	0	0	0	0.955	100	0	0	0
30	0	0	0	0	0.955	100	0	0	0
31	7	0	300	-300	0.967	100	1	107	0
32	0	0	42	-14	0.963	100	1	100	0
33	0	0	0	0	0.955	100	0	0	0
34	0	0	24	-8	0.984	100	1	100	0
35	0	0	0	0	0.955	100	0	0	0
36	0	0	24	-8	0.98	100	1	100	0
37	0	0	0	0	0.955	100	0	0	0
38	0	0	0	0	0.955	100	0	0	0
39	0	0	0	0	0.955	100	0	0	0
40	0	0	300	-300	0.97	100	1	100	0
41	0	0	0	0	0.955	100	0	0	0

42	0	0	300	-300	0.985	100	1	100	0
43	0	0	0	0	0.955	100	0	0	0
44	0	0	0	0	0.955	100	0	0	0
45	0	0	0	0	0.955	100	0	0	0
46	19	0	100	-100	1.005	100	1	119	0
47	0	0	0	0	0.955	100	0	0	0
48	0	0	0	0	0.955	100	0	0	0
49	204	0	210	-85	1.025	100	1	304	0
50	0	0	0	0	0.955	100	0	0	0
51	0	0	0	0	0.955	100	0	0	0
52	0	0	0	0	0.955	100	0	0	0
53	0	0	0	0	0.955	100	0	0	0
54	48	0	300	-300	0.955	100	1	148	0
55	0	0	23	-8	0.952	100	1	100	0
56	0	0	15	-8	0.954	100	1	100	0
57	0	0	0	0	0.955	100	0	0	0
58	0	0	0	0	0.955	100	0	0	0
59	155	0	180	-60	0.985	100	1	255	0
60	0	0	0	0	0.955	100	0	0	0
61	160	0	300	-100	0.995	100	1	260	0
62	0	0	20	-20	0.998	100	1	100	0
63	0	0	0	0	0.955	100	0	0	0
64	0	0	0	0	0.955	100	0	0	0
65	391	0	200	-67	1.005	100	1	491	0
66	392	0	200	-67	1.05	100	1	492	0
67	0	0	0	0	0.955	100	0	0	0
68	0	0	0	0	0.955	100	0	0	0
69	516.4	0	300	-300	1.035	100	1	805.2	0
70	0	0	32	-10	0.984	100	1	100	0
71	0	0	0	0	0.955	100	0	0	0
72	0	0	100	-100	0.98	100	1	100	0
73	0	0	100	-100	0.991	100	1	100	0
74	0	0	9	-6	0.958	100	1	100	0
75	0	0	0	0	0.955	100	0	0	0
76	0	0	23	-8	0.943	100	1	100	0
77	0	0	70	-20	1.006	100	1	100	0
78	0	0	0	0	0.955	100	0	0	0
79	0	0	0	0	0.955	100	0	0	0
80	477	0	280	-165	1.04	100	1	577	0
81	0	0	0	0	0.955	100	0	0	0
82	0	0	0	0	0.955	100	0	0	0
83	0	0	0	0	0.955	100	0	0	0
84	0	0	0	0	0.955	100	0	0	0
85	0	0	23	-8	0.985	100	1	100	0
86	0	0	0	0	0.955	100	0	0	0
87	4	0	1000	-100	1.015	100	1	104	0

88	0	0	0	0	0.955	100	0	0	0
89	607	0	300	-210	1.005	100	1	707	0
90	0	0	300	-300	0.985	100	1	100	0
91	0	0	100	-100	0.98	100	1	100	0
92	0	0	9	-3	0.99	100	1	100	0
93	0	0	0	0	0.955	100	0	0	0
94	0	0	0	0	0.955	100	0	0	0
95	0	0	0	0	0.955	100	0	0	0
96	0	0	0	0	0.955	100	0	0	0
97	0	0	0	0	0.955	100	0	0	0
98	0	0	0	0	0.955	100	0	0	0
99	0	0	100	-100	1.01	100	1	100	0
100	252	0	155	-50	1.017	100	1	352	0
101	0	0	0	0	0.955	100	0	0	0
102	0	0	0	0	0.955	100	0	0	0
103	40	0	40	-15	1.01	100	1	140	0
104	0	0	23	-8	0.971	100	1	100	0
105	0	0	23	-8	0.965	100	1	100	0
106	0	0	0	0	0.955	100	0	0	0
107	0	0	200	-200	0.952	100	1	100	0
108	0	0	0	0	0.955	100	0	0	0
109	0	0	0	0	0.955	100	0	0	0
110	0	0	23	-8	0.973	100	1	100	0
111	36	0	1000	-100	0.98	100	1	136	0
112	0	0	1000	-100	0.975	100	1	100	0
113	0	0	200	-100	0.993	100	1	100	0
114	0	0	0	0	0.955	100	0	0	0
115	0	0	0	0	0.955	100	0	0	0
116	0	0	1000	-1000	1.005	100	1	100	0
117	0	0	0	0	0.955	100	0	0	0
118	0	0	0	0	0.955	100	0	0	0

Table B.2 Load bus data

Bus	Type	Pd	Qd	Gs	Bs	Area	Vm	Va	Base KV	Zone	Vmax	Vmin
1	2	51	27	0	0	1	0.955	10.67	138	1	1.06	0.94
2	1	20	9	0	0	1	0.971	11.22	138	1	1.06	0.94
3	1	39	10	0	0	1	0.968	11.56	138	1	1.06	0.94
4	2	30	12	0	0	1	0.998	15.28	138	1	1.06	0.94
5	1	0	0	0	-40	1	1.002	15.73	138	1	1.06	0.94
6	2	52	22	0	0	1	0.99	13	138	1	1.06	0.94
7	1	19	2	0	0	1	0.989	12.56	138	1	1.06	0.94
8	2	0	0	0	0	1	1.015	20.77	345	1	1.06	0.94
9	1	0	0	0	0	1	1.043	28.02	345	1	1.06	0.94
10	2	0	0	0	0	1	1.05	35.61	345	1	1.06	0.94
11	1	70	23	0	0	1	0.985	12.72	138	1	1.06	0.94
12	2	47	10	0	0	1	0.99	12.2	138	1	1.06	0.94
13	1	34	16	0	0	1	0.968	11.35	138	1	1.06	0.94
14	1	14	1	0	0	1	0.984	11.5	138	1	1.06	0.94
15	2	90	30	0	0	1	0.97	11.23	138	1	1.06	0.94
16	1	25	10	0	0	1	0.984	11.91	138	1	1.06	0.94
17	1	11	3	0	0	1	0.995	13.74	138	1	1.06	0.94
18	2	60	34	0	0	1	0.973	11.53	138	1	1.06	0.94
19	2	45	25	0	0	1	0.963	11.05	138	1	1.06	0.94
20	1	18	3	0	0	1	0.958	11.93	138	1	1.06	0.94
21	1	14	8	0	0	1	0.959	13.52	138	1	1.06	0.94
22	1	10	5	0	0	1	0.97	16.08	138	1	1.06	0.94
23	1	7	3	0	0	1	1	21	138	1	1.06	0.94
24	2	0	0	0	0	1	0.992	20.89	138	1	1.06	0.94
25	2	0	0	0	0	1	1.05	27.93	138	1	1.06	0.94
26	2	0	0	0	0	1	1.015	29.71	345	1	1.06	0.94
27	2	62	13	0	0	1	0.968	15.35	138	1	1.06	0.94
28	1	17	7	0	0	1	0.962	13.62	138	1	1.06	0.94
29	1	24	4	0	0	1	0.963	12.63	138	1	1.06	0.94
30	1	0	0	0	0	1	0.968	18.79	345	1	1.06	0.94
31	2	43	27	0	0	1	0.967	12.75	138	1	1.06	0.94
32	2	59	23	0	0	1	0.964	14.8	138	1	1.06	0.94
33	1	23	9	0	0	1	0.972	10.63	138	1	1.06	0.94
34	2	59	26	0	14	1	0.986	11.3	138	1	1.06	0.94
35	1	33	9	0	0	1	0.981	10.87	138	1	1.06	0.94
36	2	31	17	0	0	1	0.98	10.87	138	1	1.06	0.94
37	1	0	0	0	-25	1	0.992	11.77	138	1	1.06	0.94
38	1	0	0	0	0	1	0.962	16.91	345	1	1.06	0.94
39	1	27	11	0	0	1	0.97	8.41	138	1	1.06	0.94
40	2	20	23	0	0	1	0.97	7.35	138	1	1.06	0.94

41	1	37	10	0	0	1	0.967	6.92	138	1	1.06	0.94
42	2	37	23	0	0	1	0.985	8.53	138	1	1.06	0.94
43	1	18	7	0	0	1	0.978	11.28	138	1	1.06	0.94
44	1	16	8	0	10	1	0.985	13.82	138	1	1.06	0.94
45	1	53	22	0	10	1	0.987	15.67	138	1	1.06	0.94
46	2	28	10	0	10	1	1.005	18.49	138	1	1.06	0.94
47	1	34	0	0	0	1	1.017	20.73	138	1	1.06	0.94
48	1	20	11	0	15	1	1.021	19.93	138	1	1.06	0.94
49	2	87	30	0	0	1	1.025	20.94	138	1	1.06	0.94
50	1	17	4	0	0	1	1.001	18.9	138	1	1.06	0.94
51	1	17	8	0	0	1	0.967	16.28	138	1	1.06	0.94
52	1	18	5	0	0	1	0.957	15.32	138	1	1.06	0.94
53	1	23	11	0	0	1	0.946	14.35	138	1	1.06	0.94
54	2	113	32	0	0	1	0.955	15.26	138	1	1.06	0.94
55	2	63	22	0	0	1	0.952	14.97	138	1	1.06	0.94
56	2	84	18	0	0	1	0.954	15.16	138	1	1.06	0.94
57	1	12	3	0	0	1	0.971	16.36	138	1	1.06	0.94
58	1	12	3	0	0	1	0.959	15.51	138	1	1.06	0.94
59	2	277	113	0	0	1	0.985	19.37	138	1	1.06	0.94
60	1	78	3	0	0	1	0.993	23.15	138	1	1.06	0.94
61	2	0	0	0	0	1	0.995	24.04	138	1	1.06	0.94
62	2	77	14	0	0	1	0.998	23.43	138	1	1.06	0.94
63	1	0	0	0	0	1	0.969	22.75	345	1	1.06	0.94
64	1	0	0	0	0	1	0.984	24.52	345	1	1.06	0.94
65	2	0	0	0	0	1	1.005	27.65	345	1	1.06	0.94
66	2	39	18	0	0	1	1.05	27.48	138	1	1.06	0.94
67	1	28	7	0	0	1	1.02	24.84	138	1	1.06	0.94
68	1	0	0	0	0	1	1.003	27.55	345	1	1.06	0.94
69	3	0	0	0	0	1	1.035	30	138	1	1.06	0.94
70	2	66	20	0	0	1	0.984	22.58	138	1	1.06	0.94
71	1	0	0	0	0	1	0.987	22.15	138	1	1.06	0.94
72	2	0	0	0	0	1	0.98	20.98	138	1	1.06	0.94
73	2	0	0	0	0	1	0.991	21.94	138	1	1.06	0.94
74	2	68	27	0	12	1	0.958	21.64	138	1	1.06	0.94
75	1	47	11	0	0	1	0.967	22.91	138	1	1.06	0.94
76	2	68	36	0	0	1	0.943	21.77	138	1	1.06	0.94
77	2	61	28	0	0	1	1.006	26.72	138	1	1.06	0.94
78	1	71	26	0	0	1	1.003	26.42	138	1	1.06	0.94
79	1	39	32	0	20	1	1.009	26.72	138	1	1.06	0.94
80	2	130	26	0	0	1	1.04	28.96	138	1	1.06	0.94
81	1	0	0	0	0	1	0.997	28.1	345	1	1.06	0.94
82	1	54	27	0	20	1	0.989	27.24	138	1	1.06	0.94
83	1	20	10	0	10	1	0.985	28.42	138	1	1.06	0.94
84	1	11	7	0	0	1	0.98	30.95	138	1	1.06	0.94
85	2	24	15	0	0	1	0.985	32.51	138	1	1.06	0.94
86	1	21	10	0	0	1	0.987	31.14	138	1	1.06	0.94
87	2	0	0	0	0	1	1.015	31.4	161	1	1.06	0.94

88	1	48	10	0	0	1	0.987	35.64	138	1	1.06	0.94
89	2	0	0	0	0	1	1.005	39.69	138	1	1.06	0.94
90	2	78	42	0	0	1	0.985	33.29	138	1	1.06	0.94
91	2	0	0	0	0	1	0.98	33.31	138	1	1.06	0.94
92	2	65	10	0	0	1	0.993	33.8	138	1	1.06	0.94
93	1	12	7	0	0	1	0.987	30.79	138	1	1.06	0.94
94	1	30	16	0	0	1	0.991	28.64	138	1	1.06	0.94
95	1	42	31	0	0	1	0.981	27.67	138	1	1.06	0.94
96	1	38	15	0	0	1	0.993	27.51	138	1	1.06	0.94
97	1	15	9	0	0	1	1.011	27.88	138	1	1.06	0.94
98	1	34	8	0	0	1	1.024	27.4	138	1	1.06	0.94
99	2	0	0	0	0	1	1.01	27.04	138	1	1.06	0.94
100	2	37	18	0	0	1	1.017	28.03	138	1	1.06	0.94
101	1	22	15	0	0	1	0.993	29.61	138	1	1.06	0.94
102	1	5	3	0	0	1	0.991	32.3	138	1	1.06	0.94
103	2	23	16	0	0	1	1.001	24.44	138	1	1.06	0.94
104	2	38	25	0	0	1	0.971	21.69	138	1	1.06	0.94
105	2	31	26	0	20	1	0.965	20.57	138	1	1.06	0.94
106	1	43	16	0	0	1	0.962	20.32	138	1	1.06	0.94
107	2	28	12	0	6	1	0.952	17.53	138	1	1.06	0.94
108	1	2	1	0	0	1	0.967	19.38	138	1	1.06	0.94
109	1	8	3	0	0	1	0.967	18.93	138	1	1.06	0.94
110	2	39	30	0	6	1	0.973	18.09	138	1	1.06	0.94
111	2	0	0	0	0	1	0.98	19.74	138	1	1.06	0.94
112	2	25	13	0	0	1	0.975	14.99	138	1	1.06	0.94
113	2	0	0	0	0	1	0.993	13.74	138	1	1.06	0.94
114	1	8	3	0	0	1	0.96	14.46	138	1	1.06	0.94
115	1	22	7	0	0	1	0.96	14.46	138	1	1.06	0.94
116	2	0	0	0	0	1	1.005	27.12	138	1	1.06	0.94
117	1	20	8	0	0	1	0.974	10.67	138	1	1.06	0.94
118	1	33	15	0	0	1	0.949	21.92	138	1	1.06	0.94

Table B.3 Branch data

Branch Number	From Bus	To Bus	R	X	B	rate A	rate B	rate C	ratio	Angle	Status	ang min	ang max
1	1	2	0.0303	0.0999	0.0254	0	0	0	0	0	1	-360	360
2	1	3	0.0129	0.0424	0.01082	0	0	0	0	0	1	-360	360
3	4	5	0.00176	0.00798	0.0021	0	0	0	0	0	1	-360	360
4	3	5	0.0241	0.108	0.0284	0	0	0	0	0	1	-360	360
5	5	6	0.0119	0.054	0.01426	0	0	0	0	0	1	-360	360
6	6	7	0.00459	0.0208	0.0055	0	0	0	0	0	1	-360	360
7	8	9	0.00244	0.0305	1.162	0	0	0	0	0	1	-360	360
8	8	5	0	0.0267	0	0	0	0	0.99	0	1	-360	360
9	9	10	0.00258	0.0322	1.23	0	0	0	0	0	1	-360	360
10	4	11	0.0209	0.0688	0.01748	0	0	0	0	0	1	-360	360
11	5	11	0.0203	0.0682	0.01738	0	0	0	0	0	1	-360	360
12	11	12	0.00595	0.0196	0.00502	0	0	0	0	0	1	-360	360
13	2	12	0.0187	0.0616	0.01572	0	0	0	0	0	1	-360	360
14	3	12	0.0484	0.16	0.0406	0	0	0	0	0	1	-360	360
15	7	12	0.00862	0.034	0.00874	0	0	0	0	0	1	-360	360
16	11	13	0.02225	0.0731	0.01876	0	0	0	0	0	1	-360	360
17	12	14	0.0215	0.0707	0.01816	0	0	0	0	0	1	-360	360
18	13	15	0.0744	0.2444	0.06268	0	0	0	0	0	1	-360	360
19	14	15	0.0595	0.195	0.0502	0	0	0	0	0	1	-360	360
20	12	16	0.0212	0.0834	0.0214	0	0	0	0	0	1	-360	360
21	15	17	0.0132	0.0437	0.0444	0	0	0	0	0	1	-360	360
22	16	17	0.0454	0.1801	0.0466	0	0	0	0	0	1	-360	360
23	17	18	0.0123	0.0505	0.01298	0	0	0	0	0	1	-360	360
24	18	19	0.01119	0.0493	0.01142	0	0	0	0	0	1	-360	360
25	19	20	0.0252	0.117	0.0298	0	0	0	0	0	1	-360	360
26	15	19	0.012	0.0394	0.0101	0	0	0	0	0	1	-360	360
27	20	21	0.0183	0.0849	0.0216	0	0	0	0	0	1	-360	360
28	21	22	0.0209	0.097	0.0246	0	0	0	0	0	1	-360	360
29	22	23	0.0342	0.159	0.0404	0	0	0	0	0	1	-360	360
30	23	24	0.0135	0.0492	0.0498	0	0	0	0	0	1	-360	360
31	23	25	0.0156	0.08	0.0864	0	0	0	0	0	1	-360	360
32	26	25	0	0.0382	0	0	0	0	0.96	0	1	-360	360
33	25	27	0.0318	0.163	0.1764	0	0	0	0	0	1	-360	360
34	27	28	0.01913	0.0855	0.0216	0	0	0	0	0	1	-360	360
35	28	29	0.0237	0.0943	0.0238	0	0	0	0	0	1	-360	360
36	30	17	0	0.0388	0	0	0	0	0.96	0	1	-360	360
37	8	30	0.00431	0.0504	0.514	0	0	0	0	0	1	-360	360
38	26	30	0.00799	0.086	0.908	0	0	0	0	0	1	-360	360
39	17	31	0.0474	0.1563	0.0399	0	0	0	0	0	1	-360	360
40	29	31	0.0108	0.0331	0.0083	0	0	0	0	0	1	-360	360
41	23	32	0.0317	0.1153	0.1173	0	0	0	0	0	1	-360	360
42	31	32	0.0298	0.0985	0.0251	0	0	0	0	0	1	-360	360
43	27	32	0.0229	0.0755	0.01926	0	0	0	0	0	1	-360	360
44	15	33	0.038	0.1244	0.03194	0	0	0	0	0	1	-360	360
45	19	34	0.0752	0.247	0.0632	0	0	0	0	0	1	-360	360
46	35	36	0.00224	0.0102	0.00268	0	0	0	0	0	1	-360	360
47	35	37	0.011	0.0497	0.01318	0	0	0	0	0	1	-360	360
48	33	37	0.0415	0.142	0.0366	0	0	0	0	0	1	-360	360
49	34	36	0.00871	0.0268	0.00568	0	0	0	0	0	1	-360	360
50	34	37	0.00256	0.0094	0.00984	0	0	0	0	0	1	-360	360
51	38	37	0	0.0375	0	0	0	0	0.94	0	1	-360	360
52	37	39	0.0321	0.106	0.027	0	0	0	0	0	1	-360	360
53	37	40	0.0593	0.168	0.042	0	0	0	0	0	1	-360	360
54	30	38	0.00464	0.054	0.422	0	0	0	0	0	1	-360	360
55	39	40	0.0184	0.0605	0.01552	0	0	0	0	0	1	-360	360
56	40	41	0.0145	0.0487	0.01222	0	0	0	0	0	1	-360	360
57	40	42	0.0555	0.183	0.0466	0	0	0	0	0	1	-360	360
58	41	42	0.041	0.135	0.0344	0	0	0	0	0	1	-360	360
59	43	44	0.0608	0.2454	0.06068	0	0	0	0	0	1	-360	360
60	34	43	0.0413	0.1681	0.04226	0	0	0	0	0	1	-360	360
61	44	45	0.0224	0.0901	0.0224	0	0	0	0	0	1	-360	360
62	45	46	0.04	0.1356	0.0332	0	0	0	0	0	1	-360	360

63	46	47	0.038	0.127	0.0316	0	0	0	0	0	1	-360	360
64	46	48	0.0601	0.189	0.0472	0	0	0	0	0	1	-360	360
65	47	49	0.0191	0.0625	0.01604	0	0	0	0	0	1	-360	360
66	42	49	0.0715	0.323	0.086	0	0	0	0	0	1	-360	360
67	42	49	0.0715	0.323	0.086	0	0	0	0	0	1	-360	360
68	45	49	0.0684	0.186	0.0444	0	0	0	0	0	1	-360	360
69	48	49	0.0179	0.0505	0.01258	0	0	0	0	0	1	-360	360
70	49	50	0.0267	0.0752	0.01874	0	0	0	0	0	1	-360	360
71	49	51	0.0486	0.137	0.0342	0	0	0	0	0	1	-360	360
72	51	52	0.0203	0.0588	0.01396	0	0	0	0	0	1	-360	360
73	52	53	0.0405	0.1635	0.04058	0	0	0	0	0	1	-360	360
74	53	54	0.0263	0.122	0.031	0	0	0	0	0	1	-360	360
75	49	54	0.073	0.289	0.0738	0	0	0	0	0	1	-360	360
76	49	54	0.0869	0.291	0.073	0	0	0	0	0	1	-360	360
77	54	55	0.0169	0.0707	0.0202	0	0	0	0	0	1	-360	360
78	54	56	0.00275	0.00955	0.00732	0	0	0	0	0	1	-360	360
79	55	56	0.00488	0.0151	0.00374	0	0	0	0	0	1	-360	360
80	56	57	0.0343	0.0966	0.0242	0	0	0	0	0	1	-360	360
81	50	57	0.0474	0.134	0.0332	0	0	0	0	0	1	-360	360
82	56	58	0.0343	0.0966	0.0242	0	0	0	0	0	1	-360	360
83	51	58	0.0255	0.0719	0.01788	0	0	0	0	0	1	-360	360
84	54	59	0.0503	0.2293	0.0598	0	0	0	0	0	1	-360	360
85	56	59	0.0825	0.251	0.0569	0	0	0	0	0	1	-360	360
86	56	59	0.0803	0.239	0.0536	0	0	0	0	0	1	-360	360
87	55	59	0.04739	0.2158	0.05646	0	0	0	0	0	1	-360	360
88	59	60	0.0317	0.145	0.0376	0	0	0	0	0	1	-360	360
89	59	61	0.0328	0.15	0.0388	0	0	0	0	0	1	-360	360
90	60	61	0.00264	0.0135	0.01456	0	0	0	0	0	1	-360	360
91	60	62	0.0123	0.0561	0.01468	0	0	0	0	0	1	-360	360
92	61	62	0.00824	0.0376	0.0098	0	0	0	0	0	1	-360	360
93	63	59	0	0.0386	0	0	0	0	0.96	0	1	-360	360
94	63	64	0.00172	0.02	0.216	0	0	0	0	0	1	-360	360
95	64	61	0	0.0268	0	0	0	0	0.99	0	1	-360	360
96	38	65	0.00901	0.0986	1.046	0	0	0	0	0	1	-360	360
97	64	65	0.00269	0.0302	0.38	0	0	0	0	0	1	-360	360
98	49	66	0.018	0.0919	0.0248	0	0	0	0	0	1	-360	360
99	49	66	0.018	0.0919	0.0248	0	0	0	0	0	1	-360	360
100	62	66	0.0482	0.218	0.0578	0	0	0	0	0	1	-360	360
101	62	67	0.0258	0.117	0.031	0	0	0	0	0	1	-360	360
102	65	66	0	0.037	0	0	0	0	0.94	0	1	-360	360
103	66	67	0.0224	0.1015	0.02682	0	0	0	0	0	1	-360	360
104	65	68	0.00138	0.016	0.638	0	0	0	0	0	1	-360	360
105	47	69	0.0844	0.2778	0.07092	0	0	0	0	0	1	-360	360
106	49	69	0.0985	0.324	0.0828	0	0	0	0	0	1	-360	360
107	68	69	0	0.037	0	0	0	0	0.94	0	1	-360	360
108	69	70	0.03	0.127	0.122	0	0	0	0	0	1	-360	360
109	24	70	0.00221	0.4115	0.10198	0	0	0	0	0	1	-360	360
110	70	71	0.00882	0.0355	0.00878	0	0	0	0	0	1	-360	360

111	24	72	0.0488	0.196	0.0488	0	0	0	0	0	1	-360	360
112	71	72	0.0446	0.18	0.04444	0	0	0	0	0	1	-360	360
113	71	73	0.00866	0.0454	0.01178	0	0	0	0	0	1	-360	360
114	70	74	0.0401	0.1323	0.03368	0	0	0	0	0	1	-360	360
115	70	75	0.0428	0.141	0.036	0	0	0	0	0	1	-360	360
116	69	75	0.0405	0.122	0.124	0	0	0	0	0	1	-360	360
117	74	75	0.0123	0.0406	0.01034	0	0	0	0	0	1	-360	360
118	76	77	0.0444	0.148	0.0368	0	0	0	0	0	1	-360	360
119	69	77	0.0309	0.101	0.1038	0	0	0	0	0	1	-360	360
120	75	77	0.0601	0.1999	0.04978	0	0	0	0	0	1	-360	360
121	77	78	0.00376	0.0124	0.01264	0	0	0	0	0	1	-360	360
122	78	79	0.00546	0.0244	0.00648	0	0	0	0	0	1	-360	360
123	77	80	0.017	0.0485	0.0472	0	0	0	0	0	1	-360	360
124	77	80	0.0294	0.105	0.0228	0	0	0	0	0	1	-360	360
125	79	80	0.0156	0.0704	0.0187	0	0	0	0	0	1	-360	360
126	68	81	0.00175	0.0202	0.808	0	0	0	0	0	1	-360	360
127	81	80	0	0.037	0	0	0	0	0.94	0	1	-360	360
128	77	82	0.0298	0.0853	0.08174	0	0	0	0	0	1	-360	360
129	82	83	0.0112	0.03665	0.03796	0	0	0	0	0	1	-360	360
130	83	84	0.0625	0.132	0.0258	0	0	0	0	0	1	-360	360
131	83	85	0.043	0.148	0.0348	0	0	0	0	0	1	-360	360
132	84	85	0.0302	0.0641	0.01234	0	0	0	0	0	1	-360	360
133	85	86	0.035	0.123	0.0276	0	0	0	0	0	1	-360	360
134	86	87	0.02828	0.2074	0.0445	0	0	0	0	0	1	-360	360
135	85	88	0.02	0.102	0.0276	0	0	0	0	0	1	-360	360
136	85	89	0.0239	0.173	0.047	0	0	0	0	0	1	-360	360
137	88	89	0.0139	0.0712	0.01934	0	0	0	0	0	1	-360	360
138	89	90	0.0518	0.188	0.0528	0	0	0	0	0	1	-360	360
139	89	90	0.0238	0.0997	0.106	0	0	0	0	0	1	-360	360
140	90	91	0.0254	0.0836	0.0214	0	0	0	0	0	1	-360	360
141	89	92	0.0099	0.0505	0.0548	0	0	0	0	0	1	-360	360
142	89	92	0.0393	0.1581	0.0414	0	0	0	0	0	1	-360	360
143	91	92	0.0387	0.1272	0.03268	0	0	0	0	0	1	-360	360
144	92	93	0.0258	0.0848	0.0218	0	0	0	0	0	1	-360	360
145	92	94	0.0481	0.158	0.0406	0	0	0	0	0	1	-360	360
146	93	94	0.0223	0.0732	0.01876	0	0	0	0	0	1	-360	360
147	94	95	0.0132	0.0434	0.0111	0	0	0	0	0	1	-360	360
148	80	96	0.0356	0.182	0.0494	0	0	0	0	0	1	-360	360
149	82	96	0.0162	0.053	0.0544	0	0	0	0	0	1	-360	360
150	94	96	0.0269	0.0869	0.023	0	0	0	0	0	1	-360	360
151	80	97	0.0183	0.0934	0.0254	0	0	0	0	0	1	-360	360
152	80	98	0.0238	0.108	0.0286	0	0	0	0	0	1	-360	360
153	80	99	0.0454	0.206	0.0546	0	0	0	0	0	1	-360	360
154	92	100	0.0648	0.295	0.0472	0	0	0	0	0	1	-360	360
155	94	100	0.0178	0.058	0.0604	0	0	0	0	0	1	-360	360
156	95	96	0.0171	0.0547	0.01474	0	0	0	0	0	1	-360	360
157	96	97	0.0173	0.0885	0.024	0	0	0	0	0	1	-360	360
158	98	100	0.0397	0.179	0.0476	0	0	0	0	0	1	-360	360
159	99	100	0.018	0.0813	0.0216	0	0	0	0	0	1	-360	360
160	100	101	0.0277	0.1262	0.0328	0	0	0	0	0	1	-360	360
161	92	102	0.0123	0.0559	0.01464	0	0	0	0	0	1	-360	360
162	101	102	0.0246	0.112	0.0294	0	0	0	0	0	1	-360	360
163	100	103	0.016	0.0525	0.0536	0	0	0	0	0	1	-360	360
164	100	104	0.0451	0.204	0.0541	0	0	0	0	0	1	-360	360
165	103	104	0.0466	0.1584	0.0407	0	0	0	0	0	1	-360	360

166	103	105	0.0535	0.1625	0.0408	0	0	0	0	0	1	-360	360
167	100	106	0.0605	0.229	0.062	0	0	0	0	0	1	-360	360
168	104	105	0.00994	0.0378	0.00986	0	0	0	0	0	1	-360	360
169	105	106	0.014	0.0547	0.01434	0	0	0	0	0	1	-360	360
170	105	107	0.053	0.183	0.0472	0	0	0	0	0	1	-360	360
171	105	108	0.0261	0.0703	0.01844	0	0	0	0	0	1	-360	360
172	106	107	0.053	0.183	0.0472	0	0	0	0	0	1	-360	360
173	108	109	0.0105	0.0288	0.0076	0	0	0	0	0	1	-360	360
174	103	110	0.03906	0.1813	0.0461	0	0	0	0	0	1	-360	360
175	109	110	0.0278	0.0762	0.0202	0	0	0	0	0	1	-360	360
176	110	111	0.022	0.0755	0.02	0	0	0	0	0	1	-360	360
177	110	112	0.0247	0.064	0.062	0	0	0	0	0	1	-360	360
178	17	113	0.00913	0.0301	0.00768	0	0	0	0	0	1	-360	360
179	32	113	0.0615	0.203	0.0518	0	0	0	0	0	1	-360	360
180	32	114	0.0135	0.0612	0.01628	0	0	0	0	0	1	-360	360
181	27	115	0.0164	0.0741	0.01972	0	0	0	0	0	1	-360	360
182	114	115	0.0023	0.0104	0.00276	0	0	0	0	0	1	-360	360
183	68	116	0.00034	0.00405	0.164	0	0	0	0	0	1	-360	360
184	12	117	0.0329	0.14	0.0358	0	0	0	0	0	1	-360	360
185	75	118	0.0145	0.0481	0.01198	0	0	0	0	0	1	-360	360
186	76	118	0.0164	0.0544	0.01356	0	0	0	0	0	1	-360	360